

RETURNING MATERIALS:
Place in book drop to remove this checkout from your record. FINES will be charged if book is returned after the date stamped below.

Determination of the Rabbit  $\alpha$  and  $\beta$  Globin Nascent Polypeptide Size Distribution: Correlation of Nascent Peptide Accumulations with mRNA Secondary Structure

Ву

Calvin P. H. Vary

#### A Dissertation

Submitted to
Michigan State University
in partial fulfillment of the requirements
for the degree of

DOCTOR OF PHILOSOPHY

Department of Biochemistry

1980

Determination of the Rabbit  $\alpha$  and  $\beta$  Globin Nascent Polypeptide Size Distribution: Correlation of Nascent Peptide Accumulations with mRNA Secondary Structure

by

#### Calvin P.H. Vary

Polysome derived rabbit globin nascent polypeptides were isolated and the size distribution of the  $\alpha$  and  $\beta$  globin nascent polypeptide components was determined. The size distributions of the  $\alpha$  and  $\beta$  globin nascent polypeptides were shown to be non-uniform and unique. Previous work (1) has established a correlation between the accumulation of certain size classes of nascent polypeptides and the presence of elements of secondary structure in a mRNA molecule which, we propose, hinders ribosomal transit in certain regions of the mRNA molecule giving rise to the observed nascent polypeptide size non-uniformity.

Globin nascent polypeptides were prepared by isolation of peptidyl tRNA from polysomes which had been labeled to steady state with a particular radiolabeled amino acid. Following base catalyzed hydrolysis of the tRNA-nascent peptide linkage, the size distribution of the nascent polypeptides was determined by analytical gel chromatography. The  $\alpha$  globin polypeptide size distribution was determined by labeling polysomes in a reticulocyte

cell the p

incor

s glo

tion

**30**00

ja 62

lati

tion

non

çlo io

i i

ci( be:

.,

ě.

1

cell free protein synthesizing system derived from rabbits homozygous for the  $\beta$ 112 isoleucine valine polymorphism. Such a lysate was shown to incorporate radiolabeled isoleucine into  $\alpha$  globin precursors only since the  $\beta$  globin molecule contains no isoleucine residues.

The  $\beta$  globin component of the globin nascent polypeptide size distribution was determined by fractionation of tryptophan labeled nascent peptides according to size, treatment of various fractions with trypsin and separation of the two  $\beta$  and one  $\alpha$  tryptophan labeled tryptic peptides by high pressure liquid chromatography followed by quantitation by liquid scintillation spectrometry.

The resolved  $\beta$  globin nascent peptide size distribution was found to be non-uniform and substantially different from the size distribution of the  $\alpha$  globin nascent polypeptides. The  $\beta$  globin nascent peptide size distribution was compared to a primary and secondary structural model of the  $\beta$  globin mRNA. Nascent peptide accumulations were found to correlate with predicted regions of stable secondary structure (2) providing a correlation between the secondary structure of a mRNA  $\underline{in\ vivo}$  and the secondary structure of the same mRNA determined with the aid of chemical probes in vitro.

The  $\alpha$  globin nascent polypeptide size distribution was used to determine if agents which can modify RNA secondary or tertiary structure would alter the non-random distribution of ribosomes along the mRNA as reflected in changes in the size distribution of nascent  $\alpha$  globin polypeptides. Thermal perturbation was effected by temperature shift experiments between 15 and 37°C following steady state labeling of polysomes. Such experiments revealed a moderate and reproducible shifting of discreet components of the  $\alpha$  globin size distribution as a function of temperature under conditions

which span 10-15% of the total thermal hypochromic shift of the globin mRNA molecules.

Perturbation experiments were carried out with a short mRNA complimentary oligodeoxyribonucleotide. The reticulocyte lysate was incubated in the presence of 100  $\mu$ Molar tetradeoxycytidylic acid which is complimentary to three positions in the  $\beta$  globin mRNA and has no complimentary sequences in the  $\alpha$  globin mRNA molecule. Tetradeoxycytidylate had little effect on the  $\alpha$  globin nascent peptide size distribution but caused shifts in discreet regions of the combined  $\alpha$  plus  $\beta$  nascent polypeptide size distribution. This is consistent with tetradeoxycytidylate interaction with the  $\beta$  globin mRNA molecule resulting in a perturbation of the mRNA structure which was effectively monitored in solution by the redistribution of the nascent polypeptide size distribution.

Further experiments involving the effects of the elongation inhibitors cycloheximide, gougerotin and sparsomycin on the  $\alpha$  globin nascent peptide size distribution were conducted. It was found that ribosomal loading of the mRNA produced by all the above elongation inhibitors resulted in the reproducible relative loss of high molecule weight nascent polypeptides of the approximate size of completed  $\alpha$  globyl tRNA. Similar results were observed when polysomes were fractionated by sucrose density gradient sedimentation. The size distribution of a  $\alpha$  globin nascent polypeptide determined as a function of polysome size for both sparsomycin inhibited and control polysomes all revealed diminishing amounts of completed and near completed globyl chains in larger polysomes relative to smaller length oligopeptides. These results are consistent with the facilitated release of completed globyl polypeptides from larger polysomes indicating possible ribosomal relaxation of mRNA conformation in or near the termination codon.

- Chaney, W.G. and Morris, A.J. Archs. Biochem. Biophys. <u>194</u>, 283-291 (1979).
- 2. Vary, C.P.H., Pavalakis, G.N., Vournakis, J.N. and Morris, A.J. Nature (1981) in Press.

<u>:r:</u>

¥.

## TABLE OF CONTENTS

I	n	t	r	d	u	C	t	i	0	r	Ì

	RNA Primary Structure	•	•	•	•	•	•	• 1
	RNA Secondary Structure	•	•	•	•	•	•	. 1
	Optical Properties of RNA Helices	•	•	•	•	•	•	. 3
	Thermodynamic Properties of RNA Helices	•	•	•	•	•	•	. 5
	Experimental Approaches to RNA Structural Analysis	•		•	•	•	•	. 5
	Secondary Structure and RNA Function	•	•	•	•	•	•	. 9
	Rabbit Globin mRNA, Sequence and Translation	•	•	•	•	•	•	11
	mRNA Translational Dynamics	•	•	•	•	•	•	13
Mate	rials	•	•	•	•	•	•	18
Meth	<u>ods</u>							
	Preparation of Rabbit Reticulocytes	•	•	•	•	•	•	21
	Preparation of the Reticulocyte Lysate	•	•	•	•	•	•	21
	Conditions for Cell-free Protein Synthesis	•	•	•	•	•	•	21
	Cell-free Globin Biosynthesis: Confirmation of Proclementity, Separation of $\alpha$ and $\beta$ Globin Chains .			•	•	•	•	22
	Preparation of Peptidyl tRNA - Polysomal Labeling .	•	•	•	•	•	•	22
	Dissociation of Polysomal Structures	•	٠.	•	•	•	•	23
	Purification of Peptidyl tRNA	•	•	•	•	•	•	23
	Recrystallization of Guanidinium Chloride	•	•	•	•	•	•	25
	Analysis of Peptide Size Distribution	•	•	•	•	•	•	26
	Preparation of Cyanogen Bromide Fragments of Labeled and β Globin			•	•	•	•	27
	Determination of Distribution Coefficients	•	•	•	•	•	•	28
	Identification of 8112 (Val/Val) Homozygous Rabbits	_	_	_		_		29

	By Rapid Estimation of L-Isoleucine Incorporation SDS-gel Electrophoresis	30
	Preparation of Uniformly Labeled L-[ $^{14}$ C]-Trp-Globins	32
	Tryptic Peptide Analysis of L-[3H]-Trp Labeled Nascent Peptides	32
	Tryptic Digestion of Nascent Peptides	32
	Preparation of Bio-gel P-2 (-400 mesh) Column Buffer	33
	Preparation of Bio-gel P-2 (-400 mesh) Analytical Column	34
	Bio-gel P-2 (-400 mesh) Chromatography of Tryptic Digestion Products	34
	Construction of the High Pressure Liquid Chromagraphic System.	35
	Preparation of Buffers for High Pressure Liquid Chromatography	35
•	High Pressure Liquid Chromatographic Analysis of Tryptic Digestion Products	36
	Qualitative Analysis of Tryptic Digest Products - Desalting of Bio-gel P-2 Digestion Products	37
	Identification of Resolved Tryptic Digestion Components	37
	Paper Chromatographic Analysis of Resolved Tryptophan- Labeled β Globin Tryptic Digestion Products	38
	Calibration of the Bio-gel P-2/Urea Chromatographic System for Double Isotope Analysis	38
	Calibration of the HPLC System for Double Isotope Analysis	39
	Separation of the Different Polysomal Size Classes by Sucrose Density Gradient Centrifugation	40
Resu	<u>lts</u>	
	Analysis of the Products of the Reticulocyte Lysate System	42
	Incorporation of Radiolabel into Peptidyl-tRNA	42
	Calibration of the Bio-gel A 0.5 m Column	50
	Identification of Homozygous $\beta_{112}$ (Val/Val) Rabbits	60
	Assessment of $\alpha$ and Total Globin Synthetic Requirements for Potassium and Magnesium Ions	61

Pist Revo

	Labeling of $\beta_{112}$ (Val/Val) $\alpha$ Polysomes with L-[3H]-Isoleucine
	Double Label Analysis of Nascent Polypeptides Using L-[ $^{14}$ C]-Isoleucine and L-[ $^{3}$ H]-Tryptophan
	Characterization of the Bio-gel P-2 (-400 mesh) Analytical System for Quantitation of L-[3H]-Tryptophan Labeled Tryptic Peptides
	Determination of the α and β Globin Nascent Peptide Size Distribution by HPLC of Tryptophan Labeled Tryptic Peptides
	Labeling of Reticulocyte Polysomes with [ $^{35}$ S]-N-formyl methionyl tRNA $_f$ and L-[ $^3$ H]-Methionine 103
	Perturbation of the Nascent Peptide Size Distribution with L-O-Methylthreonine
	Perturbation of the Nascent Polypeptide Size Distribution with a Complimentary Deoxyribooligonucleotide
	Analysis of the Nascent Polypeptide Size Distribution as a Function of Polysomal Size
	Inhibition of Globin Translation by Sparsomycin and Gougerotin. 132
	Thermal Perturbation of the Nascent Polypeptide Size Distribution
	The Effect of K <sup>+</sup> Concentration on the Nascent Polypeptide Size Distribution
<u>Disc</u>	<u>ussion</u>
<u>Refe</u>	<u>rences</u>

Eigure figure figure Eigure igure rigure figure Figure igun ווטנוי :iguri :: 110 ti Bun :/ }U**r**(

## Index of Figures

Figure 1	CM-Cellulose chromatography of the products of the reticulocyte cell-free synthesis system
Figure 2	Bio-gel P-10 column chromatography of peptidyl tRNA material
Figure 3	Elution of peptidyl tRNA material from DE-52 anion exchange cellulose
Figure 4	Size fractionation of L-[ $^3$ H]-tryptophan-labeled nascent polypeptides on the Bio-gel A 0.5 m analytical column51
Figure 5	Placement of selected amino acid residues in the $\alpha$ and $\beta$ globin polypeptide sequence
Figure 6	Calibration of the Bio-gel A 0.5 m analytical sizing column with the L-[ $^{14}$ C]-tryptophan-labeled cyanogen bromide peptides of $\alpha$ and $\beta$ globin
Figure 7	Calibration of the Bio-gel A 0.5 m analytical sizing column with the L-[ $^3$ H]-leucine-labeled cyanogen bromide peptides of $\alpha$ and $\beta$ globin
Figure 8	CM-cellulose chromatography of L-[ $^3$ H] isoleucine-labeled products of a $\beta$ 112 Val/Val reticulocyte cell-free protein synthesizing system
Figure 9	Dependence of $\alpha$ globin and total globins synthetic rates on magnesium chloride concentration in the $\beta_{112}$ Val/Val Lysate
Figure 10	Dependence of the $\alpha$ globin and total globin synthetic rates on potassium acetate concentration
Figure 11	Nascent peptide size distribution of a globin nascent polypeptides
Figure 12	Comparison of the mascent peptide size distribution of $\alpha$ and total mascent peptides
Figure 13	Bio-gel P-2 (-400) chromatography of L-[3H]-tryptophan-labeled globin tryptic peptides from nascent polypeptide material
Figure 14	Bio-gel P-2 (-400) chromatography of $\alpha$ globin L-[3H]-tryptophan-labeled and tryptic peptides
Figure 15	Bio-gel P-2 (-400) chromatography of β globin [ <sup>3</sup> H]- tryptophan-labeled tryptic peptides

Figur Figur Figur Figu: figur Figur 1991 Figu Figur iigur figur Figur :igur Figure

Figure	16	High pressure liquid chromatography of L-[ $^{14}$ C] tryptophan-labeled $\alpha$ globin tryptic peptides
Figure	17	High pressure liquid chromatography of L-[ $^{14}$ ] tryptophan-labeled $\beta$ globin tryptic peptides
Figure	18	Preparative high pressure liquid chroamtography of L-[3H] tryptophan-labeled globin tryptic peptide for subsequent paper chromatographic analysis
Figure	19	Paper chromatography of L-[ $^3$ H]-tryptophan-labeled ß tryptic peptide no. 2 obtained by high pressure liquid chromatography
Figure	20	Paper chromatography of L-[3H]-tryptophan-labeled β tryptic peptide no. 3 obtained by high pressure liquid chromatography
Figure	21 a	b High pressure liquid chromatographic analysis of nascent polypeptide derived tryptic peptides from selected positions of the Bio-gel A 0.5 m nascent peptide size distribution95
Figure	22	L-[ $^3$ H]-tryptophan-labeling of the $\beta$ T2 and $\beta$ T4 tryptic peptide as a function of the Bio-gel A 0.5 m distribution coefficient
Figure	23	$L-[^3H]$ -tryptophan-labeled mascent peptide size distribution used for tryptic peptide analysis
Figure	24	$\alpha$ and $\beta$ globin nascent peptide size distribution as determined from HPLC analysis of [ $^3\text{H}$ ] tryptophan-labeled tryptic peptides
Figure	25	Time course of $[^{35}S]$ -formylmethionine incorporation into protein
Figure	26	L-[ $^{35}$ S]formylmethionine/L-[ $^{3}$ H]-tryptophan-labeling of the $\alpha$ and $\beta$ globin nascent polypeptides 109
Figure	27	L-[ $^3$ H]methionine-labeling of the $\alpha$ and $\beta$ globin nascent polypeptides
Figure	28	The effect of L-O-Methylthreonine on the $\alpha$ and total mascent peptide size distributions
Figure	29	Subtraction of L-[ $^3$ H]-tryptophan/L-[ $^{14}$ C]-isoleucine-labeled nascent peptide size distributions obtained with and without L-0-methylthreonine treatment

Figure 30	The effect of tetradeoxycytidylate on the tryptophan- labeled nascent peptide size distribution
Figure 31	The effect of tetradeoxycytidylate on the $\alpha$ globin nascent peptide size distribution
Figure 32	The a globin mascent peptide size distribution as a function of polysomal size
Figure 33	The effect of 0.5 x $10^{-6}$ M aurine tricarboxylic acid on the rate of $\alpha$ globin synthesis
Figure 34	The effect of low levels of aurine tricarboxylic acid on the size distribution of $\alpha$ -nascent peptides
Figure 35	Effect of sparsomycin and gougerotin on the rate of globin synthesis
Figure 36	Dosage dependence of the rate of protein synthesis on sparsomycin concentration
Figure 37	Effect of cycloheximide on the rate of globin synthesis 138
Figure 38	Effect of cycloheximide on the rate of $\alpha$ globin synthesis 140
Figure 39	Dosage dependence on the rate of total globin and $\alpha$ globin synthesis on cycloheximide concentration
Figure 40	Evaluation of the levels of cycloheximide, sparsomycin and gougerotin which provide 70% inhibition of protein synthesis
Figure 41	The effect of low levels of sparsomycin on the $\alpha$ globin nascent peptide size distribution
Figure 42	The effect of low levels of gougerotin on the $\alpha$ globin nascent peptide size distribution
Figure 43	Sedimentation profile of sparsomycin inhibited, control and mixed (inhibited and uninhibited) polysomes 153
Figure 44	The effect of low levels of sparsomycin on the size distribution of $\alpha$ nascent peptides from small polysomes 155
Figure 45	The effect of low levels of sparsomycin on the size distribution of a nascent peptides from medium sized polysomes
Figure 46	The effect of low levels of sparsomycin on the size distribution of $\alpha$ -nascent peptides from large sized polysomes

Figure 4	The effect of L-[ $^3$ H]-isoleucine-labeling conducted at 15°C on the $\alpha$ nascent peptide size distribution 162
Figure 4	The effect of a temperature shift from 37°C to 22°C on the nascent peptide size distribution
Figure 4	The effect of a temperature shift from 37°C to 15°C on the α nascent peptide size distribution
Figure 5	The effect of different potassium levels on the $\alpha$ and $\beta$ globin nascent peptide size distribution
Figure 5	A comparison of nuclease susceptible regions of a proposed globin mRNA structure and the accumulation of nascent globin peptides
Figure 5	Proposed regions of single stranded β globin mRNA structure and the β nascent peptide accumulations
Figure 5	B Location of mascent peptide accumulation on the secondary structure of the 5' region of the $\alpha$ and $\beta$ globin mRNAs 194

## List of Tables

Table 1	Analysis of Globin Polypeptides for the Incorporation of L-[ $^3$ H]-Isoleucine into $\alpha$ and $\beta$ Globins by SDS Polyacrylamide
Table 2	The Positions of the a Globin Nascent Peptide Accumulations as Determined by L-Isoleucine Labeling of ß112 Val/Val Lysates
Table 3	The Positions of the ß Globin Nascent Peptide Accumulations as Determined by Tryptic Analysis
Table 4	The Recovery of [3H]dpm Present in Peptidyl tRNA Relative to Control dpm ([14C]) From Polysomes Following Thermal Shift to 22°C and 15°C From 37°C

Intro

RNA P

of nu

tives Matur

polyr the b

bases

of proints

into.

certa speci

950

Prote

prote

below nucle

ships

BK 20

struct

ŝρζ,

#### Introduction

#### RNA Primary Structure

Polyribonucleic acids are naturally occurring or synthetic polymers of nucleoside monophosphates. These are the monophosphorylated derivatives of β-D-ribofuranosyl adenine, guanine, cytosine and uracil. Natural polynucleotides contain varying amounts of modified bases. polyribonucleotides other than tRNA these modifications are predominantly the base N-methyl and 2'-0-methyl-ribose derivatives. The sequence of bases contains not only the information necessary to direct the synthesis of proteins as in the case of messenger RNA but presumably also contains information which results in the folding of the polynucleotide backbone into a unique molecular conformation necessary for the determination of certain aspects of the functional behavior of the polynucleotides such as specific initiation rate, and metabolic half life (1,2). These functions also include interaction of the polyribonucleotide with various specific proteins (3), specific molecular interactions with regulatory cations (4) as well as internucleotide interactions which occur at many levels of the protein biosynthetic apparatus (5). A number of studies to be mentioned below have indicated that knowledge of the primary structure of a polynucleotide will not immediately describe all of the structural relationships which are needed to account for known RNA function (6).

#### RNA Secondary Structure

Rich and co-workers (7) published definitive studies of the crystal structures of the self-complimentary dinucleoside monophosphates, ApU and GpC. Analysis of the crystal structures of these molecules permitted

observation of the C-2 rotational axis of symmetry between the two halfs of the (ApU)<sub>2</sub> and (GpC)<sub>2</sub> dimers and provided, for the first time, direct visualization of a segment of a right-handed helix exhibiting Watson-Crick base pairing. Additional information from these studies indicated that the sugar phosphate backbone promoted the spontaneous formation of W-C base pairing in helices of nucleotides (8). These studies also confirmed predictions of strong base stacking interactions among the dinucleoside monophosphates in solution. Extension of these studies to helical polyribonucleotides and polydeoxyribonucleotides revealed tendencies towards large scale helical ordering.

Helical polynucleotides are described physically by their respective genus. This term reflects ranges in the axial translation (h) and rotation (t) nucleotide. These parameters may vary from 2.56A-3.14A for (h) and from  $30^\circ-45^\circ$  for (t).

Genus A helices are characterized by C(3') endofuranose conformations and a large range of values for (h) (2.56-3.29 A) as well as a restricted range for (t) exhibiting values from 30-32.7°. This is in contrast to genus B helices which exhibit a preference for C3' exo- or C2' endofuranose conformations, narrower ranges of (h) values (3.04-3.4 A) and a broader range of (t) from 31.3° to 45°. The A genus helics have their bases positioned 3 to 5 A forward of the major helix axis and tilted positively with respect to a normal with the major axis in contrast with genus B helics in which the bases are translated to the rear of the helix major axis by 0-3 A and exhibit a negative base tilt (9). These parameters reflect differences in helical dynamics, stability and configuration which can occur to varying extents in any helical region or group of helices. In particular, the forward positioning of the bases in

the A helix creates a deep groove opposing the glycosidic linkages providing an opportunity for tertiary interactions such as triple strand formation as is found in tRNA (10).

Natural RNA helices such as those found in localized regions of mRNA molecules seem to fall predominantly into the A genus (11). However, it cannot be excluded that short regions of a particular sequence may result in unusual and potentially important alternate helical forms. This has been found to be the case in DNA following the observation by Rich and coworkers of an extreme conformational variant termed Z-DNA (12).

#### Optical Properties of RNA Helices

One of the best known properties of helical polynucleotides is the dramatic decrease in the extinction coefficient per residue of the primary ultraviolet absorption transition upon transfer of a nucleotide residue from a random coil to a helical environment. This change is primarily due to the interaction of the aromatic electrons of each base residue with bases stacked above and below it in the helix. This phenomenon is known as base stacking and is reflected in a hypochromic shift upon helix formation and is thought to be the primary stabilizing force for helix formation providing a hydrophobic environment for Watson-Crick hydrogen bonding which in turn leads to the high specificity or complimentarity of the helical interaction. The technique of thermal denaturation and the resultant hyperchromic shift has been used to characterize the helical content of many natural and synthetic polyribonucleotides. Using this property, total mRNA, 18S and 28S ribosomal RNA, ovalbumin mRNA and procollagen mRNAs were found to have from 55 to 75% of their bases present in base paired form (13). It has also been determined that

in the case of ovalbumin mRNA (14) and globin mRNA (15) greater than 90% of the helical structure is preserved at physiological values of ionic strength, pH and temperature. O'Malley et al. were able to carry these analyses further to demonstrate, with the aid of high resolution thermal denaturation and heat capacity measurements, that different mRNAs had characteristic dH/dT profiles which suggested the presence of discreet helical structures of different classes of stability and of varying amounts in tRNA, 18S and 28S rRNA, globin, ovalbumin mRNAs and MS-2 RNA. These studies also indicated the absence of long GC rich structures in ovalbumin mRNA in contrast to data obtained for tRNA and 28S RNA (14). In general, it was found that mRNAs had fewer GC rich regions than is the case for 28S RNA. This result was taken as evidence that the secondary structure present was not due to random complimentarity of sequence, which would be expected to give upwards of 50% helicity (16), but rather was an indication of specific stable structures present in the RNA molecular structure.

Similar results have been obtained using the techniques of optical rotatory dispersion and circular dichroism (15). Globin mRNA showed a positive Cotton effect which upon shift of the temperature from 20° to 85°, gradually decreased with a concomittant shift of the 285 nm peak and zero rotation crossover point to longer wavelengths. Decrease in the Cotton effect is characteristic of loss of asymmetry during the helix coil transition. This process was found to be reversible upon cooling indicating that renaturation to the original state or to a very similar state had occurred. The reversibility of nucleic acid denaturation is well substantiated in the case of tRNA but remains only partially substantiated by experiment in the case of structural studies on larger molecules.

#### Thermodynamic Properties of RNA Helices

Pioneering work of Uhlenbeck, Tinoco and others on the thermodynamics of formation of homopolymeric (17) mixed sequence complimentary (18), and imperfect helices (19), and helical fragments from natural sources (20) has resulted in the accumulation of a large body of data concerning the thermodynamics and stability constraints on helix formation. Evaluation of the enthalpies and entropies for formation of the dimeric units of helical structures and recognition and characterization of the contributions of nearest neighbor base pairs, helix nucleation, and the steric constraints of loops and bulges to overall helix stability has culminated in a set of parameters which allow systematic estimation of the free energy of formation of helices of known primary sequence (21) and provide a systematic criterion by which the relative stabilities of alternative helical representations of a given sequence may be adduced and the most stable or probable structure chosen.

These parameters have been coupled with algorithms (22,23) which allow searches to be made of all possible base pairing schemes for a given polynucleotide primary structure. These results provide hypothelical polynucleotide secondary structures based on maximal hydrogen bonding and minimized free energy content. These highly tentative structure proposals will gradually be supported or rejected as the appropriate experimental approaches become available.

#### Experimental Approaches to RNA Structural Analysis

It has been pointed out by Fresco and demonstrated experimentally with synthetic random sequence polynucleotides (16) that a random polynucleotide sequence would be expected to exhibit base pairing involving

50% or more of the bases. It has been argued that the levels of base pairing found in natural polynucleotides is in many cases only slightly higher than the amount estimated for a random sequence. This model predicts that no critical conformation or molecular state need exist for a particular polynucleotide. Initial experimental evidence at variance with this position was obtained demonstrating that random polymers had very low thermal stability reflecting lowered Tm's and shallow hyperchromic transitions concomittant with thermal denaturation. This result was in contrast to natural RNAs which exhibited similar amounts of base pairing but had distinctly sharper hyperchromic shifts upon denaturation indicating a high cooperativity of melting as well as significantly higher Tm values for these transitions. More evidence has accumulated in support of the view that natural RNAs will have discreet molecular structures. The early studies of Tinoco et al. (24) and Wrede et al. (25) on the ability of tRNA and 5S RNAs to bind some complimentary oligonucleotides to regions of a known polyribonucleotide primary sequence while other complimentary oligonucleotides would not associate supported a model of secondary structure composed of helical elements, inaccessible to the complimentary oligonucleotides probes, separated by accessible single strand sequences. These techniques allowed demonstration of single strandedness at the anticodon, amino acid acceptor stem and T U loops of tRNA molecules in solution.

Further evidence for discreet molecular conformations in larger polynucleotides came from the work of Adams et al. (26). Using limited nuclease digestion of R-17 bacteriophage RNA protected by initiation complex formation these workers isolated in high yield, and sequenced, a 55 nucleotide long fragment which exhibited extensive helical structure

in solution. The increased sensitivity of single stranded regions of polynucleotide to nuclease attack relative to double stranded regions came to the foreground during efforts by Fiers et al. to determine the primary sequence of the bacteriophage MS-2 genomic RNA (28). It was observed that limited digestion with nucleases such as T1 released certain fragments in high yield from the polycistronic RNA. Further analysis showed that different guanylate residues varied dramatically in their susceptibility to enzymatic cleavage by T1 nuclease. Completion of the sequence of the MS-2 RNA led to the proposal of an extensively base paired secondary structural map of the RNA molecule in which the residues of highest nuclease susceptibility resided predominantly in single stranded regions while guanylate residues which were hydrolyzed slowly, if at all, under the same conditions resided in the regions of proposed stable helical structure (28).

Further exploitation of this approach was used by Flashner and Vournakis (29) to demonstrate discreet and different patterns of nuclease resistant fragments characteristic of the rabbit  $\alpha$  and  $\beta$  globin mRNAs indicating the presence of helical elements of structure characteristic of the rabbit  $\alpha$  and  $\beta$  globin mRNAs.  $\alpha$  and  $\beta$  globin mRNAs which had been radioiodinated were subjected to limited digestion with the single strand specific nuclease S1. Analysis of the products by denaturing polyacrylamide gel electrophoresis demonstrated that a limited set of fragments, which were different for  $\alpha$  and  $\beta$  RNAs, had been released under the conditions of the incubation. This result was interpreted as evidence for unique discreet molecular conformations for the  $\alpha$  and  $\beta$  globin mRNAs and judged inconsistent with a model for RNA structure based on a large number of random molecular structures. The susceptibility of specific

regions of natural polynucleotides has been noted by others. Hela cell 5.8S ribosomal RNA was observed to have two internal sequences susceptible to S<sub>1</sub> nuclease hydrolysis which allowed the proposal of a hypothetical secondary structure consistent with this observation (30). T<sub>1</sub> ribonuclease digestion of human, hamster and Xenopus laevus 18S ribosomal RNA also showed limited sensitivity to the nuclease used as a structure probe and led Maden et al. (31) to propose that the 3' terminus of this RNA existed in a highly exposed conformation in the intact ribosomal subunit. Maden supported the possibility of interaction of the 3'-termini of 18S ribosomal RNA with other components of the protein synthetic apparatus.

Nucleolytic enzymes as structural probes have recently been used to map regions of secondary structure on the polynucleotide backbone of several RNAs. Wurst et al. (32) have developed a methodology based on rapid RNA sequencing techniques Gilbert and Maxam (33).

RNAs which have been terminally labeled with <sup>32</sup>Phosphorous are bjected to limited hydrolysis of S<sub>1</sub> nuclease or T<sub>1</sub> ribonuclease. Products are then separated on high resolution denaturing polyacrylate sequencing gels. Bands appear on the gels at positions correspondto nuclease susceptable single stranded sites along the polynucleode sequence. This method allows determination of the relative susceptility and hence accessibility of each phosphodiester bond to the clease structural probe throughout the molecule. These data can be do support a particular hypothetical secondary structure at the pense of possible alternative structures.

An alternative approach was used to determine interacting sequences large RNA molecules and, in particular, the 16S ribosomal RNA from

E. coli. This method uses nucleases to hydrolyze the polynucleotide preferentially at single stranded regions to release helical fragments.

These fragments are separated under non-denaturing conditions which allow the halves of the helices to remain intact. The separated fragments are then subjected to electrophoresis at right angles to the original separation under denaturing conditions and interacting sequences appears as a linear array of spots along the direction of the second separation procedure. The approach provided evidence allowing Brimacombe and Ross to propose a secondary structure map of the 16S ribosomal RNA and demonstrated several long range intramolecular interactions (34). These studies, cited above, are consistent with conserved unique structural conformations in a given class of RNA molecules and begin to provide a molecular basis for various functional interactions which have been observed.

### Secondary Structure and RNA Function

Early work attempting to relate RNA structure to RNA function began in the 1960's. Work by Lodish utilizing f-2 bacteriophage RNA addressed the sensitivity of the translational process to severe perturbants of secondary structure (35). Using reagents such as formaldehyde to permanently denature regions of the phage mRNA it was found that unrestricted initiation occurred at the correct initiator codon resulting in a large excess of the normal polypeptide products. In addition, a large number of Polypeptides were generated which were found to bear no relationship to the primary sequence of the normal phage proteins implying that erroneous initiation had occurred at various points other than the true initiation codon. These results were taken as evidence that secondary

structure which was specifically removed by formaldehyde treatment was necessary for the correct functioning of the RNA.

In other studies, the coat proteins of the RNA phages f-2, MS-2 and R-17 were found to play a key role in the regulation of the synthesis of the product of the RNA polymerase cistron (36). Later studies showed that the coat protein bound specifically to a helical region of the RNA which contained the initiator AUG for the phage polymerase enzyme and thus affected its protection from nuclease attack allowing isolation of the protein binding fragments.

Analysis of the primary and secondary structure of the MS-2 genome by Fiers et al. (28) provided a molecular explanation for the effect of coat protein binding on suppression of replicase production through binding of coat protein to a helical fragment of the phage RNA which contains the replicase initiation codon. In addition, the secondary structure of the coat protein/replicase initiation region, as determined by Fiers et al.. Provides confirmation of a proposal by Lodish and Robertson that part of the coat protein cistron must be translated to expose the viral replicase AUG initiator codon since the initiator codon appears to be heavily involved in secondary structure with a region of the coat protein genome (37). These results led to the proposal of a molecular explanation for the strongly polar effect of coat protein synthesis on replicase synthesis (28).

Additional evidence for an influence of secondary structure on the events leading to initiation of protein synthesis was obtained by Pavlakis et al. (38). These workers used nuclease probes of primary and secondary structure, as described above, to show that the 5'-terminal regions of the  $\alpha$  and  $\beta$  globin mRNAs of mouse and rabbit possessed ele-

ments of structural similarity between the homologous  $\alpha$  or  $\beta$  mRNAs respectively of each species. Analysis of structure revealed that the initiation codon and flanking sequences in the mouse and rabbit  $\alpha$  mRNAs were inaccessible to nuclease structure probes. This finding was in contrast to the extensive nuclease susceptibility of the AUG codons in the homologous  $\beta$  mRNAs. These results may be of considerable functional significance since it is known that the  $\beta$  mRNA initiates synthesis of the  $\beta$  globin polypeptide at about 1.5 times the rate of  $\alpha$  globin initiation in the rabbit reticulocyte (1).

Other aspects of the initiation process have been studied within the context of mRNA structure. Robertson and Legon performed a series of studies on ribosome binding to radioiodinated globin mRNA (39). These workers were able to isolate and sequence a specific fragment which was protected from nuclease digestion by bound ribosomal subunits. These studies revealed that the 40S subunit protected a fragment approximately 80 nucleotides in length from nuclease degradation whereas the complete 80S ribosome protected a much smaller portion of the same region of RNA of approximately 40 nucleotides, suggesting a conformational change in the polynucleotide backbone during construction of the preinitiation and initiation complexes.

# Rabbit Globin mRNA, Sequence and Translation

The question of the relevance of mRNA secondary structure to mRNA function has been evaluated from other points of view. Analysis of the primary sequence of coding and noncoding regions in terms of the degree of conservation of sequence in homologous RNAs from different species, codon usage, and the presence of highly conserved oligonucleotide

sequences, has had considerable impact on the question of the role of secondary structure in mRNA function.

Early studies of the globin mRNAs from rabbit revealed the presence of the conserved hexanucleotide, AAUAAA within the 3'-noncoding region of the  $\alpha$  and  $\beta$  globin mRNAs (40,41). This same sequence has been found in the 3' noncoding region of all other poly(A) containing mRNAs sequenced thus far. The function of this hexanucleotide is not known at this time. The hexanucleotide ACACUU is found to be present within the 5' regions of both  $\alpha$  and  $\beta$  globin mRNAs. Although no function is known for this hexanucleotide its conservation would seem significant given that the  $\alpha$  and  $\beta$  5' nontranslated regions bear little other sequence homology. Presumably there has been an accumulation of a relatively large number of mutations in this region of the RNA molecules since divergence of the  $\alpha$  and  $\beta$  sequences.

Sequence analysis of a number of eukaryotic mRNAs has demonstrated the nonrandom use of synonymous codons. Work by Adams et al. (27) on sequence analysis of the 57 nucleotide long region of the coat protein cistron of R-17 bacteriophage indicates that degeneracy in the genetic code and nonrandom usage of synonymous codons has allowed maximization of secondary structure without alteration of the resultant polypeptide sequence. This view has been carried further by Ball who suggests that some of the selective pressure on an amino acid sequence reflects changes which maximize secondary structure (42). This proposal was suggested following sequence analysis of the MS-2 coat protein gene. It was demonstrated that the codons for the most conserved amino acids occur in extensively base paired regions. Although it is difficult to make conclusive statements from such studies, sequence analysis and asymetric

codon usage argue in favor of structural constraints on certain aspects of mRNA function.

#### mRNA Translational Dynamics

The globin biosynthetic system has been extensively studied in terms of the rate and dynamics of the process of protein synthesis. Theoretical studies by Gibbs et al. on template directed polymerization processes allowed prediction of some of the properties found in protein synthetic systems (43,44). These workers indicated, as Lodish later underscored (45), that for polymerizing systems for which the initiation step is rate limiting, inhibition of initiation will result in more severe restriction of a slower initiating messenger RNA relative to a faster initiating mRNA. Later studies using inhibitors of mRNA initiation allowed demonstration of this phenomenon with the  $\alpha$  and  $\beta$  globin mRNA. Jacobsen et al. (46), building on previous studies which established that the overall (average) rate of elongation and termination were roughly equal for  $\alpha$  and  $\beta$  globin mRNAs, determined that the  $\alpha$  globin mRNA initiates synthesis only 60% as efficiently as the  $\beta$  mRNA and that there is approximately 1.4 times as much  $\alpha$  globin mRNA as  $\beta$  mRNA resulting in a **net** ratio of  $\alpha$  to  $\beta$  synthesis of unity. Although there were technical difficulties with both of these studies, the conclusions of Jacobsen and Lodish concerning the differences in apparent initiation rates and the assignment of rate limiting step in globin synthesis at the level of initiation remain valid.

Other studies involving analysis of the effects of elongation inhibitors such as gougerotin, cycloheximide and amicetin and the initiation inhibitors edeine and pactamycin established the dependence of polysome

size on the initiation and elongation rates. Evidence was obtained that the number of ribosomes on a mRNA at a steady state is proportional to the length of the coding region of a mRNA and to the rate of initiation of protein synthesis. The mean polysomal size is inversely dependent on the rate of elongation and termination. Recent studies on the regulation of mRNA structural and functional half life seem to indicate that control of mRNA ribosomal loading may be used to effect control on mRNA turnover (47). Cohn et al. used elongation and initiation inhibitors to demonstrate that certain of the T7 early mRNAs are significantly protected from nuclease inactivation when they are present in larger polysomes. This result was taken to indicate that ribosomes may be spending more of their time residing over nuclease susceptable sites in the mRNA, reducing the effective level of that site as a target for nuclease attack. Other mRNAs were found to be stabilized by inhibitors which allowed ribosomal density to increase near the initiation region, indicating the possibility of ribosomal protection of a nuclease susceptible site near the initiator region. These studies raise the question of whether structural aspects of a mRNA can modulate polysomal size through effects upon the rates of initiation, elongation and termination and in turn upon ribosomal density on a mRNA thus altering the observed half life.

A fairly large body of evidence is accumulating concerning the effect of mRNA secondary structure on the rates of elongation and termination. Protzel et al. have demonstrated that the size distribution of the nascent polypeptide intermediates of globin synthesis is nonuniform (48). Gel chromatographic analysis of uniformly labeled nascent polypeptides conducted under denaturing conditions has been used to demonstrate

that the population of nascent polypeptide intermediates is composed predominantly of discreet size classes of nascent polypeptides which are disproportionately represented throughout the population of  $\alpha$  and  $\beta$ alobin nascent polypeptides. Since the nascent polypeptide molecular weight uniquely corresponds to the position of the associated ribosome along the coding region of the particular mRNA being translated, the disproportionate representation of a particular size class of nascent polypeptides was taken as an indication of an increased probability of finding ribosomes occupying this region of the mRNA. The most likely explanation for this observation is that the rate of ribosomal translocation is not uniform but changes locally along the mRNA. Later work by Chaney and Morris sought to identify the origin of the **nonuniformity** of local translocation rates (49). These workers were unable to identify any rate limiting components of the protein biosynthetic apparatus which could account for the production of nonuniform elongation rates during globin synthesis. Translation of Poly(A)+ RNA from rabbit reticulocytes in a wheat germ cell-free protein **synthes**izing system permitted demonstration of an identical nascent Peptide size distribution to that observed in the reticulocyte system. These findings were taken as evidence that the origin of local nonuniform rates of elongation was associated with some property of the mRNA itself not due to a limitation of some component of the biosynthetic apparatus.

Further studies sought to analyze the nascent peptide size distribution in a different system reflecting the translation of a single mRNA sequence. Chaney et al. observed a nonuniform size distribution of nascent polypeptide precursors in the synthesis of MS-2 coat protein (50). The nascent peptide accumulations were used to map points of slow

translocation on the coding region of the coat protein cistron and these results were compared with the "flower" conformation proposed by Fiers et al. as the most stable secondary structure for this part of the MS-2 RNA molecule. It was found that the accumulations of nascent peptides corresponded to single stranded stretches at or near the 5' side of regions of stable helical structure. This result was taken as evidence that helical regions of the RNA molecule retard ribosomes entering these helical regions. This model predicts that ribosomes will tend to occupy regions of the mRNA at the points of entry into regions of secondary structure. This model provides a basis for the formulation of a mechanism by which the amount of stable helical structure in a mRNA may modulate the average elongation rate by virtue of its effect on local translocation rates which contribute to the average elongation rate. Independent evidence for this is indicated by the observation of Schimke et al. (51) that irreversible denaturation of several mRNAs by treatment with methyl mercury hydroxide resulted in an increase in the rate of elongation as well as an increase in the ability of these mRNAs to direct the synthesis of full length reverse transcripts instead of partial transcripts. Partial reverse transcripts are thought to arise from premature termination brought about by stable structures present in the template. These arguments indicate that mRNA secondary structure may be involved in a  ${f dual}$  role in determination of mRNA half life, directly through modulation of the amount of nuclease susceptable regions per mRNA molecule and indirectly by providing a mechanism by which ribosomal coverage of  ${f sus}$  Ceptable sites along the polynucleotide backbone may be maximized.

The goal of this thesis is to determine which nascent peptide  ${}^{\text{acc}}\text{cumulations, previously observed in the synthesis of the rabbit }\alpha \text{ and }$ 

β globins, correspond to α specific and β specific nascent peptide accumulations, to correlate the single mRNA specific nascent peptide accumulations thus obtained with any physical data on the α or β globin mRNAs which may become available during the time this work was in progress and finally, to test the ability of perturbative techniques applied to the protein biosynthetic apparatus, eg. inhibitors, temperatures, etc. to provide information relevant to the hypothesis analyzed herein, that mRNA secondary structure directly hinders ribosomal translocation along regions of the mRNA involved in stable secondary structural interactions.

#### Materials

Cycloheximide, guanidinium chloride (practical grade), bovine hemin (twice recrystallized), phosphocreatine, 2.4-dinitrophenyl alanine, Triton X-114, N,N,N',N'-tetramethylethylene-diamine, and creatine phosphokinase (E.C. No. 2.7.3.2) and aurine tricarboxylic acid were purchased from Sigma Chemical Co., St. Louis, Missouri. Phenylhydrazine-HCl, napthalene (scintillation grade), and diethylpyrocarbonate were purchased from Aldrich Chemical Co., Milwaukee, Wis. Gougerotin was purchased from Calbiochem Co., La Jolla, Calif. Bio-Rad Co., Richmond, Calif., was the Source of Bio-gel A 0.5m (10% agarose) and Bio-gel P-10. Nembutal (Sodium pentobarbital) was obtained from Abbott Laboratories, North Chicago, Ill. Research Products International was the source of 2,5-di-Phenyloxazole (PPO, scintillation grade), 1,4-bis 2-(4-methyl-5-phenyl-Oxazolyl)-benzene (POPOP, scintillation grade), and Triton X-100. Blue dextran 2000 was purchased from Pharmacia Co., Uppsala, Sweden. Microgranular (preswollen) diethylaminoethyl cellulose (DE52) and carboxymethyl cellulose (CM32) were obtained from Whatman Biochemicals, Ltd., Maidstone, Kent, Great Britain, as were GF/C glass fiber filters. Sodium heparin was purchased from Fisher Scientific Co., Fair Lawn, New Jersey. Sparsomycin was generously donated by Drug Research and Development, Division of Cancer Treatment, National Cancer Institute, Bethesda, Md.

Radioactive amino acids were purchased from New England Nuclear, Boston, Mass. ([ $^{3}$ H]-tryptophan, 7.9 Ci/mmole, [ $^{14}$ C]-tryptophan, 50-7 mCi/mmole, [ $^{3}$ H]-isoleucine and [ $^{14}$ C]-isoleucine) and Amer-

sham/Searle Co., Arlington Heights, Ill. ([3H]-leucine, 60 Ci/mmole. Ultra pure grade sucrose was purchased from Bethesda Research Labs, Bethesda, Md.

All other chemicals used were reagent grade.

#### Methods

#### **Preparation of Rabbit Reticulocytes**

New Zealand white male rabbits weighing 6-10 lbs were made anemic with four daily injections of 2.5% phenylhydrazine in an isotonic sodium potassium and magnesium salts solution at pH 7.30 as described by Allen and Schweet (52). Following a recovery period of three days rabbits were injected with a solution composed of 100 mg sodium nembutal and 2000 units of sodium heparin in a final volume of three ml via the marginal ear vein. Exsanguination was accomplished by cardiac puncture with a 100 ml glass syringe fitted with an 18 gauge needle. Blood so obtained was immediately chilled to 0°C on wet ice and all subsequent operations were Performed at 0-4°C. Hematocrits from such preparations ranged from 9-15%.

Blood was initially passed through two layers of glass wool to

effect removal of small pieces of tissue and then centrifuged at 4000 x g

× 20 minutes in a Sorvall GSA type rotor. Plasma was removed by aspira
tion and considerable care was taken to remove the buffy coat from the

top of the pellet. Cells were resuspended with a rubber policeman in a

volume of Ringers saline (RS) solution approximately equal to the plasma

volume (53). Cells were then isolated by centrifugation at 4000 xg x 10

minutes followed by aspiration of the RS supernatant. This washing

procedure was repeated three times to give cells which had been washed

pelleted four times.

#### Preparation of the Reticulocyte Lysate

Washed rabbit reticulocytes were lysed with an equal volume of ice cold sterile water. The lysate was then centrifuged at 25,000 xg x 20 minutes. The supernatant fraction was decanted to another centrifuge tube to ensure homogeneity of the lysate. Aliquots of 700 to 900 µl were immediately frozen by injection into vials which had been maintained at -40°C on dry ice. All glass which the lysate was to encounter was washed in a solution of 1 N KOH, 50% ETOH, rinsed first with water and then with a diethyl pyrocarbonate containing solution and placed in an oven to dry at 120°C for several days or at high temperature (270°C) for at least 6 hours prior to use. Lysate aliquots were capped and stored in liquid nitrogen until used.

#### Conditions for Cell-Free Protein Synthesis

The reticulocyte cell-free protein synthesizing system contained in a total volume of 1 ml: 800 µl lysate, 0.3 µmoles of hemin prepared as described by Darnbrough et al. (54), 11.0 µmoles of creatine phosphate as the sodium salt, 100 µg creatine phosphokinase at a specific activity of units/mg protein, 1.0 µmoles adenosine triphosphate, sodium salt, 0.20 µmoles guanosine triphosphate, potassium salt, and 0.1 times the final amino acid concentrations of Lingrel and Borsook (53).

Potassium and magnesium requirements were determined for each lysate Preparation on the basis of those levels of salt required for optimal initial velocity and extent of incorporation of L-[ $^3$ H]-leucine (10  $_{\mu}$ Ci Per 250  $_{\mu}$ l lysate) into alkali stable 10% trichloroacetic acid precipitable material. These optima were consistently found to be in the range of 1.2-1.6 millimolar for MgCl<sub>2</sub> and 130-140 millimolar for potassium acetate.

# Cell-Free Globin Biosynthesis, Confirmation of Product Identity: Separation of α and β Globin Chains

Analysis of products synthesized by the cell-free system was accomplished by CM-cellulose ion exchange chromatography according to a modification of the method of Dintzis et al. (55). Small aliquots of postribosomal supernatant obtained from the preparative ultracentrifugation of [3H]-Leu labeled lysate at 105,000 xg for 180 minutes were dialyzed against distilled water for 24 hours to remove radioactive amino acids. The retention was used to prepare globin by the method of Winterhalter and Huehns (56). Approximately 2 ml of the hemoglobin solution was dripped into a rapidly stirring solution of 200 ml acetone and HCl (final concentration, 0.6 M) maintained at -40°C in a dry ice/acetone bath. After 30 minutes stirring the precipitated globin was collected by centrifugation at 13,200 xg x 20 minutes. The pellet was washed gently with fresh acetone, dried and dissolved in .02 M pyridine, 0.2 M formic acid, .005 M 2-merceptoethanol (referred to as 1% Dintzis buffer). This solution was cleared of insoluble material by centrifugation at 25,000 xg for 20 minutes. 35,000-50,000 cpm of the globin solution was applied to  $^{\mathbf{a}}$   $^{\mathbf{O}}$   $^{\mathbf{9}}$  x 22 cm column of CM-cellulose-32 equilibrated with 1X Dintzis buffer. Following a wash cycle of 10 volumes of Dintzis 1X buffer, elution was affected with a gradient of pyridinium formate as described by Protzel and Morris (48). Fractions were collected directly into 1 1 Quid scintillation counting vials and counted in a xylene based scintillation cocktail.

# Preparation of the Peptidyl tRNA - Polysomal Labeling

Labeling of peptidyl tRNA was accomplished in reaction volumes 0.5

to 1.0 ml containing 50 to 200 µCi of tritium labeled amino acid or 5 to 20 µCi [14C]-labeled amino acid. When the labeled amino acid was other than isoleucine or tryptophan, the input level of the corresponding cold amino acid in the Borsook mix (53) was reduced 10 fold. Incubations were conducted at 37°C for 10 minutes unless otherwise indicated.

Label ing was terminated by rapid addition of 2 ml of ice cold Medium B (48) containing 0.21 mM sparsomycin and 0.059 mM cycloheximide.

Polyri bosomes were isolated by centrifugation at 105,000 xg for 2 hours at 2-4°C.

#### Dissociation of Polysomal Structures

The polysomal pellet isolated by ultracentrifugation was resuspended in O-75 ml of a solution composed of 0.25 M sucrose, 0.059 M cycloheximide and 0.21 mM sparsomycin. This suspension was then brought to concentrations of 3.0 M LiCl, 4.0 M Urea, 0.05 M 2-mercaptoethanol and 0.05 M NaAc pH 5.6. This mixture was incubated for 16 hours at 0°C followed by Centrifugation at 10,000 xg x 20 minutes. The supernatant solution was used for subsequent purification steps.

# Purification of Peptidyl-tRNA

Stock urea solutions were prepared by stirring a 9.0 <u>M</u> solution of urea for four hours with Amberlite MB-3. The amberlite was removed by filtration through a medium grade scintered glass funnel and the volume adjusted to give a final urea concentration of 8.54 <u>M</u>. This stock urea solution was used to prepare buffers for subsequent peptidyl tRNA purification steps as described by Slabaugh and Morris (57) as modified by Chaney and Morris (49). Buffer I containing 7.6 <u>M</u> urea, 0.05 <u>M</u> 2-mercap-

toethanol, 0.1 M sodium acetate (pH 5.6). Buffer II contained all components at identical concentrations as in to buffer I except that the sodium acetate concentration was raised to 0.75 M.

DEAE cellulose (Whatman DE-52 in microgranilar preswollen form) was suspended in approximately 60 ml of 0.5 N acetic acid per 7 grams of ion exchange cellulose. The fine particulate material was removed by allowing the DEAE cellulose to settle to one third the column height of the suspension followed by removal of the volume above the bulk of the settling cellulose. This procedure was repeated twice, the volume restored to its original value and the pH adjusted to 5.6 with saturated NaOH. The ion exchange cellulose was then isolated in a scintered glass funnel and washed three times with Buffer I in amount equal to the original suspension volume. The cellulose was then resuspended in Buffer I, the fine particulate material was removed once and the final volume of the suspension was brought to twice the volume of the fully settled Cellulose. Prior to adsorption of peptidyl tRNA a column containing approximately 2 g of DE-52 cellulose was washed with approximately 50 ml Of Buffer I.

Lithium chloride and contaminating amino acids were removed from the Pibosomal dissociation mixture by chromatography on a 1.9 x 40 cm column Of Bio-gel P-10 (200-400 mesh) equilibrated with Buffer I. The column was eluted with buffer I and radioactivity which eluted in the void Volume was pooled and adsorbed to a DE-52 cellulose anion exchange column and washed with approxaimately 150 column volumes of buffer I.

After peptidyl tRNA had been adsorbed to the anion exchange material and washed as described above, the peptidyl tRNA was eluted stepwise by elution of the column with Buffer II.

Fractions containing the radioactivity which was eluted were concentrated by pressure ultrafiltration with N<sub>2</sub> gas to a final volume of 0.3-0.5 ml in an Amicon model 8 MC microultrafiltration system (Amicon Corp., Lexington Ma.) over an Amicon UM-2 membrane. Three ml of 6M guanidinium chloride,  $100 \, \underline{\text{mM}}$  2-mercaptoethanol pH 6.5 were then added and the solution concentrated to 0.3-0.5 ml.

The pH of the concentrated peptidyl tRNA solution was then adjusted to a value of 13-14 with 6 N NaOH as determined by pH paper and allowed to incubate for 4 hours at 37°C to cleave all aminoacyl and peptidyl-tRNA ester bonds. The solution was then adjusted to pH 5.6-6.0 with glacial acetic acid as judged with pH indicator paper.

#### Recrystallization of Guanidinium Chloride

Practical grade guanidinium chloride was recrystallized twice by a modification of the method of Nozaki and Tanford (58). 1000 g of guanidinium chloride was dissolved in sufficient absolute ethanol at 70°C to give a final volume of 3500 ml. To this solution was added 1 gram of activated charcoal followed 5 minutes later with 1 gram of Celite and the solution filtered while hot through a Whatman 1 filter paper in an 18.5 cm buchner funnel under mild vacuum. Following redissolution of any crystallized material in the filtrate, 120-200 ml of benzene were added to the ethanol until crystals first appeared and remained. This solution was allowed to cool to room temperature and then allowed to stand overnight at 4°C.

Collection of the crystals was accomplished by vacuum filtration in an 18.5 cm buchner funnel. These crystals were then washed with a small amount of ethanol maintained at -20°C, collected and dissolved in a mini-

mum amount of absolute methanol maintained at 68-70°C. Once all the crystals were in solution the solution was allowed to stand at -20°C overnight. The crystals which formed were harvested as described above and dried to constant mass over potassium hydroxide pellets under reduced pressure.

#### Analysis of Peptide Size Distribution

The size distribution of nascent polypeptides was analyzed by the gel permeation chromatographic method described by Fish et al. (59) and by Protzel and Morris (48). Radiolabeled nascent polypeptides derived from peptidyl-tRNA (above) were subjected to gel permeation chromatography under conditions known to render polypeptide chains in a random coil configuration (6.0 M guanidinium chloride, 0.1 M 2-mercaptoethanol, PH 6.5) on Bio-gel A 0.5m agarose.

Approximately 200 ml of the Bio-gel A 0.5m slurry were brought to a final volume of 1000 ml and the slurry was allowed to settle to 50% of the column height of the vessel and particulate material in the upper 50% of the solution was removed by aspiration. This operation was repeated 5 times or until no particulate material could be seen above the slurry at 50% column height. The slurry was then allowed to settle completely, the supernatant decanted and the slurry gently resuspended in a guanidinium chloride solution (at 4°C) equal to twice the packed slurry volume. Once the slurry had settled this procedure was repeated twice or until the density of the supernatant was approximately equal to that of the fresh solution at 4°C. A final addition of 6 M guanidinium chloride solution was added to give a final volume of 400 ml and this suspension was used to prepare the analytical gel column.

The slurry was slowly and continuously poured into a Pharmacia analytical column 100 cm x 1.6 cm fitted with a 500 ml reservoir and containing 15 ml of 6 M guanidinium chloride solution. The slurry was stirred to the bottom of the column to remove any suspension inhomogeneity and, following a 5 minute standing period, the column was allowed to flow under a hydrostatic head of 8 to 10 cm. The outlet was gradually lowered to approximate a constant flow rate until the final operating hydrostatic head of 65-70 cm was reached. The slurry was allowed to continue packing until a bed height of 95 cm had been obtained. The column was washed with 3 column volumes of 6 M guanidinum chloride 100 mM 2-mercaptoethanol solution, pH 6.5. Prior to analysis of any sample, the

The sample prepared for analysis as described above had a final VOlume of 0.5 and 0.7 ml. The sample was made 50 mM in dithiothreitol and sucrose was added to a final concentration of 90 mg/ml. After two hours at room temperature, 50 µl of 3.6% Blue dextran and 50 µl of 0.1% DNP-alanine were added prior to chromatographic analysis to serve as excluded and included volume markers, respectively. The sample was applied at the top of the column under a column of the running buffer by layering the sample onto the bed with a pasteur pipet. The column was developed in the descending direction and 0.9 ml fractions were collected directly into plastic or glass liquid scintillation vials for determination of radioactivity.

## Preparation of Cyanogen Bromide Fragments of Labeled α and β Globin

A check of the calibration properties of the Bio-gel A 0.5 m column as determined by Protzel and Morris (48) was conducted using the 4

cyanogen bromide fragments of α and β globin. L-[14C]-tryptophan

labeled total (α and β) globins were used as a source of the N-terminal α

and β cyanogen bromide fragments and L-[3H]-leucine labeled globin

provided a source of all 4 α and β CNBr fragments. Globin was dissolved

in 70% formic acid at a concentration of 5.0 mg/ml. A 400 fold molar

excess of cyanogen bromide was added and the solution was placed in the

dark for 36 hours at 25°C. Following the incubation period, 15 times the

Original sample volume of water was added and the samples frozen and

lyophilized.

### **Determination of Distribution Coefficients**

Elution data from the size distribution experiments, as determined by Bio-gel A 0.5 m chromatography in 6.0  $\underline{M}$  guanidinium chloride, were treated as described by Fish et al. (59). The distribution coefficient (Kd) was calculated according to the formula:

Kd = (Ve-Vo)/(Vi-Vo)

where We is the mass of solvent which corresponds to the peak concentration of the eluting solute.

Vo is the void volume in mass of solvent.

Vi is the mass of solvent contained within the gel matrix and Column. In this work these parameters were determined in terms of volume instead of mass.

Blue Dextran 2000 was used as a marker for the void volume and dinitrophenylalanine was used to determine the total volume of the column and matrix which was accessible to solvent. In the experiments described herein the location of the blue dextran peak maximum was determined either visually or spectrophotometrically at a wavelength of 637.5 nm in the visible range. The fractions corresponding to the elution maxima of

the DNP alanine were determined spectrophotometrically at a wavelength of 360 nm in the near ultraviolet.

### **Identification** of $\beta_{112}$ (Val/Val) Homozygous Rabbits

Identification of individual rabbits homozygous for the substitution of isoleucine for valine at position 112 of the  $\beta$  globin chain present in the population of white New Zealand male rabbits was determined on the basis of the absence of incorporation of radiolabel (presented as L-[3H]-isoleucine) into purified  $\beta$  globin, with incorporation into  $\alpha$  91 obin polypeptides as a reference.

White New Zealand male rabbit (8-10 pounds) were made mildly anemic With a single injection of 1.5 ml of 2.5% phenylhydrazine prepared as described above. After a four day period approximately 5-10 ml of blood were collected from each rabbit from the marginal ear vein into nalgene Centrifuge tubes containing 200-500 units of heparin sulfate per tube. Subsequent operations were performed at 0-4°C. After the blood was Collected and chilled the tubes were balanced and the cells isolated by Centrifugation at 4000 xg for 10 minutes. The cells were then washed twice by resuspension in Ringer's saline (60) followed by centrifugation at 4000 xg for 10 minutes. Washed, packed cells (1 ml) were then transferred to glass culture tubes containing per tube 5.0 µCi of L-[3H]-ile at a specific activity of 16 Curies/mmole, 0.15 ml of a solution of 10.5 mg/ml ferrous ammonium sulfate in Ringer's saline and 2.85 ml of incubation mixture components. The  $\beta_{112}$  Val/Val incubation mixture contained, per 100 ml total volume, 13.9 ml of 10X amino acid mixture pre-Pared as described by Lingrel and Borsook (53) except that isoleucine was maintained at one tenth the specified final concentration, 30.4 ml Ringer's isotonic saline solution, 1.81 ml of 0.25 M MgCl<sub>2, 10%</sub>

glucose, 18 ml 0.164 M Tris·HCl (pH 7.75), 14.37 ml 1 mM sodium citrate in Ringer's saline (1 mM) and 21.56 ml sodium bicarbonate in Ringer's saline. Cells were suspended in the labeling medium by gentle swirling and allowed to incubate for 60 minutes at 37°C. Following incubation cells were chilled on wet ice and transferred to plastic centrifuge tubes. Ice cold RS (15 ml) was added and the cells were collected by centrifugation at 4000 xg for 15 minutes. Following removal of the supernatant a lysate was prepared by the addition of 4 ml of water, 1.0 mM in glutathione. Cells were incubated on ice with frequent swirling for 10 minutes, followed by removal of cell debris by centrifugation at 17,500 xg for 20 minutes. This supernatant solution was stored at -20°C and subsequently used to prepare globin as described above.

### Rapid Estimation of L-Isoleucine Incorporation by SDS-Gel Electrophoresis

The SDS gel electrophoresis procedure used here is essentially that described by Wood and Schaeffer (61). Hemoglobin solutions prepared as above were made 0.5 to 1 mg/ml in protein. Samples were made 1% in SDS and 2-mercaptoethanol and then heated to 100°C for 3 minutes. The mixtures were dialyzed at room temperature against 0.1 M sodium phosphate buffer, pH 7.2, containing 1% SDS and 0.1% 2-mercaptoethanol. Immediately prior to application of samples to gels a volume of 0.05% bromophenol blue dye in 50% glycerol was added equal to 5% of the sample volume. The electrophoresis buffer was 0.1 M sodium phosphate, pH 7.2, 0.1% in SDS. Gels were composed of 12.5% acrylamide with a bis acrylamide to acrylamide ratio of 1 to 20. The Bis acrylamide solution was prepared prior to use by dissolving 6.072 g of acrylamide and 0.304 g bis acrylamide in the electrophoresis buffer. Following removal of particulate

material by filtration through Whatman 1 filter paper the solution was degassed and TEMED and ammonium persulfate were added to a final concentration of 0.05% each. Disk gel columns were poured in 0.6 x 15 cm silanized glass tubes to a height of 13 cm and allowed to polymerize at room temperature. Pre-electrophoresis of the gels was conducted at room temperature at a current of 2 mA per gel for one hour.

Samples were applied to the gel column in a volume 25-50 µl depending on the number of counts per minutes per microliter available. For these analyses 8,000-10,000 cpm were present in a sample volume of 25 µl. Electrophoresis was conducted at 8 mA per gel for approximately 13 hr or until the marker dye had migrated 12 cm. Cells were stained with cyanin brilliant G stain (62) for 4-8 hr and destained with 0.02% sulfuric acid in water. In this system, the band which migrates farthest toward the anode is a globin as expected for a separation according to molecular weight. For this analysis bands were excised by cutting the gel halfway between the two stained bands and taking gel to a length of 1 cm in both directions. Each gel slice which contained either an  $\alpha$  or a  $\beta$  band was then diced with a razor blade, placed in 0.5 ml 30% H<sub>2</sub>O<sub>2</sub> and incu-40°C for 4 hours. Ten ml of formula C scintillation coctail was then added and the samples counted for radioactivity in a Beckman LS-230 liquid scintillation spectrometer. Formula C scintillation coctail contained in 1 liter, 60.6 g napthalene, 6.06 g 2,5-diphenyloxazole, 0.49 g 1,4-bis[2-(4-methyl-5-phenyloxazolyl)]benzene, 606 ml xylenes and 333 ml Triton X-114. Samples which gave an  $\alpha$  to  $\beta$  cpm ratio of 9:1 or greater were subjected to further analysis by CM-cellose column chromatography as described above for confirmation of the \$112 val/val pheno-Type. Rabbits determined to be of this phenotype were used to prepare reticulocyte lysate cell free protein synthesizing system as described above.

### Preparation of Uniformly Labeled L-[140]-trp Globins

1.0 ml of the β112 Val/Val lysate was incubated with the master mix components as described above and 50 μCi L-[14C]-tryptophan for one hour at 37°C. Following exhaustive dialysis against distilled deionized water, globin was prepared by the dry ice acetone method of Winterhalter and Huehns (56). Precipitated globin was collected by centrifugation as described above, dissolved in Dintzis 1X buffer (see separation of α and β globin chains) and chromatographed on a 2.5 x 90 cm column of Bio-gel P-60 equilibrated in Dintzis 1X buffer to remove a high molecular weight contaminant. The fractions corresponding to the major component of radioactivity (80% of the total cpm eluted) was collected and lyophilized. The globin was redissolved in distilled deionized water, centrifuged at 25,000 xg for 20 minutes and lyophilized. Analysis of this sample by Bio-gel A 0.5 M chromatography in 6 M guanidine hydrochloride, 100 mM 2-mercaptoethanol revealed a single component of average molecular weight corresponding to that expected for the globins.

## Tryptic Peptide Analysis of L-[3H]-Trp-Labeled Nascent Polypeptides

20 ml of lysate and master mix was incubated with 5 mCi of trypto-Phan at an initial specific acitivity of 23 Ci/mmole. Purified nascent Polypeptides derived from polysomal peptidyl tRNA were fractionated as described above by Bio-gel A 0.5 m column chromatography except that every third fraction was counted for radioactivity and the remaining fractions were subjected to tryptic peptide analysis.

### <u>Tryptic Digestion of Nascent Polypeptides</u>

To each Bio gel A 0.5 m fraction of approximately 400  $\mu$ l was added 20  $\mu$ l of a solution containing 1-2 mg/ml uniformly labeled L-[14 $_{\text{C}}$ ]--

trp globins as an internal standard providing radioactivity, as [14c] cpm, to an upper limit of 10% of the [3H] cpm in each sample. To this solution was added sufficient carrier globin chains to bring the total globin mass to 5 mg. This solution was brought to a final volume of 5 ml following the addition of 250 µl of 1 M CaCl<sub>2</sub> and 1 M Tris·HCl (pH 8.3) to give a final concentration of 50 mM CaCl<sub>2</sub> and 50 mM Tris·HCl (pH approximately 8.0) and 1 mg/ml globin. After equilibration of the sample under vacuum at 37°C for 10 minutes, 10 ml of a 4 mg/ml solution of TPCK-trypsin (Worthington) was added to give an initial globin to trypsin mass ratio of 125:1 and allowed to incubate for two hours. Two additional 10 µl additions were made and each addition was followed by a 2 hr incubation period for a total incubation time of 6 hr. The reaction was terminated by the addition of 250 µl of glacial acetic acid. Samples were stored at -20°C until needed for further analysis. Under these digestion conditions, no protein precipitate was apparent.

## Preparation of Bio-gel P-2 (-400 mesh) Column Chromatography Buffer

5 moles (300.3 g) of urea were dissolved in sufficient deionized distilled water to a volume of 900 ml or 90% of the total final volume. Following equilibration of the solution to room temperature, 25 g of Amberlite MB-3 mixed bed ion exchanger was added to effect deionization and the mixture was stirred for 4 hr or until the solution had a conductivity less than 1.5 μMho at 23°C. The resin was removed by filtration through a medium grade fitted glass funnel. The solution was then made 5 mM in 2-mercaptoethanol and sufficient 1 M Tris HCl (pH 8.0) was added to give a final conductivity of 115-120 μMhO. The solution was then brought to a final volume of 1 l, filtered through 0.45 μ millipore membrane

(pore size) and stored at 4°C prior to use. Large batches may be made and frozen at -20°C prior to use. This buffer should not be used if the conductivity exceeds 200 µMho. Each lot of Bio-Gel P-2 (-400 mesh) must be tested for the optimal buffer conductivity for peptide separation.

#### Preparation of Bio-Gel P-2 (-400 Mesh) Analytical Column

Approximately 85 g of Bio-Gel P-2 (-400 mesh) column support material is added to 200 ml of column equilibration buffer with slow stirring until all of the support material is suspended. The suspension is then allowed to stand for 48 hours at 4°C. The support material is then resuspended and fine particulate material was removed following settling of the bulk of the support through 50% of the total column volume. This Procedure is repeated once and in most cases further removal of fine Particulate material is unnecessary. The support material is then resuspended in a final volume of buffer equal to twice the approximate settled gel volume and this suspension was slowly poured down the side of a 1.1 x 100 cm Glenco analytical gel column to a fritted unit with a 500 ml reservoir. Packing was conducted at a hydrostatic head height of 100 cm for 4 hours. At this point excess gel was removed by aspiration to give a final bed height of 95 cm and washing was allowed to continue for 24 hr under a 100 cm hydrostatic head.

## Bio-Gel P-2 (-400 mesh) Chromatography of Tryptic Digestion Products

Following tryptic digestion, samples were flash evaporated to dryness and the residue was dissolved in a minimal volume of distilled deionized water to give a final sample of volume 0.3-0.5 ml. This sample was loaded directly onto a 1.4  $\times$  95 cm column of Bio-gel P-2 (-400

mesh) gel support and eluted with urea/Tris/mercaptoethanol buffer (pH 7.9, 115-120  $\mu$ MhO) at a flow rate of 0.2 ml per minute directly into liquid scintillation vials for a final sample volume of 0.4 ml/vial. Samples were analyzed for [<sup>3</sup>H] and [<sup>14</sup>C] content following addition of 8.0 ml of Formula C liquid scintillation mixture.

#### Construction of the High Pressure Liquid Chromatographic System

A high pressure liquid chromatographic system was designed following an extensive modification of the procedure of Jones et al. (63) to facilitate analysis of the large number of samples encountered in this study. A 1/16" bore 1/4" OD column of length 40 cm fitted at one end with a steel frit and 1/16" OD tubing was used as the column. A Milton Roy (Milton Roy Co., St. Petersburg, Fla.) dual pump system and an oil dia-Phragm pressure gauge (max psi, 2000) were placed on the inlet line of the column system. The column tube was completely filled with dry Pellionex SCX strong cation exchange resin (Reeve Angel Co., Clifton, NJ) by slow pouring of the dry resin in fine granule form with constant Vigorous tapping of the column tubing to insure uniform packing. Once the column had been filled to capacity the inlet lines were purged of air with the initial buffer system (0.05 M pyridinium acetate, pH 4.0), and the inlet fittings attached to the column. Buffer was allowed to percolate through the support under pressure and extensive washing and equilibration of the column was conducted at an inlet pressure of 300 psi at ambient temperature.

# Preparation of Buffers for High Pressure Liquid Chromatography

Pyridine was purified by distillation at one atmosphere pressure

over ninhydrin. To approximately 1.5 l of reagent grade, glass distilled, pyridine in a 2 liter round bottom flask was added 5 g of reagent grade ninhydrin. The flask was fitted to a glass water jacketed condenser and heating mantle and the solution was heated until a mild even boil was achieved. The first 10% (150 ml) of pyridine was discarded and approximately 1200 ml was obtained as a constant boiling fraction at the expected T<sub>b</sub> of 113-116°C. The redistilled pyridine was stored at room temperature in ground glass bottles wrapped in aluminum foil to exclude light.

The initial gradient eluent was prepared by adding 4.0 ml of pyridine to 900 ml degassed deionized distilled water which had undergone millipore filtration over a 45  $\mu$  membrane. The pH of the solution was then adjusted to 4.0 with glacial acetic acid and the volume brought to 1 liter in a volumetric flask. The limit gradient eluent was prepared by adding 160 ml of pyridine to 800 ml water. The pH was then adjusted to 6.0 and the volume brought to 1 liter.

# High Pressure Liquid Chromatographic Analysis of Tryptic Digestion Products

Following tryptic digestion, samples were flash evaporated to dryness and then brought to a final volume of 120 ml with distilled deionized water. Following adjustment of the pH to a value of 3.5 with 91 acial acetic acid, the preparation was pumped onto a 0.15 x 40 cm column of Pellionex strong cation exchanger previously equilibrated with 0-05 M pyridinium acetate, pH 4.0, at an inlet pressure of 200-300 psi.

Following a wash cycle of 5 minutes (two column volumes), elution was effected with a convex gradient generated by a series arrangement of two chambers containing 40 ml each of 0.05 M pyridinium acetate, pH 4.0, followed by a single chamber containing 40 ml of 2.0 M pyridinium acetate, pH 6.0 in a chamber rectangular Varigrad gradient mixer.

Fractions (2.0 ml) were collected directly into liquid scintillation vials and counted for [3H] and [14C] radioactivity content following addition of 10 ml of Formula C scintillation fluid.

# Qualitative Analysis of Tryptic Digest Products - Removal of Urea from the Bio-gel P-2 Resolved [3H]-Tryptophan-Labeled Tryptic Peptides

Fractions corresponding to individual peaks of radioactivity eluting

from the Bio-Gel P-2 (-400 mesh) analytical column were pooled and the

salts and urea present were removed by chromatography of the peptides on

a O.9 x 20 cm column of Bio-Gel P-2 (100-200 mesh) equilibrated with 0.2

M ammonium bicarbonate pH 7.0. These fractions were later used to

establish the identity of the components isolated by the analytical

Bio-Gel P-2 (-400) urea column.

Individual components obtained above as well as from the high

Pressure liquid chromatographic analysis of the tryptic digests were

Collected and lyophilized to dryness.

# Identification of Resolved L-[3H]-Tryptophan-Labeled Tryptic Digestion Components

 $\hbox{Identification of the resolved components of the tryptic digestion} \\ \hbox{$^{11}$ $$\times$ tures on each analytical system was accomplished by analysis via:}$ 

- 1. Tryptic digestion of L-[ $^{14}$ C]-tryptophan-labeled  $\alpha$  or  $\beta$  globins (prepared by CM-cellulose chromatography) with [ $^{3}$ H]-L-trp-labeled  $\alpha$  and  $\beta$  globins.
- 2. Paper chromatography of resolved [ $^3$ H]-tryptophan-labeled peptides from each analytical system with standards of [ $^{14}$ C]-tryptophan-labeled  $\alpha$  and  $\beta$  globin tryptic peptides by the method of Hunt, Hunter and Munroe (64).

# Paper Chromatographic Analysis of Resolved Tryptophan-Labeled β Globin Tryptic Digestion Products

Lyophilized samples from the high pressure liquid chromatographic system or the P-2/urea system after removal of urea were dissolved in a minimal amount of water and spotted onto a 50 x 8 cm strip of Whatman 3 mm chromatography paper. These chromatograms were equilibrated over the organic phase of a mixture of n-Butanol, pyridine, glacial acetic acid and water (90:120:18:72, volume ratios) for 24 hours. The chromatograms were developed in the decending direction with the aqueous phase of the above solvent mixture. Chromatograms were dried for 24 hours at room temperature. The sample lanes were cut into approximately 100 strips, which were of 0.5 cm length in the direction of chromatography and 1.0 cm wide. These strips were placed in liquid scintillation vials, with 5 ml formula C liquid scintillation coctail and the radioactivity determined.

# Calibration of the Bio-gel P-2/Urea Chromatographic System for Double Isotope Analysis

Calibration of the Bio-gel P-2/urea chromatographic system for double isotope analysis was accomplished by standard methods. The column

was run for 48 hours without a sample present and then 30 blank 0.4 ml fractions were collected into plastic liquid scintillation vials. Nitromet hane was used as the quenching agent and 5 sets of triplicate points reflecting quench produced by 0, 2, 4, 6, 8 µl of nitromethane on 9,880 dpm of [14c]-toluene and 126,000 dpm of [3H]-toluene were analyzed, after addition of 8 ml Formula C, by the method of automatic external standardization as described in the Beckman LS-230 handbook (65b). Quench was found to increase slightly as a function of time in plastic vials but sample homogeneity was maintained and the progressive increase in quench followed the quench dependence with external standard value throughout a 72 hr counting period.

### Calibration of the HPLC System for Double Isotope Analysis

Since sample volume and pyridine and acetate concentrations change continuously due to generation of a gradient of eluent concentration and PH, a special calibration procedure was developed to account for the effect of the changing sample composition during elution. A sham run of the HPLC system was performed except no radioactive sample was included. To alternate samples in plastic vials containing 1.0 ml formula C were then added alternately either [3H]-toluene (1.26 x 105 dpm) or [14C]-toluene (9.88 x 103 dpm) and the S value was correlated with the quench caused by the increasing concentration of the eluent components. This relationship was found to be linear for [14C] and [3H] quench and [14C] spill into the [3H] channel over the entire range of S values encountered and was not identical to nitromethane calibration samples containing either initial or limit gradient buffers. Quench and in increased slightly with time for plastic vials as compared with

glass but followed the initially determined quench dependence with external standard S value for 72 hr. Decreasing S values diverged from the dependence with quench established after this time period due to extensive change in sample composition because of sample permeation of, and evaporation from the plastic vials. This deterioration of the sample necessitated determination of radioactivity within 48 hr of sample preparation.

# Separation of the Different Polysomal Size Classes by Sucrose Density Gradient Centrifugation

Polysome profiles were prepared on linear 15-50% sucrose gradients in Buffer A of Lodish et al. (66), which contained 100 mM Hepes (pH 7.0 at 22°C), potassium chloride and magnesium acetate. Gradients were poured from a two chamber (20 ml each) gradient mixer with 17 ml of 50% sucrose in the proximal chamber and 19 ml of 15% sucrose in the distal chamber. Gradients were poured at 4°C and used within 12 hr of preparation.

2X Buffer A was prepared (at twice the concentration specified by Lodish et al.) with distilled deionized diethylpyrocarbonate treated water. To 450 ml of water was added 5.96 g Hepes (hydroxymethyl piperazine 2-ethane sulfonic acid) 3.73 g potassium chloride and 0.429 g magnesium acetate. The pH was adjusted to 7.0 at 22°C. The final concentration of Hepes, potassium chloride and magnesium acetate were 0-05 M, 0.10 M and 0.004 M, respectively.

The initial gradient material was prepared by adding 15 g of ultraPure sucrose to 50 ml 2X Buffer A, and this mixture was brought to a

Volume of 95 ml and agitated until the sucrose dissolved. Following

Solution of the sucrose, 25 mg of cycloheximide, 5.0 mg sparsomycin

and 205  $\mu$ l of a solution of 9.74 mg/ml globin was added. The volume was then brought to 100 ml and filtered through a disposable 22  $\mu$  (pore size) millipore membrane prior to use. The limit gradient material was prepared as above except 50 g of sucrose was used.

#### Results

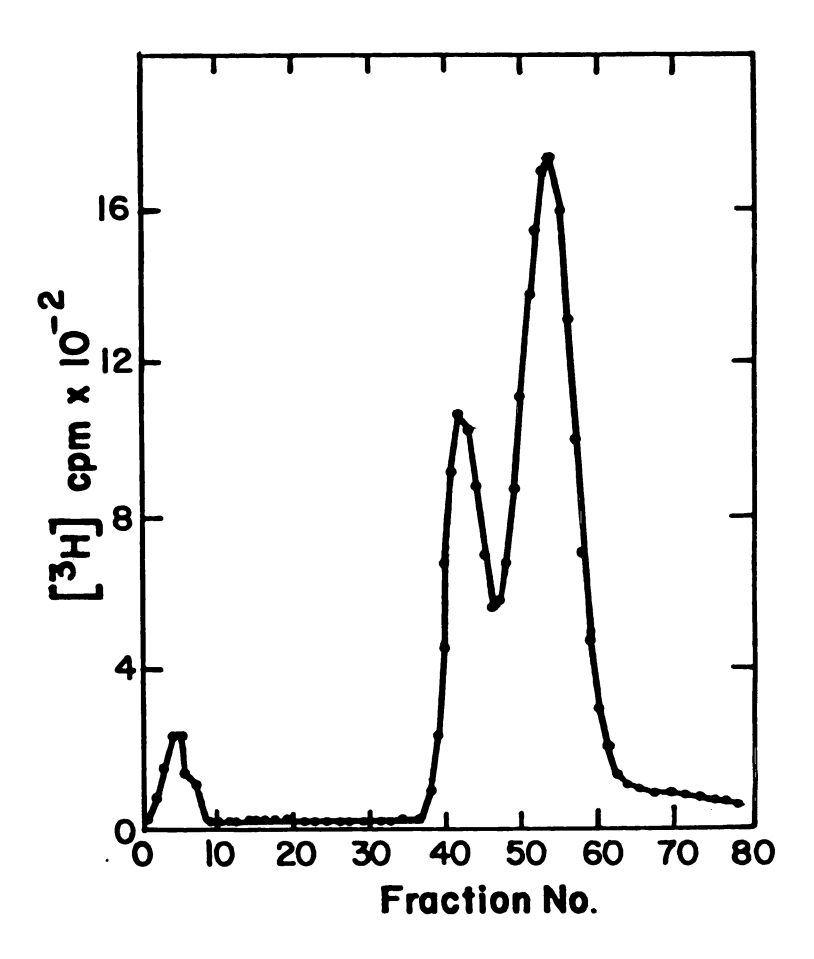
#### Analysis of the Products of the Reticulocyte Lysate System

Incubation of lysate derived from rabbit reticulocytes in the presence of hemin, GTP, ATP, creatine phosphate and creatine phosphokinase and supplemented with potassium and magnesium resulted in rapid incorporation of [ $^3$ H]-labeled tryptophan or leucine into TCA precipitable material. To ascertain that this TCA precipitable material was in fact authetic  $\alpha$  and  $\beta$  globin polypeptides, analysis of the post ribosomal supernatant was conducted. Globin polypeptides, labeled in the cell free system as described in methods, were prepared by the acid-acetone method of Winterhalter and Huehns ( $^5$ 6) and chromatographed in a CM-cellulose column as described by Dintzis ( $^5$ 5). The results of this procedure are illustrated in Figure 1. It can be seen that over  $^9$ 7% of the total cpm eluted from the column as expected for authentic  $\alpha$  and  $\beta$  globins. Recovery was typically  $^8$ 0- $^9$ 0% of the imput cpm. Very little material was found to elute in the void volume or at high ionic strength at the end of the elution program.

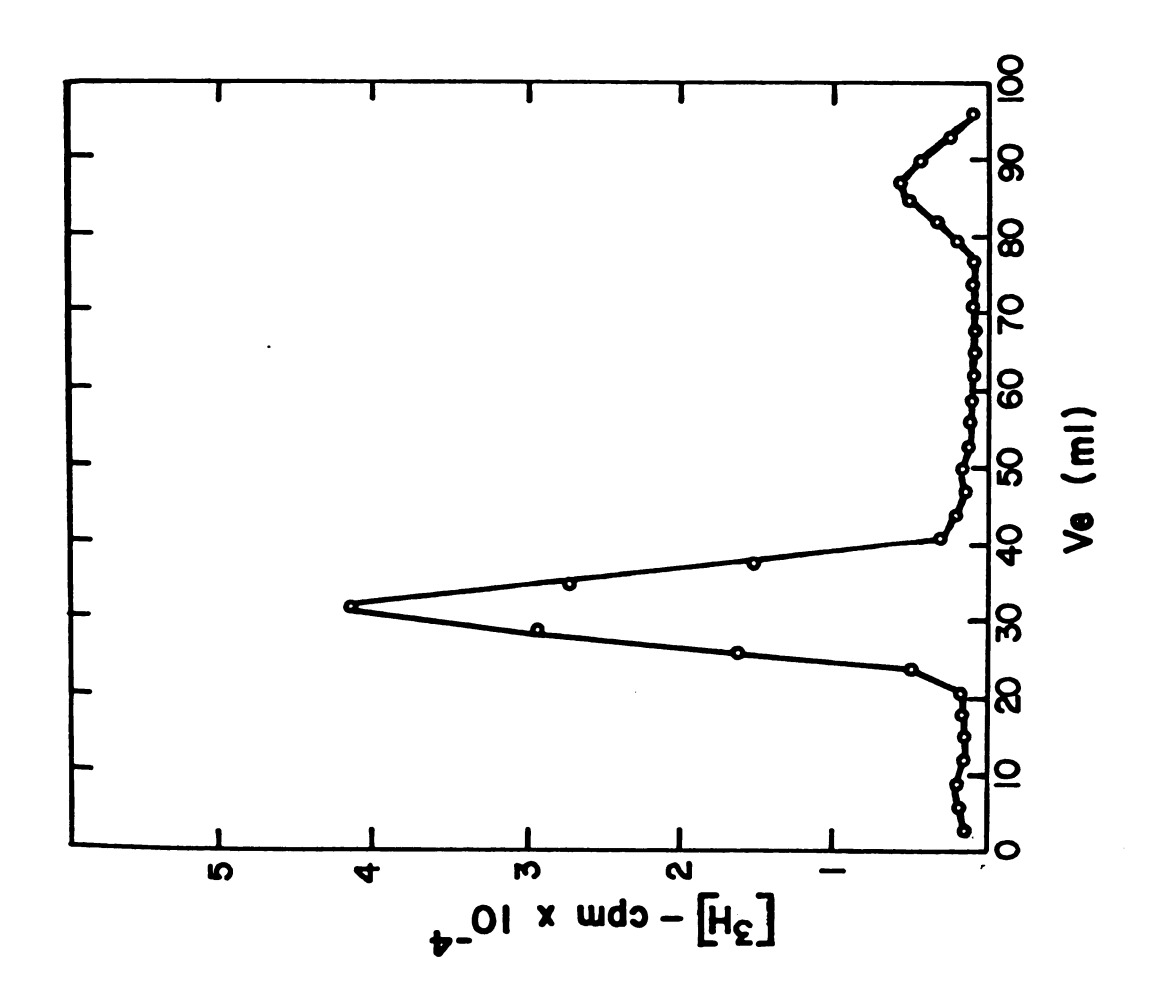
### Incorporation of Radiolabeled Amino Acids into Peptidyl-tRNA

Incubation of 1 ml of the lysate and master mix components (above) in the presence of 100  $\mu$ Ci of [ $^3$ HC]-tryptophan resulted in the incorporation of approximately 0.8-1.0 x 10 $^6$  cpm into purified peptidyl--tryptophan resulted in the incorporation of approximately 0.8-1.0 x 10 $^6$  cpm into purified peptidyl--tryptophan resulted in the incorporation of approximately 0.8-1.0 x 10 $^6$  cpm into purified peptidyl--tryptophan resulted in the incorporation of approximately 0.8-1.0 x 10 $^6$  cpm into purified peptidyl--tryptophan resulted in the incorporation of approximately 0.8-1.0 x 10 $^6$  cpm into purified peptidyl--tryptophan resulted in the incorporation of approximately 0.8-1.0 x 10 $^6$  cpm into purified peptidyl--tryptophan resulted in the incorporation of approximately 0.8-1.0 x 10 $^6$  cpm into purified peptidyl--tryptophan resulted in the incorporation of approximately 0.8-1.0 x 10 $^6$  cpm into purified peptidyl--tryptophan resulted in the incorporation of approximately 0.8-1.0 x 10 $^6$  cpm into purified peptidyl--tryptophan resulted in the incorporation of approximately 0.8-1.0 x 10 $^6$  cpm into purified peptidyl--tryptophan resulted in the incorporation of approximately 0.8-1.0 x 10 $^6$  cpm into purified peptidyl--tryptophan resulted in the incorporation of approximately 0.8-1.0 x 10 $^6$  cpm into purified peptidyl--tryptophan resulted in the incorporation of approximately 0.8-1.0 x 10 $^6$  cpm into purified peptidyl--tryptophan resulted in the incorporation of approximately 0.8-1.0 x 10 $^6$  cpm into purified peptidyl--tryptophan resulted in the incorporation of approximately 0.8-1.0 x 10 $^6$  cpm into purified peptidyl--tryptophan resulted in the incorporation of approximately 0.8-1.0 x 10 $^6$  cpm into purified peptidyl--tryptophan resulted in the incorporation of approximately 0.8-1.0 x 10 $^6$  cpm into purified peptidyl--tryptophan resulted in the incorporation of approximately 0.8-1.0 x 10 $^6$  cpm into purified peptidyl--tryptophan resulted in the incorporation of approximately 0.8-1.0 x 10 $^6$  cpm into

CM-Cellulose chromatographic analysis of  $\alpha$  and  $\beta$  globin polypeptides. The order of elution is (from left to right)  $\alpha$ ,  $\beta$ . L-[ $^3$ H]-leucine (——). Figure 1

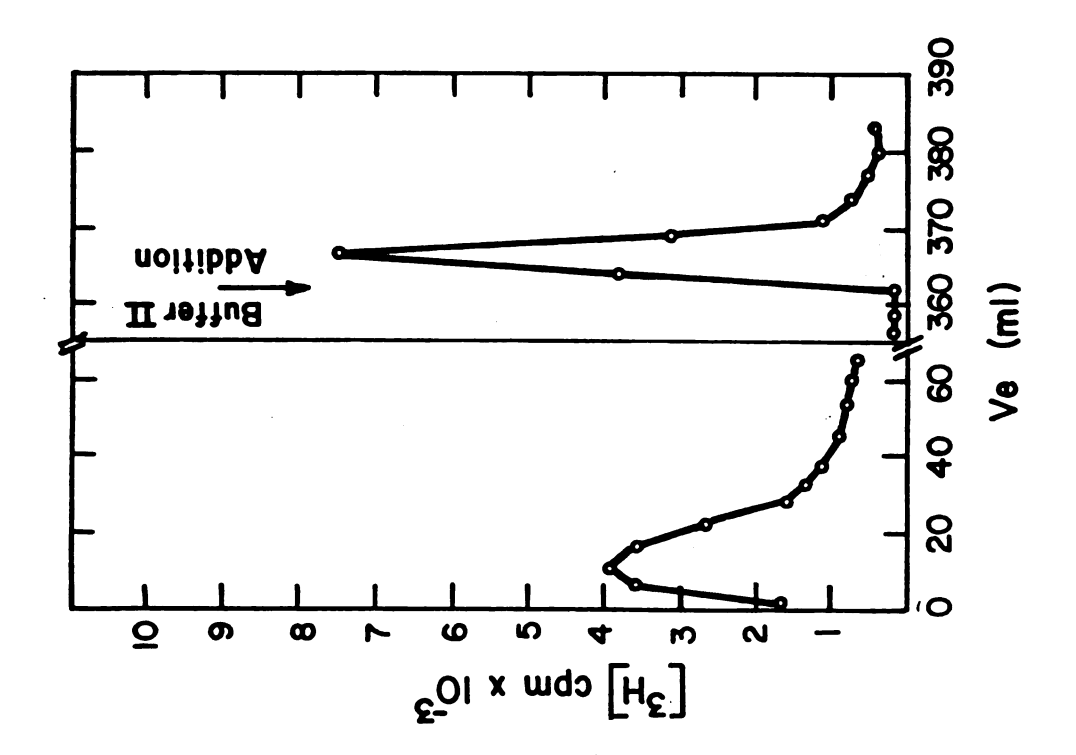


the purification (DE-52 chromatography). The included volume corresponds to contaminating Void volume fractions containing radioactivity were pooled and used in the next step of Elution behavior of L-[ $^3$ H]-tryptophan-labeled peptidyl tRNA on a Bio-gel P-10 column. salts and radioactive amino acids. Figure 2



void volume. Adsorption of the void volume fractions onto a column of DE-52 anion exchange cellulose followed by extensive washing removed all detectable contaminating globin resulting in the elution of a radiochemically pure fraction of peptidyl tRNA plus aminoacyl-tRNA corresponding to a 60-80% yield on the basis of cpm obtained from the Bio-gel P-10 step (Fig. 3). Subsequent concentration over a UM-2 ultrafiltration membrane resulted in 5-10% loss of cpm to the membrane surface while no more than 2-3% was ever detected in the ultrafiltrate. This resulted in overall yields with respect to total radioactivity from the P-10 chromatographic step consistently greater than 55% but rarely higher than 75%. Radioactivity which was associated with the ultrafiltration membrane was not removed by immersion in 6 M guanidinum chloride for 1 hour at 4°C and hence seemed to be tightly bound to the membrane or associated with the membrane in such a way that the solvent could not come into contact with the bound radioactivity. It is unlikely that this loss of material represents a nonrandom loss of peptidyl tRNA since very heavily labeled material obtained from a 5 mCi labeling of peptidyl tRNA and subsequently concentrated on a small (0.8 ml) DE-52 column was subjected to size distribution analysis by Bio-gel A 0.5m column chromatography directly (without ultrafiltration) and this material gave essentially the same size distribution profile as an aliquot of the same sample which was further concentrated by ultrafiltration.

Fractionation of tryptophan-labeled nascent polypeptide material derived from peptidyl tRNA was accomplished on a Bio-gel A 0.5 m column equilibrated with 6 M guanidinum chloride 100 mM 2-mercaptoethanol as



tides labe
shascent
lat Kd valinsertion
and the se
reacer may
referred t
previously
and sinasc
independen
This is to
the nascer
solypeptic

described

acids which

ile to a r

xlypeptic

ine mixed

; componer

incub

n'th cyano

ition have

described in methods. Figure 4 shows a size distribution analysis of L-[ $^{3}$ H]-tryptophan-labeled nascent peptides representing  $\alpha$  nascent peptides labeled once, at the single tryptophan residue al4 and a mixture of  $\beta$  mascent peptides labeled once ( $K_d$  values greater than .55) or twice (at Kd values less than 0.55) with L-[3H]-tryptophan. The point of insertion of the first  $\alpha$  and  $\beta$  tryptophan residues occurs at Kd 0.76-0.80 and the second ß tryptophan residue is encountered at Kd 0.55-0.60. The reader may refer to Figure 5 for the locations of the key amino residues referred to in this work. Analyses of this type have been conducted previously by other workers (48,49) and characterization of such mixed a and 8 mascent peptide size distributions was found to be essentially independent of the choice of amino acid used to perform the labeling. This is true to the extent that the different amino acids used to label the nascent peptides have similar distributions and frequencies along the Polypeptide sequences for the  $\alpha$  and  $\beta$  globins. However, labeled amino acids which are chosen to strongly weight one globin chain over the other due to a relatively high frequency of occurrence of that residue in one Polypeptide would be expected to enhance either the  $\alpha$  or  $\beta$  components of the mixed profile, and effect a qualitative change in the profile if the Components differ from the β components.

### Calibration of the Bio-gel A 0.5 m Column

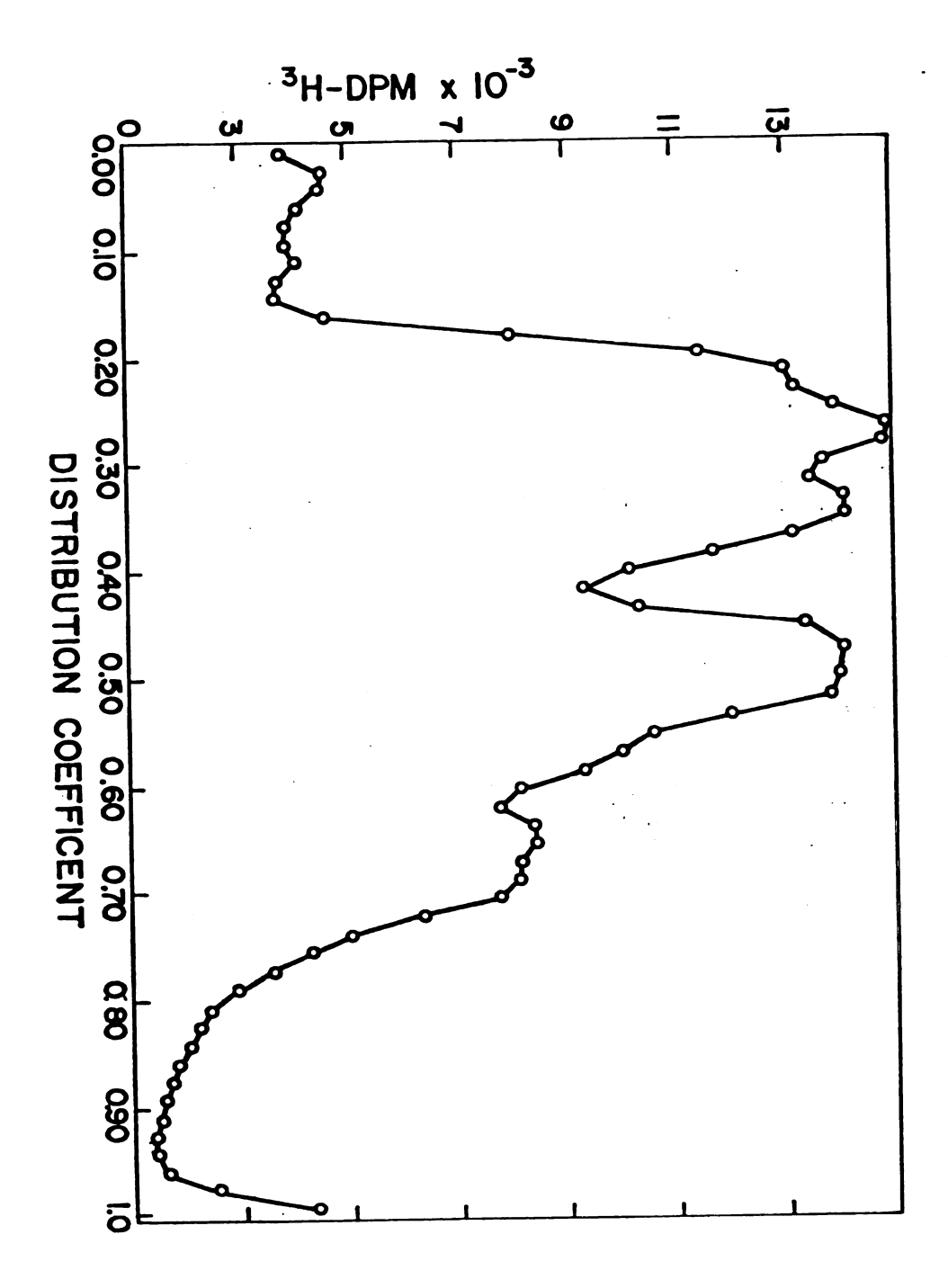
Incubation of either [14C]-Trp globins or [3H]-Leu globins

with cyanogen bromide results in the two sets of molecular weight markers

which have been used in calibration of the analytical gel column for the

0.00 0.10

A nascent polypeptide elution profile of L-[3H]-tryptophan-labeled nascent polypeptides from a Bio-gel A 0.5 m column following hydrolysis of the tRNA ester linkage of the peptidyl tRNA. Figure 4



bromide c found only of the glo designate the unread labeled a of the a and ident [-[<sup>3</sup>H]-le ents. Th and provi tiqures 6 [-[3H]-Le Sictin ma Eio-gel A expected

relations

€3.333

ierce of

Plation:

sis of t

equation

Cope and

<sup>?</sup>₹°č⊑ete

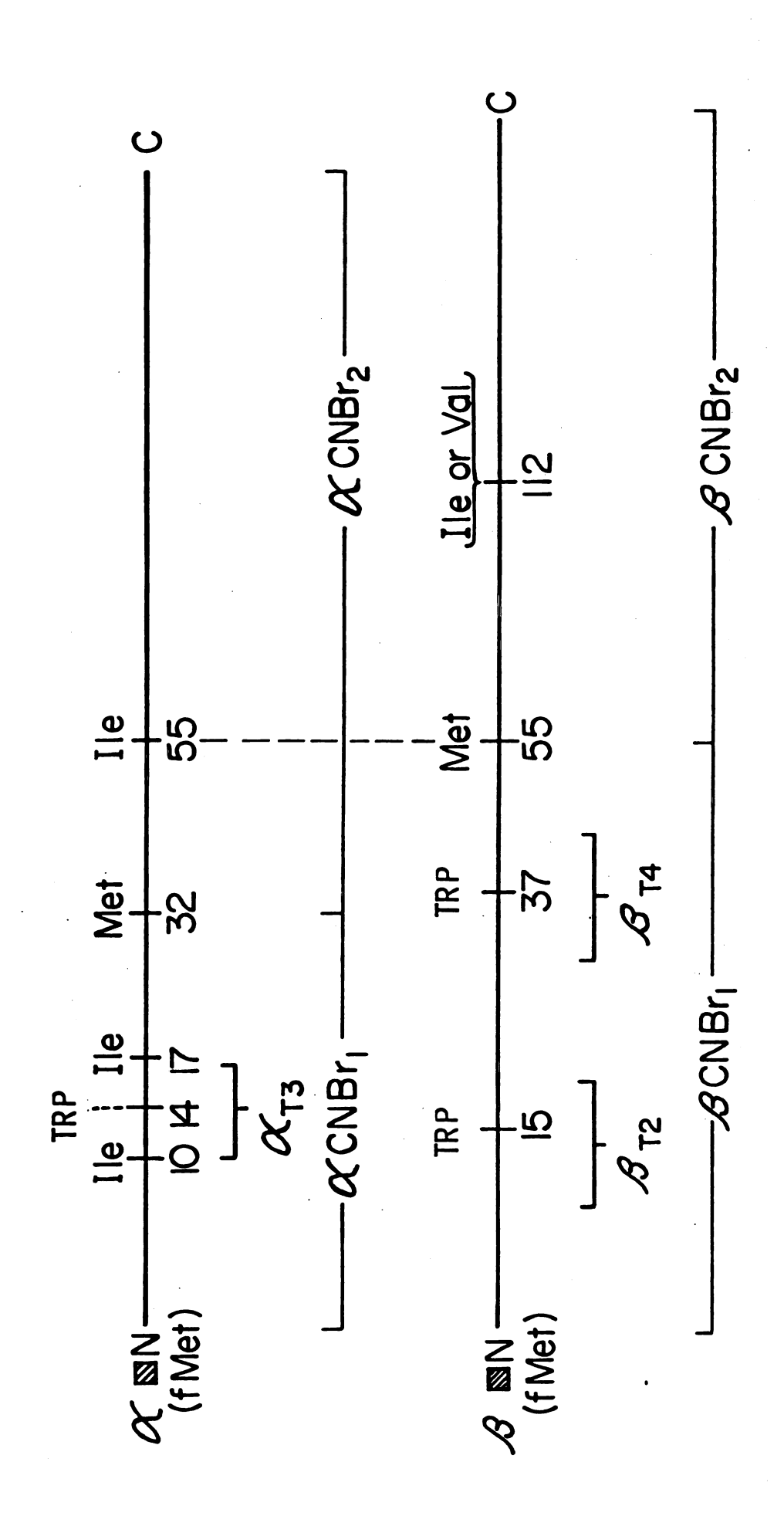
relationship between molecular weight and elution volume. Since cyanogen bromide cleaves the polypeptide backbone at methionine residues which are found only once in each of the  $\alpha$  and  $\beta$  globin chains (Fig. 5), incubation of the globins with this reagent results in the production of 4 fragments designated aCNBr1,2 and BCNBr1,2. An additional marker corresponding to the unreacted  $\alpha$  and  $\beta$  globins is also present. The use of [140]-trplabeled  $\alpha$  and  $\beta$  globin results in two labeled cyanogen bromide fragments of the  $\alpha$  and  $\beta$  globin ( $\alpha$ CNBrl,  $\beta$ CNBrl) facilitating their identification and identification of the two C terminal fragments present in the L-[3H]-leucine-labeled globin digest which elute as unresolved components. These products were used to check the calibration of new columns and provide a comparison with calibration parameters obtained previously. Figures 6 and 7 show the positions of the L-[14c]-trp and L-[ $^3\text{H}$ ]-Leu labeled cyanogen bromide derived fragments from  $\alpha$  and  $\beta$ globin markers respectively as eluted during a calibration run of the Bio-gel A 0.5 m analytical column. The markers are found to elute in the expected order as demonstrated by Protzel and Morris (48) and the dependence of molecular weight with the elution volume was found to obey the ralationship of  $Kd^{0.333}$  vs.  $MW^{0.555}$ . Linear regression analy-Sis of the data shows that the points are well represented by the linear equation:

$$Kd^{0.333} = (-2.00869 \times 10^{-3}) \text{ MW}^{0.555} + 1.02576 \quad r = -0.996$$

Protzel and Morris (48) and Chaney and Morris (49) and represent the

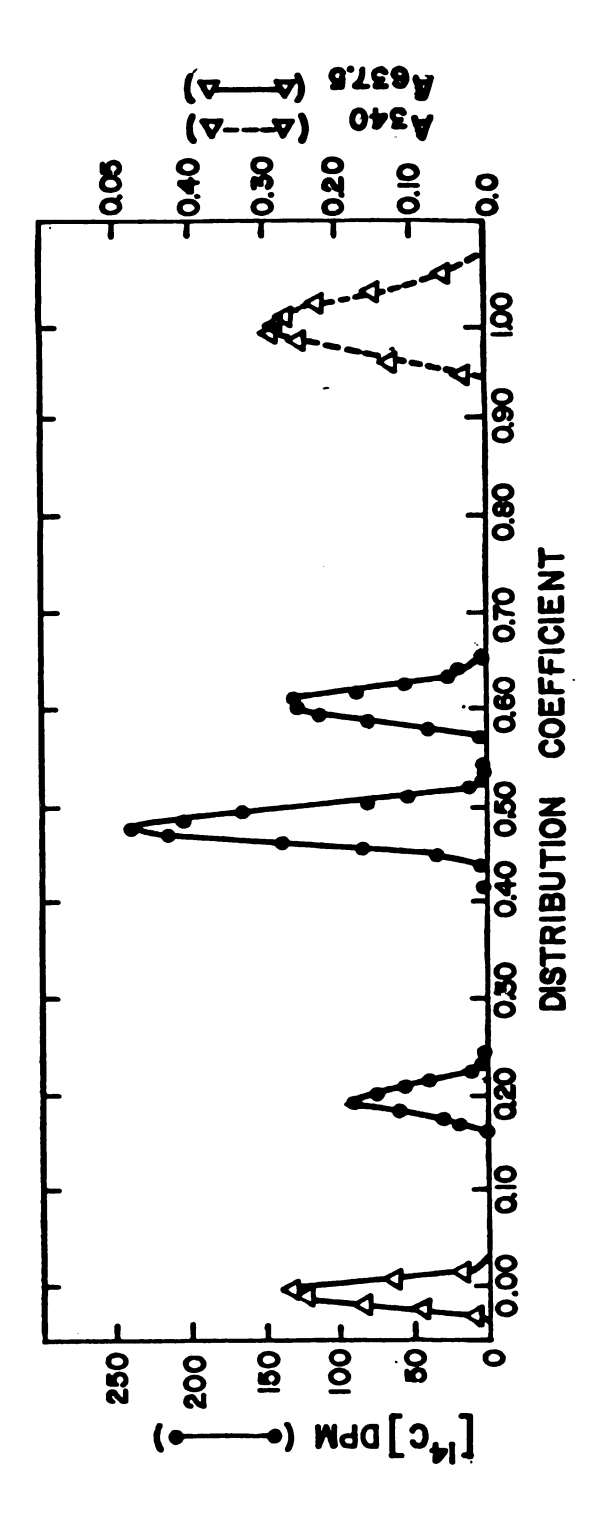
The peptides obtained by cleavage of the  $\alpha$  and  $\beta$  methionine residues by cyanogen bromide The location of selected amino acid residues in the  $\alpha$  and  $\beta$  globin polypeptide sequence. are indicated. Figure 5

Location of Selected Residues in Rabbit Globin



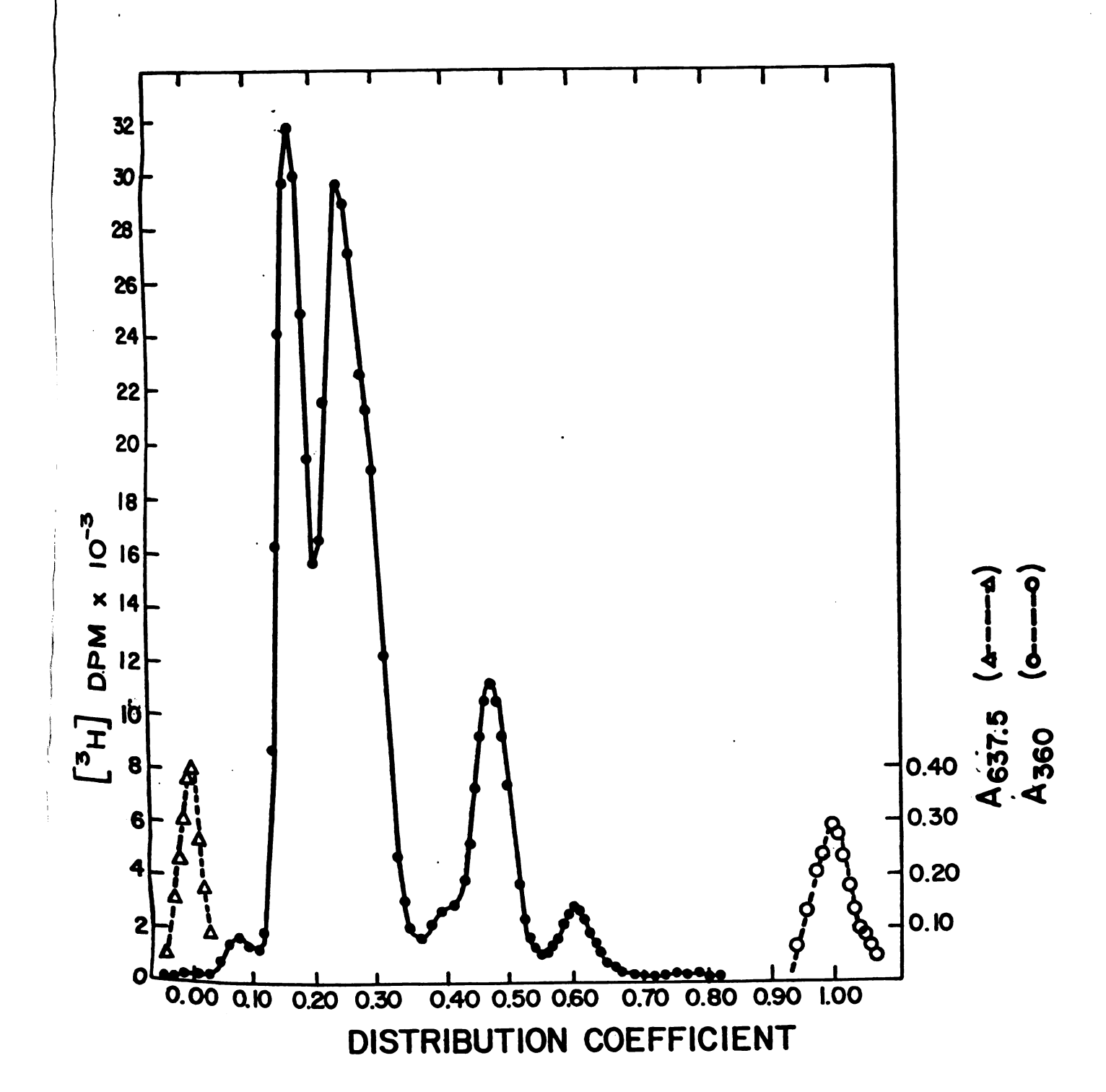
	Γ				
	1				
	}				
	!				
					:
					!
7					
	_				

N-terminal, [ $^{14}$ C]-tryptophan-labeled, cyanogen bromide peptides  $\alpha$ CNBr1 and  $\beta$ CNRr1 and Calibration of the Bio-gel A 0.5 m analytical gel column was accomplished with the 2 respectively. The order of elution is (increasing Kd) blue dextran, globin, gCNBrl, globin. Dinitrophenylalanine and blue dextran mark the included and void volumes,  $\alpha CNBrl$ , dinitrophenylalanine. Figure 6



;				

Calibration of the Bio-gel A 0.5 m column was reexamined in a subsequent analysis using (increasing Kd) blue dextran, globin, aCNBr2 and BCNBr2 (partially resolved), BCNBr1, the four L-[ $^3 ext{H}$ ]-leucine labeled cyanogen bromide peptides. The order of elution is  $\alpha CNBrl$ , dinitrophenylalanine. Figure 7



allows senting profile m21A mo

### <u>Icentif</u>

size.

In tide si due to accepted polymor the onl

tana. screens

[-[34].

incorpo

results

the a c

3:1/2 o

iinaliy

isoleuc

allows determination of the mean molecular weight of the regions representing maxima and minima in the nascent peptide size distribution profile and at the same time allows alignment of the position, on a given mRNA molecule, of a ribosome carrying a nascent polypeptide chain of that size.

### Identification of Homozygous $\beta_{112}$ Val/Val Rabbits

In order to determine which components of the mixed mascent polypeptide size distribution were due to  $\alpha$  nascent polypeptides and which are due to β nascent polypeptides, several experimental approaches were adopted. The discovery by Shamsuddin et al. (65) of a rabbit ß globin polymorphism which results in the substitution of a valine residue for the only g globin isoleucine residue providing an opportunity to directly determine the  $\alpha$  globin nascent polypeptide size distribution from a L-[ $^{3}$ H]-isoleucine labeled radiochemically pure population of  $\alpha$  peptidyl tRNA. To obtain a reticulocyte lysate of this type requires the use of a screening procedure to assess the ability of rabbit reticulocytes to incorporate L-[3H]-Ile into  $\beta$  globin chains as compared to incorporation into the three  $\alpha$  ile position of the  $\alpha$  chain. Three types of results were expected. Homozygous  $\beta_{112}$  Ile/Ile rabbits should reflect levels of Ile incorporation into the  $\alpha$  and  $\beta$  globins giving a value of 3:1 for the observed  $\alpha/\beta$  ratio. Heterozygotes in which half of the  $\beta$  chains are of the phenotype  $\beta_{\mbox{\scriptsize 112}}$  Val would give a value of 3:1/2 or 6:1 for the extent of labeling of  $\alpha$  relative to  $\beta$  globin. Finally, the homozygous  $\beta_{112}$  Val/Val phenotype should exhibit no isoleucine labeling of the ß globin compared to normal levels of

'so'eucine screening each rabbi time label Schaeffer . ratio of  $\alpha$ 1. Diffic statter in tise value espected v ed 6 shou .-.<sup>3</sup>--]-ile Mether the itims the i "ternal st inst the ch tat virtua :;'ooin c : the pher intein sy: 'I both 1

istes: um

Simult Figl.Ile

Verella V

isoleucine incorporation (3 residues) into  $\alpha$  globin. Since the usual screening method involving CM-cellulose chromatography of the globin from each rabbit, a procedure involving preliminary screening of the isoleucine labeled globin samples by SDS gel electrophoresis as described by Schaeffer et al. (61) was adopted in order to expedite the analyses. The ratio of a to B labeling with isoleucine for 8 rabbits is shown in Table 1. Difficulty in accurately counting the gel pieces accounts for the scatter in the values for  $\alpha/\beta$  obtained here as compared to the more precise values obtained from CM-cellulose chromatography which reflect the expected values of 3:1, 3:0 and 6:1. These data indicated that samples 4 and 6 should be further analyzed by CM-cellulose chromatography for L-[3H]-ile incorporation into the  $\alpha$  and  $\beta$  globin chains to establish whether these samples are from  $\beta_{112}$  Val/Val homozygotes. Figure 8 shows the results of CM-cellulose chromatography of these samples. An internal standard of [140]-Trp-labeled globins was included to insure that the chromatographic system was working properly. It can be seen that virtually all of the radioactive tritium present comigrates with the  $^{\alpha}$  globin chains in both samples, confirming an assignment of both rabbits to the phenotype of homozygous Val/Val ß112. A cell-free reticulocyte protein synthesis system was prepared from pooled blood samples obtained from both rabbits as described in materials and methods.

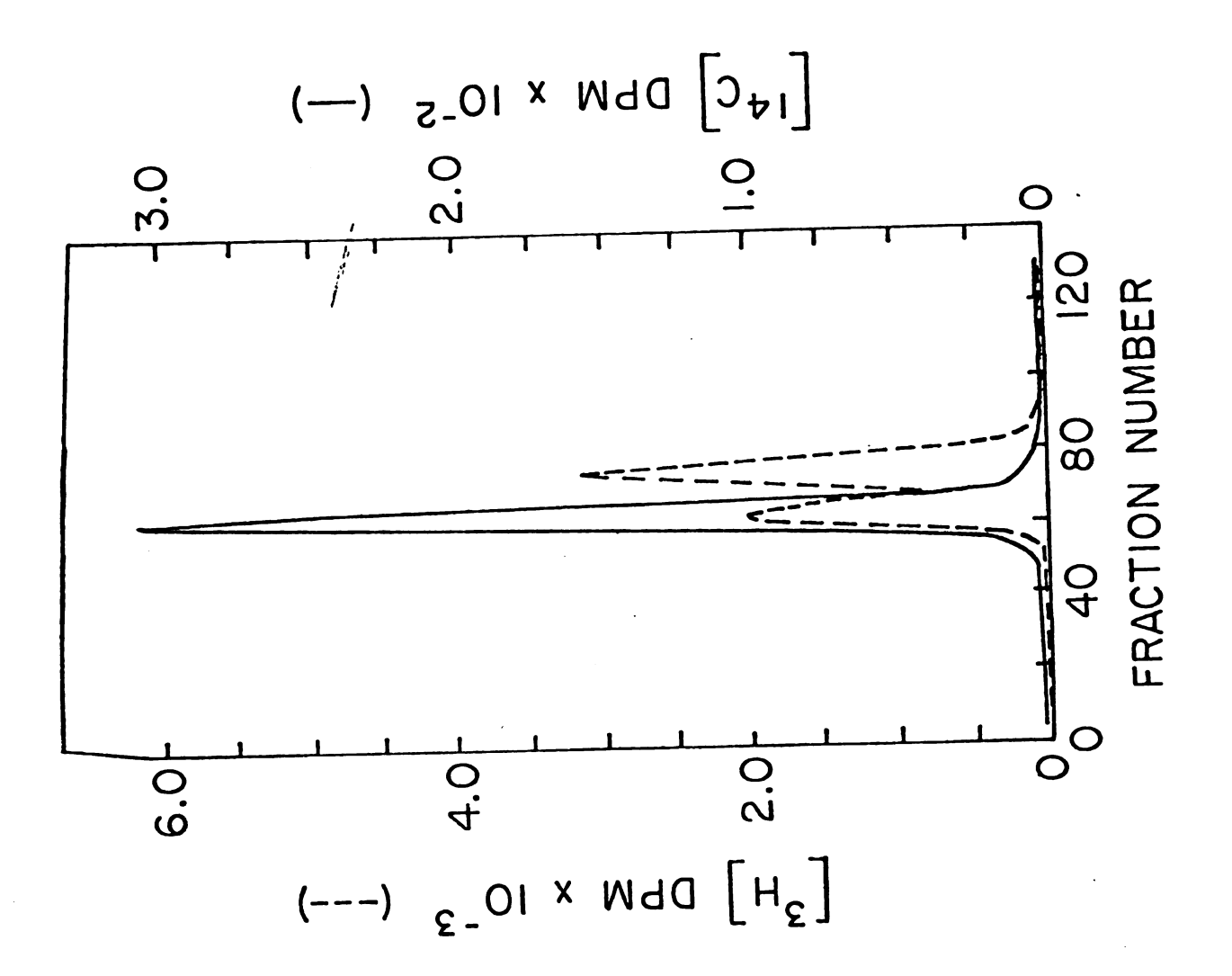
# Assessment of $\alpha$ and Total Globin Synthetic Requirements for Potassium and Magnesium

Simultaneous analysis of the rate and extent of incorporation of  $^{L-}$ [14C]-Ile and  $^{L-}$ [3H]-Leu into TCA precipitable material produced by a  $^{by}$  a  $^{B}$ 112 Val/Val lysate system as a function of  $^{Mg^{++}}$  and  $^{K^{+}}$ 

Sample No.	Cpm(a)	Cpm(ß)	Ratio(α/β)	
1	1506	494	3.0	
2	1340	618	2.2	
3	976	157	6.2	
4	2750	228	12.1	
5	1350	185	7.3	
6	935	103	9.1	
7	1257	<b>37</b> 8	3.3	
8	1893	289	6.6	

included as internal standards for comparison. The B112 Val/Val phenotype renders the B CM-cellulose chromatography of globins labeled with L-[ $^3$ H]-isoleucine in a homozygous globin polypeptide without isoleucine. The order of elution is  $\alpha,\;\beta$  (left to right). ß112 Val/Val reticulocyte lysate. L-[ $^{14}\mathrm{C}$ ] tryptophan labeled  $\alpha$  and ß globins are Figure 8

 $[^{3}H]$  (---),  $[^{14}C]$  (----).



wes carrie

I<sup>†</sup> require sizilar or

for the de

o([140]-is

the Mg++ c

140 rM KAC

into a and

concentrat

These

ight for (

inference

the reticu

iteling

Spec

15 yearnes

rith L-[3

im pepti

ictording ध्यांlibra

Je stre

inmo in

^àri⊑a ar

it the

:<sup>jj‡ju</sup>ent

was carried out in order to ascertain whether the optimal Mg<sup>++</sup> and K<sup>+</sup> requirements for  $\alpha$  synthesis and total ( $\alpha$  and  $\beta$ ) synthesis were similar or different. The result of such an assay is shown in Figure 9 for the dependence of the rate of incorporation of radioactivity into  $\alpha([^{14}C]$ -isoleucine label) and total ( $[^{3}H]$ -leucine label) globin on the Mg<sup>++</sup> concentration in the presence of a final concentration of 140 mM KAc. Figure 10 shows the dependence of incorporation of label into  $\alpha$  and total globin on K<sup>+</sup> concentration at the optimal Mg<sup>++</sup> concentration.

These studies indicate that the optimal concentrations of K<sup>+</sup> and Mg<sup>++</sup> for  $\alpha$  and total globin synthesis are indentical and that by inference the optima for  $\beta$  synthesis cannot be significantly different in the reticulocyte lysate.

#### <u>Labeling of $\beta_{112}$ (Val/Val) $\alpha$ Polysomes with L-[3H]-isoleucine</u>

Specific labeling of  $\alpha$  peptidyl-tRNA on  $\alpha$  globin mRNA programmed polysomes was accomplished by incubation of the  $\beta_{112}$  val/val lysate with L-[3H]-isoleucine. Peptidyl-tRNA was prepared as described above and peptidyl tRNA derived nascent polypeptide chains were fractionated according to molecular weight on a calibrated Bio-gel A 0.5 m column equilibrated with 6 M guanidinium chloride and 100 mM 2-mercaptoethanol. The size distribution of radiochemically pure  $\alpha$ -nascent polypeptides is shown in Figure 11. Table 2 lists the positions of the accumulation maxima and minima for the  $\alpha$  globin nascent polypeptides. It can be seen that the size distribution is nonuniform and is comprised of at least 7 components exclusive of the peak at Kd = 1 (derived from aminoacyl tRNA).

The dependence of the  $\alpha$  globin (L-[  $^{14}\text{C}$  ]-isoleucine) and total ( $\alpha$  and ß) globin  $m B_{112}$  Val/Val reticulocyte lysate. L-[ $^{14}$ C]-isoleucine (----), L-[ $^{3}$ H]-leucine synthetic rates (L-[ $^3$ H]-leucine) on  $^{\mathrm{Mg}^{++}}$  concentration was evaluated in the Figure 9

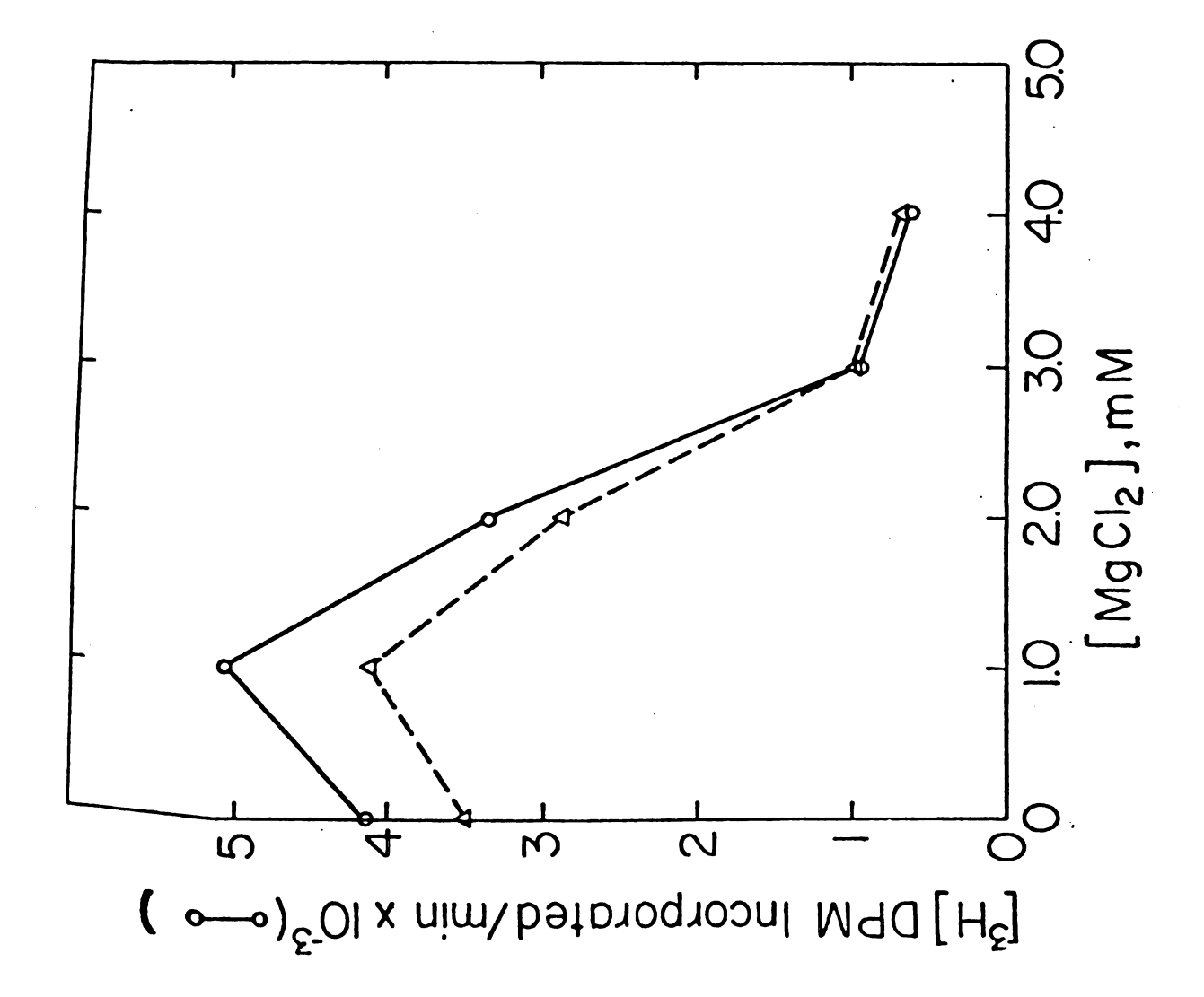
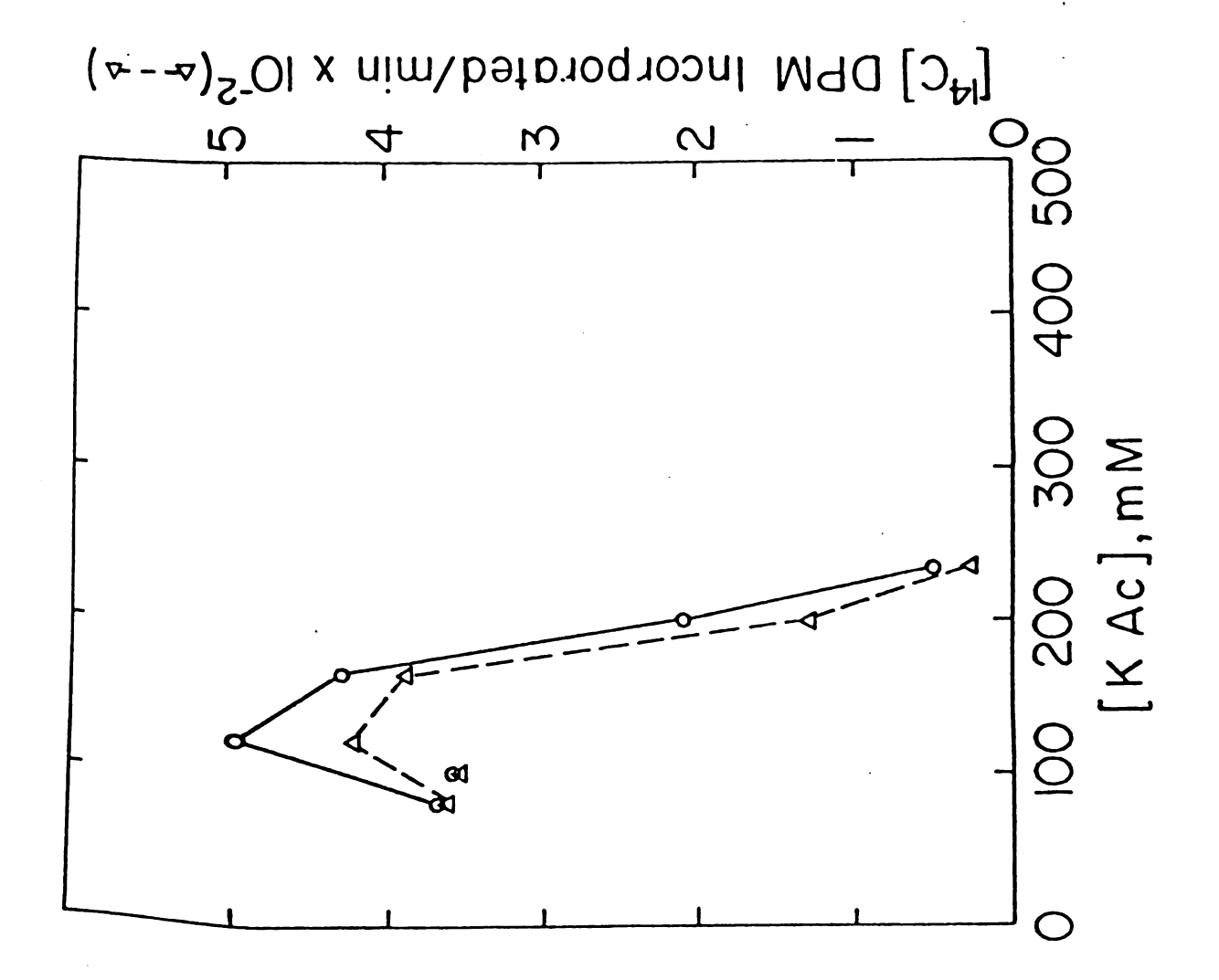
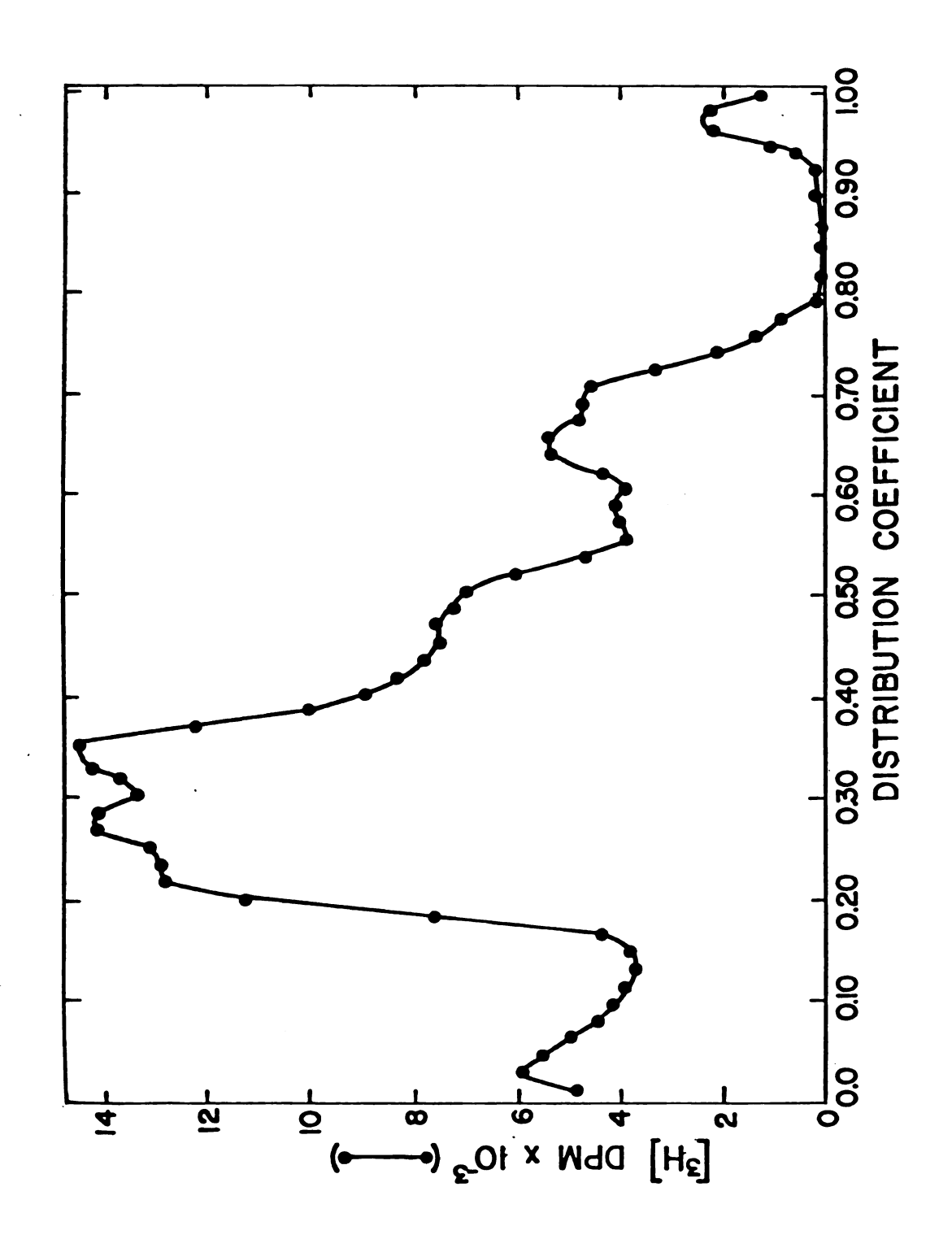


Figure 10 The dependence of the  $\alpha$  globin (L-[  $^{14}\text{C}$  ]-isoleucine) and total globin (L-[  $^{3}\text{H}$  ]-leucine) synthetic rates on potassium acetate concentration in the  $\mathfrak{g}_{112}$  Val/Val reticulocyte lysate. L-[ $^{14}$ C]-isoleucine (----), L-[ $^{3}$ H]-leucine (----).





was conducted simultaneously on the same polysome population allowing direct comparison of polypeptides (  $-\!-\!-\!-$  ) from a lysate of a  $\mathsf{g}_{112}$  Val/Val Rabbit. Double isotopic labeling nascent polypeptides (----) and L-[ $^3\mathrm{H}]\text{-tryptophan}$  labeled total (a and B) globin Figure 12 Bio-gel A 0.5 m chromatographic analysis of L-[ $^{14}\mathrm{C}$ ]-isoleucine labeled  $^{\alpha}$  globin the  $\alpha$  and total nascent peptide size distributions.

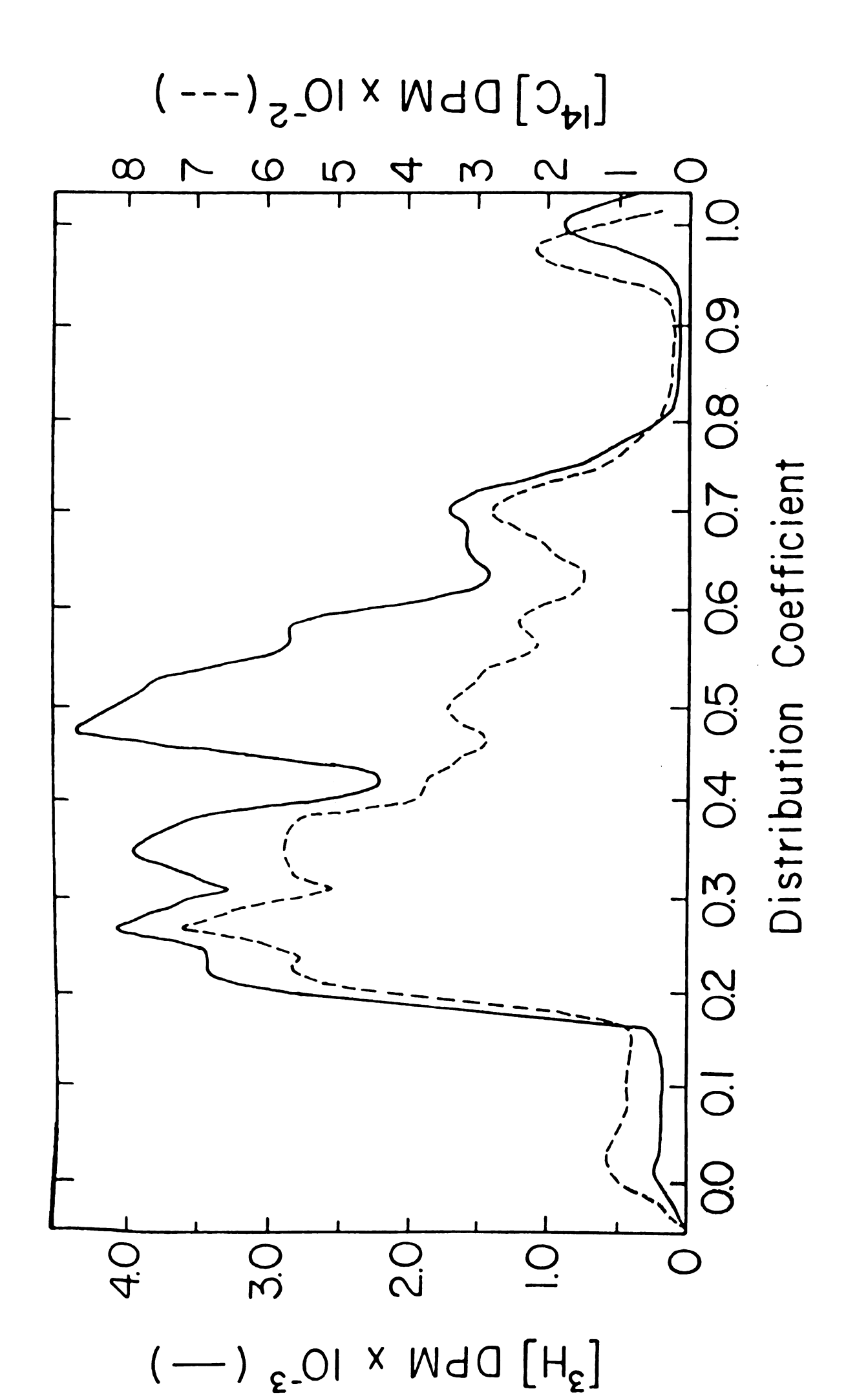


TABLE 2 The Positions of the  $\alpha$  Globin Nascent Peptide Accumulations as Determined by L-Isoleucine Labeling of  $\beta112\ Val/Val$  Lysates

α Peak	Kd	MW	Codon No.
I	0.22	15042.3	138-139
II	0.27	12754.3	116-117
III	0.35	9330.6	86-87
IV	0.43	6982.5	63-64
V	0.50	5242.1	47-48
VI	0.53	4510.5	41-42
VII	0.59	3557.4	32-33
VIII	0.66	2502.9	23-24
IX	0.73	1714.1	15-16

The most striking feature is the absence of a group of components in the Kd range from 0.45-0.55 which is seen in nascent chain size distribution profiles when other amino acids, such as tryptophan (see Figure 12), are used for labeling, indicating that the large accumulation of nascent chains in this Kd 0.45-0.55 region is due primarily to  $\beta$  nascent polypeptide components.

## Double Label Analysis of Nascent Polypeptides Using $L-[^{14}C]-Isoleu$ cine and $L-[^{3}H]-Tryptophan$

To allow simultaneous comparison of the alpha globin nascent polypeptide size distribution and the mixed  $\alpha$  and  $\beta$  globin size distribution polysomes were labeled simultaneously with L-[3H]-tryptophan and L-[14C]-isoleucine. This choice of isotopically enriched amino acids allows a direct comparison to be made between the  $\alpha$  size distribution and the composite total  $\alpha$  and  $\beta$  size distribution. The tryptophan labeled mixed ( $\alpha$  and  $\beta$ ) size distribution will be represented as weighted by a factor of two towards the  $\beta$  size distribution over the  $\alpha$  size distribution component due to the presence of two tryptophan residues near the N-terminus of the β chain in contrast with only one tryptophan residue near the N-terminus of the a globin polypeptide. The result of such an analysis is illustrated in Figure 12. The size distributions revealed by the isoleucine and tryptophan labeled nascent polypeptides show striking differences in the region corresponding to a Kd of 0.45 to 0.55 revealing the presence of at least two large B components centered approximately at Kd 0.47 and Kd 0.50. The remainder of the size distribution profile

shows a fairly similar though not identical distribution of components in the  $\alpha$  profile as compared to the composite  $\alpha$  and  $\beta$  profile.

## Characterization of the Bio-gel P-2 (-400 mesh) Analytical System for Quantitation of L-[3H]-tryptophan-Labeled Tryptic Peptides

It was found that under the correct conditions of ionic strength, and to a lesser extent pH, Bio-gel P-2 (-400) mesh gel filtration separates the two  $\beta$  and one  $\alpha$  tryptophan labeled tryptic peptides by a mixed sieving adsorptive process. In this system, the three peptides elute in order opposite to that expected for a separation based on molecular size but in order of increasing basicity. Control chromatographic analyses indicated that undigested globins elute with the void volume. Figure 13 shows separation obtained following tryptic digestion of a sample nascent polypeptides plus an internal standard of L-[14C]-Trp-labeled  $\alpha$  and  $\beta$  globins. Separation of the  $\beta$ T2 and  $\beta$ T4 tryptic peptides was less reproducible than the separation between the  $\alpha$ T3 and the two  $\beta$  peptides. This system was used for analysis of the extent of digestion of the sample and as an independent method for confirmation of the ratio  $\alpha$ T3 to  $\beta$ T2 as determined by high pressure liquid chromatography (below).

Identification of these tryptic peptides was accomplished by two methods. Figures 14 and 15 show the result of chromatography of a tryptic digest of [ $^3$ H]-Trp-labeled  $_\alpha$  and  $_\beta$  globin derived tryptic peptides with either [ $^1$ 4C]-tryptophan-labeled  $_\alpha$  or  $_\beta$  globins (previously isolated by CM-cellulose chromatography according to the method of Dintzis). This procedure allowed immediate identification of the  $_\alpha$  and two  $_\beta$  tryptophan labeled tryptic peptides. Further identification

provide an internal standard which allows a correction to be made for spurious loss of uniformly labeled, globin was co-digested with the  $[^3\mathrm{H}]$  labeled nascent peptides to Bio-gel P-2 (-400 mesh) column chromatography of L-[ $^3\mathrm{H}$ ]-tryptophan labeled globin tryptic peptides obtained from nascent polypeptide material. L-[ $^{14}\mathrm{C}$ ]-tryptophan, peptide material during the procedure.  $[^3\mathrm{H}]$  (----),  $[^{14}\mathrm{C}]$  (----). The order of elution is globin, aT3, BT2, BT4. Figure 13

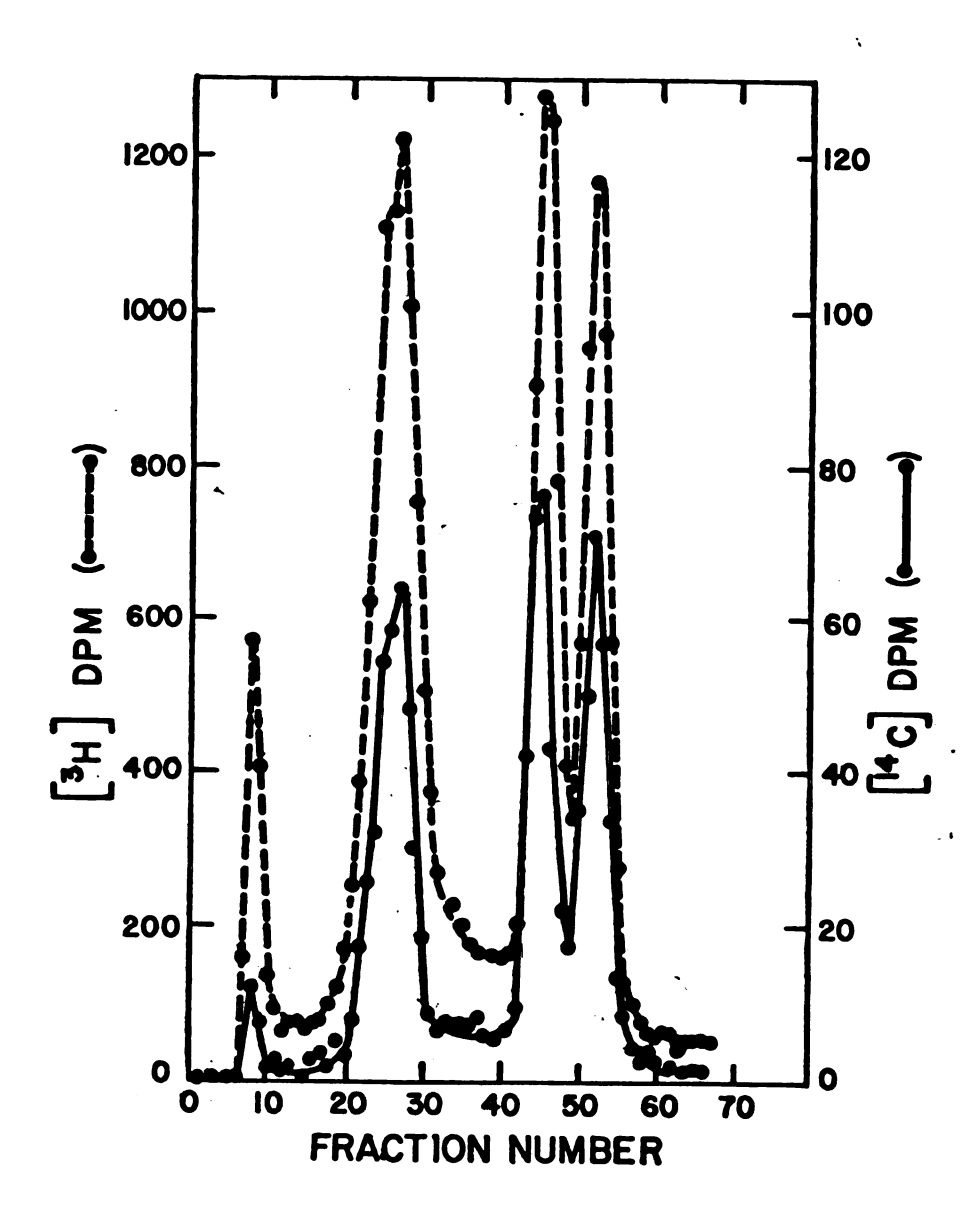
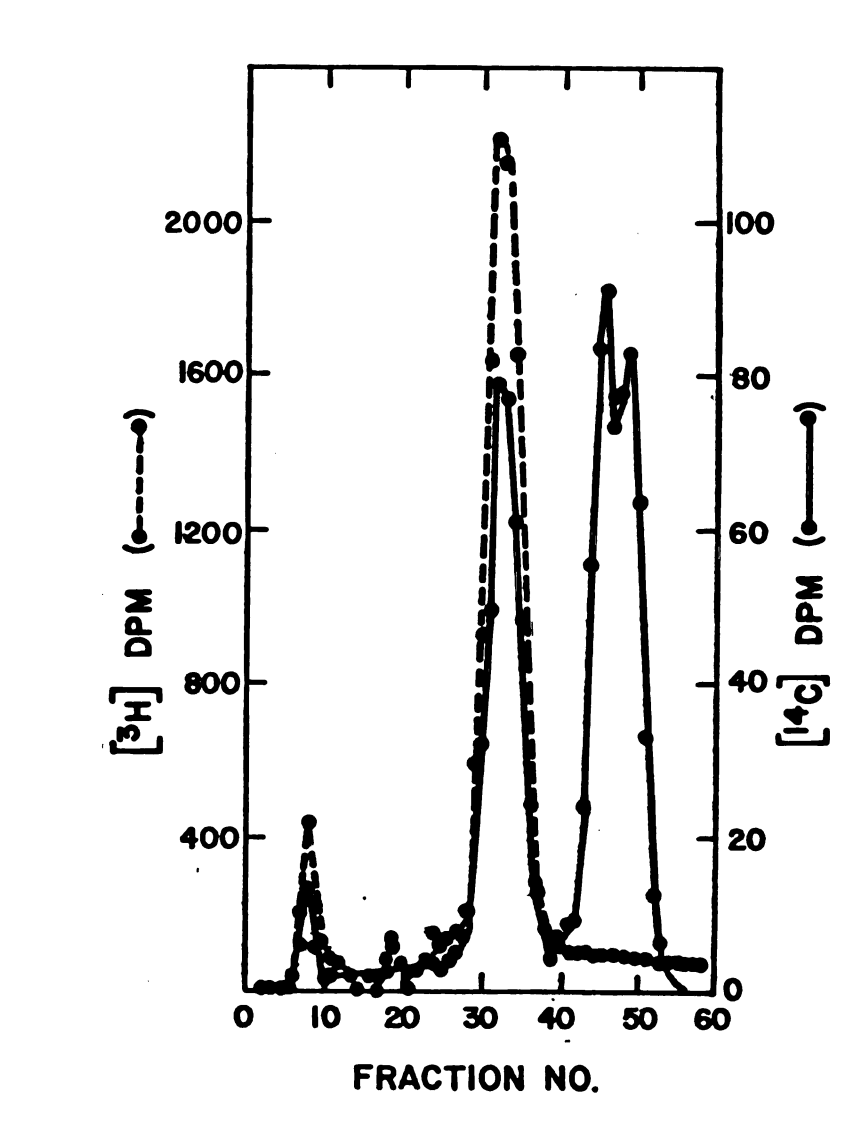
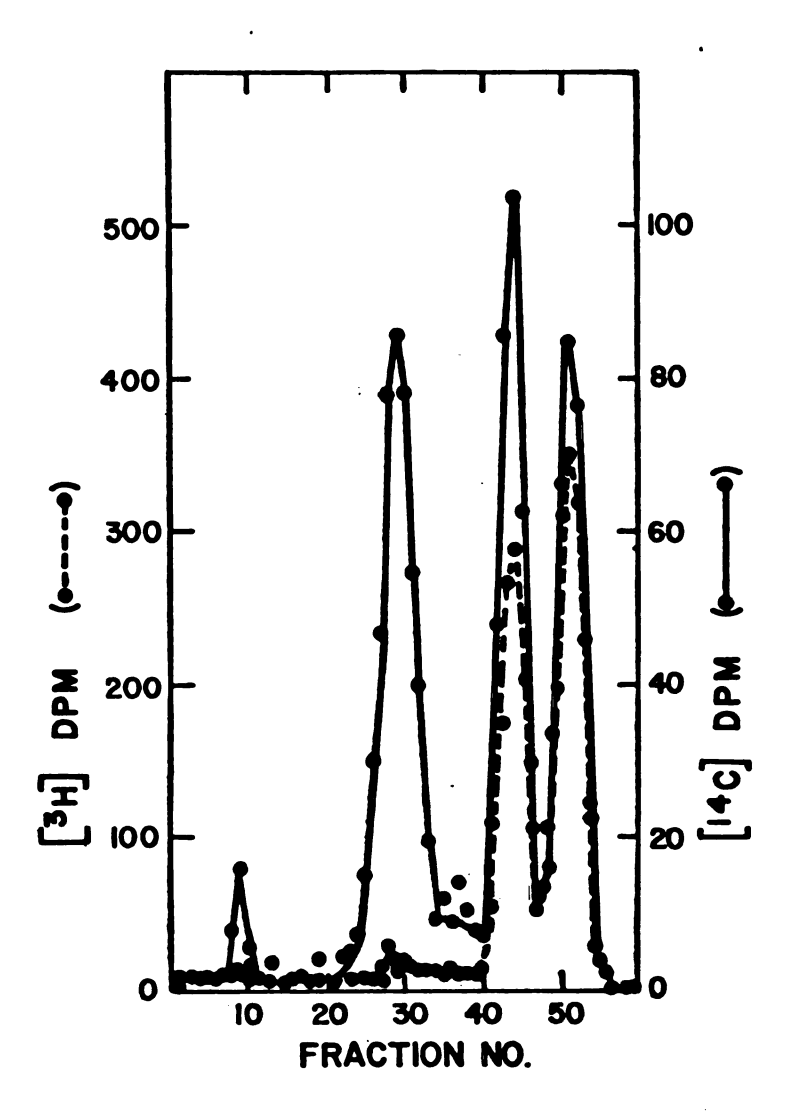


Figure 14 Bio-gel P-2 (-400 mesh) chromatography of L-[ $^3$ H]-tryptophan-labeled  $^{\alpha}$  globin tryptic chromatography as described in methods.  $[^3\mathrm{H}]$  (----),  $[^{14}\mathrm{C}]$  (----). The order of peptides with [  $^{14}\text{CJ-tryptophan}$  labeled tryptic peptides from  $\alpha$  and  $\beta$  globins. Separated  $\lceil ^3\text{H} \rceil$ -labeled- $\alpha$  and  $\beta$  globins were obtained by CM-cellulose column elution is globin, aT3, BTxz2, BT4.



[14c]-tryptophan labeled  $\alpha$  and  $\beta$  globins. [3H] (----), [14c] (----). The order  $\lceil 3H \rceil$ -tryptophan labeled  $\beta$  globins, obtained by CM-cellulose chromatography, and Figure 15 Bio-gel P-2 (-400 mesh) chromatography of the products of tryptic digestion of of elution is globin,  $\alpha T_3$ ,  $\beta T_2$ ,  $\beta T_4$ .



wa:

re

and

Qua Pre

874

rap

50 res

[3<sub>H]</sub>

sepa

tryp labe

Dept

Pept

[3H]gccou

(Fig.

٤٤١٦زو

of page

:131re

was accomplished high pressure liquid chromatography with ultimate reference to the established paper chromatographic system of Hunt, Hunter and Monroe (64) (below).

## Quantiation of the L-[3H]-tryptophan-Labeled Tryptic Peptides by High Pressure Liquid Chromatography.

The three tryptophan labeled globin tryptic peptides  $\alpha T3$ ,  $\beta T2$  and  $\beta T4$  were resolved and quantified by high pressure liquid chromatography on Pellionex SCX cation exchange support equilibrated initially in 50 mM pyridinium acetate pH 4.0. Figures 16 and 17 illustrate the results of fractionation of a mixture produced by codigestion of [3H]-Trp-labeled  $\alpha$  or  $\beta$  globin nascent polypeptides with [14C]-Trp uniformly labeled  $\alpha$  and  $\beta$  globins. The results of co-chromatography, in separate experiments, of [14C]-tryptophan labeled  $\alpha$  and  $\beta$  globin tryptic peptides with tryptic peptides derived from [3H]-tryptophan labeled  $\alpha$  or  $\beta$  nascent globin chains reveals that the first tryptic peptide eluting is  $\alpha T3$  and that the latter two are the  $\beta$  tryptic peptides.

Identification of the remaining  $\beta$  components as  $\beta$ T2 and  $\beta$ T4, was accomplished by pooling of the appropriate eluate fractions of [ $^3$ H]-tryptophan-labeled tryptic peptides from the Pellionex column (Fig. 18). Following concentration by lyophilization, the samples were subjected to paper chromatography as described in Methods. The results of paper chromatography of  $\beta$  first and second tryptic peptides eluted from a high pressure liquid chromatographic analysis is presented in Figures 19 and 20, respectively. These results indicate that the order

Figure 16 High pressure liquid chromatographic analysis of the tryptic peptides of

L-[  $^{14}\text{C}$  ]-trytophan-labeled  $\alpha$  and ß globins and L-[  $^{3}\text{H}$  ]-tryptophan labeled  $\alpha$  globin. [3H] (----), [14c] (----). The order of elution is globin,  $\alpha T_3$ ,  $\beta T_2$ ,  $\beta T_4$ .

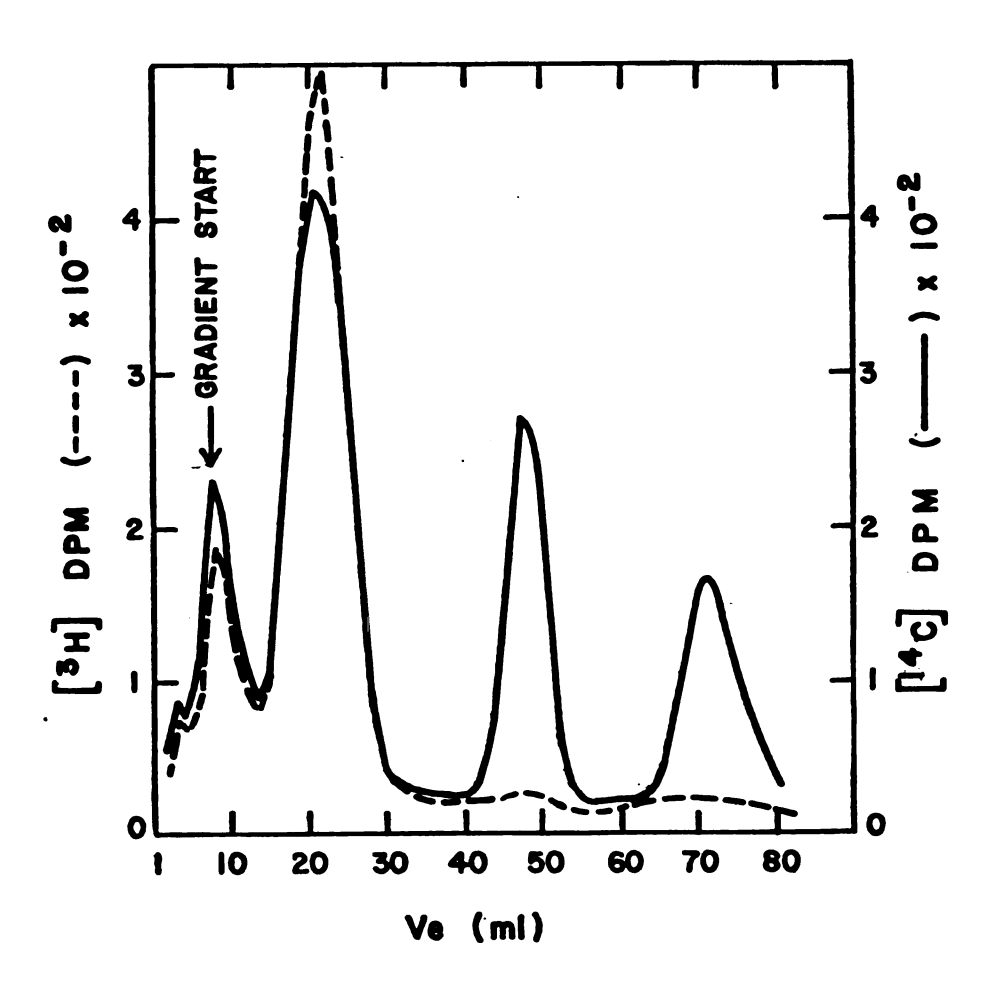
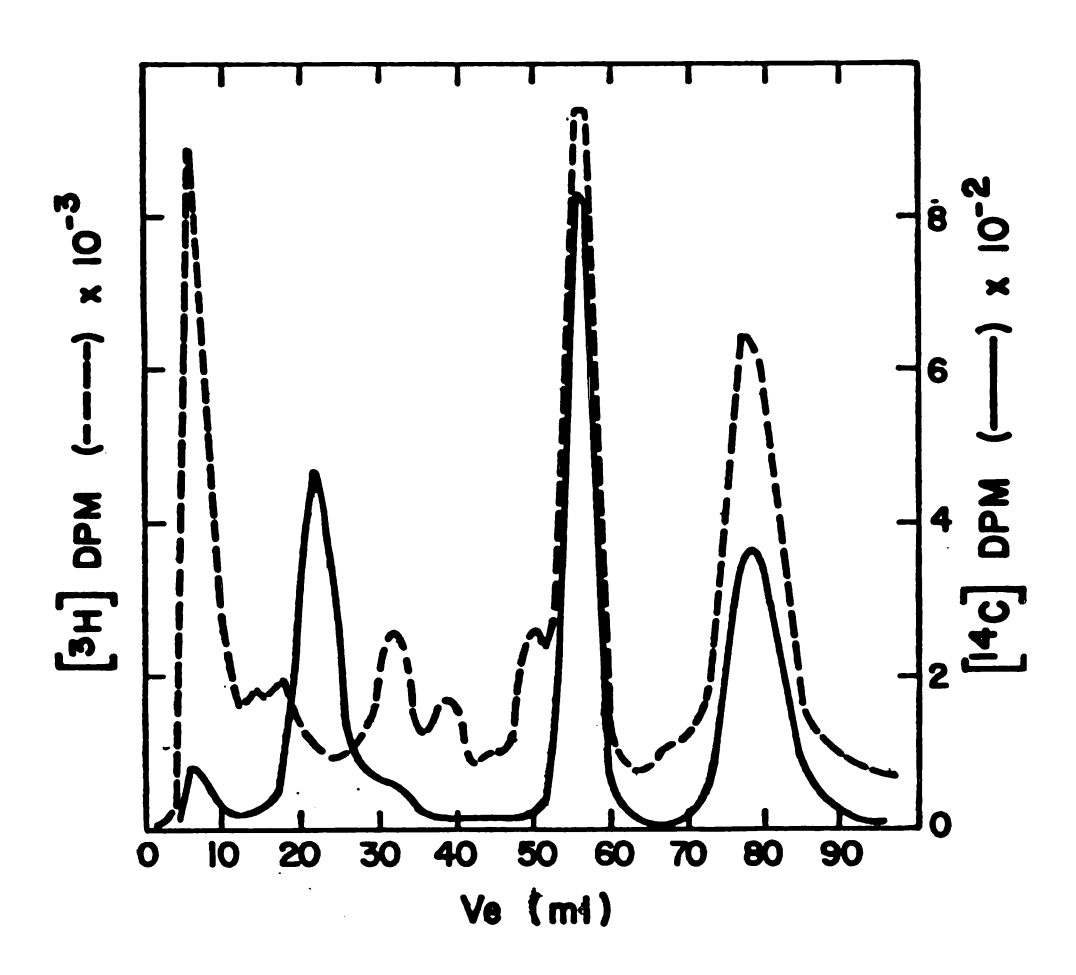


Figure 17 High pressure liquid chromatographic analysis of the tryptic peptides of

L-[ $^{14}$ C]-tryptophan-labeled  $\alpha$  and  $\beta$  globins and L-[ $^{3}$ H]-tryptophan labeled  $\beta$  globin.

[ $^3\mathrm{H}$ ] (----), [ $^{14}\mathrm{C}$ ] (----). The order of elution of the [ $^{14}\mathrm{C}$ ]-labeled material

is globin aT3, BT2, BT4.



chromatographic to allow determination of the identity of the ß peptides as BT2 and BT4, globin tryptic peptides. The fractions indicated (peaks 2 and 3) were used for paper Figure 18 Preparative high pressure liquid chroamtography of heavily labeled ( $[^3\mathrm{H}]$ -tryptophan) respectively. The order of elution is globin, aT3, BT2, BT4.

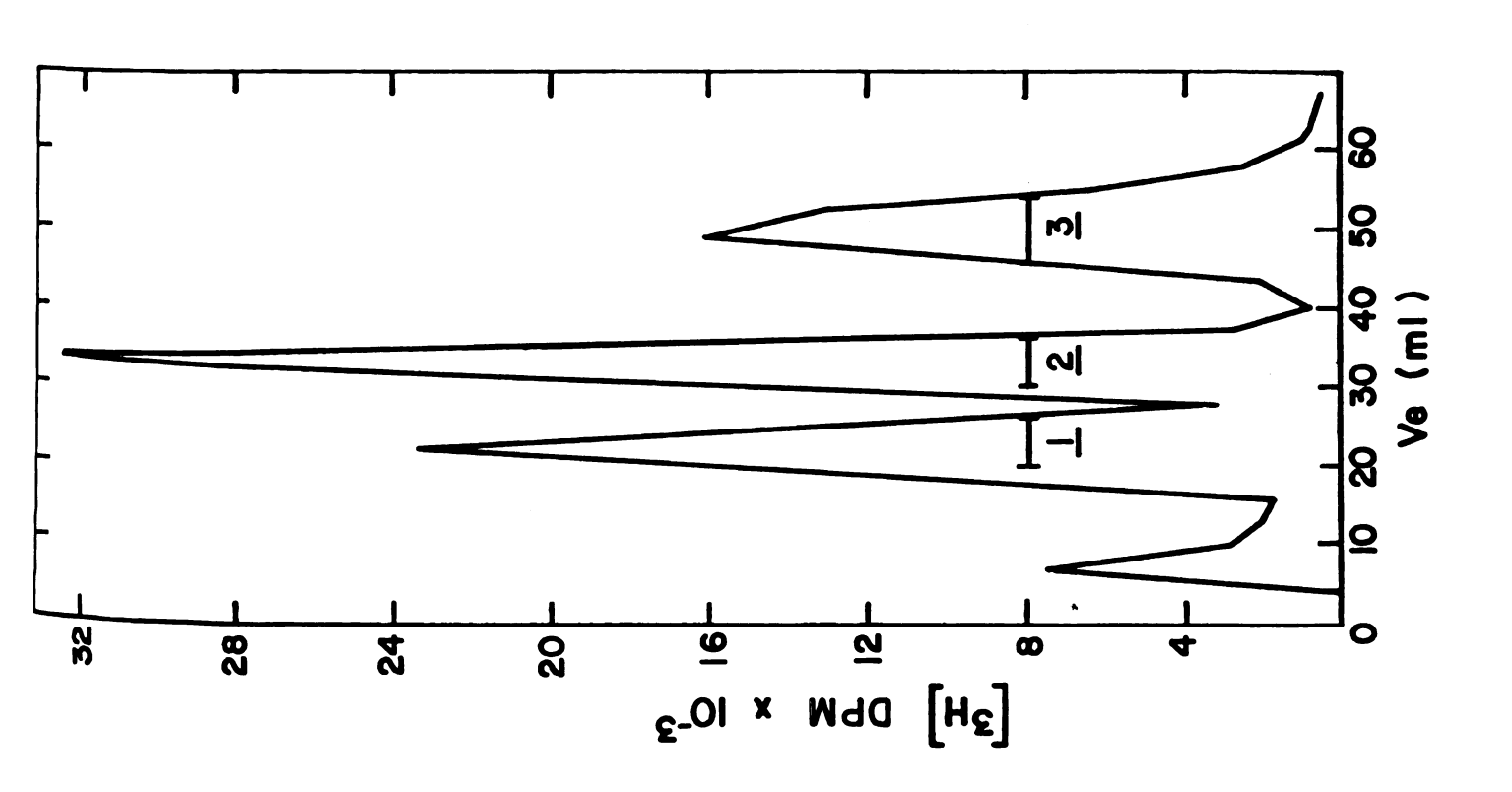


Figure 19 Paper chromatographic analysis of the L-[ $^3$ H]-tryptophan peptide no. 2 obtained by high corresponding to the first & globin tryptophan residue at osition &15. Cross hatching pressure liquid chromatography. The identity of this peptide was found to be BT2 indicates region of ultraviolet absorption by tryptophan.

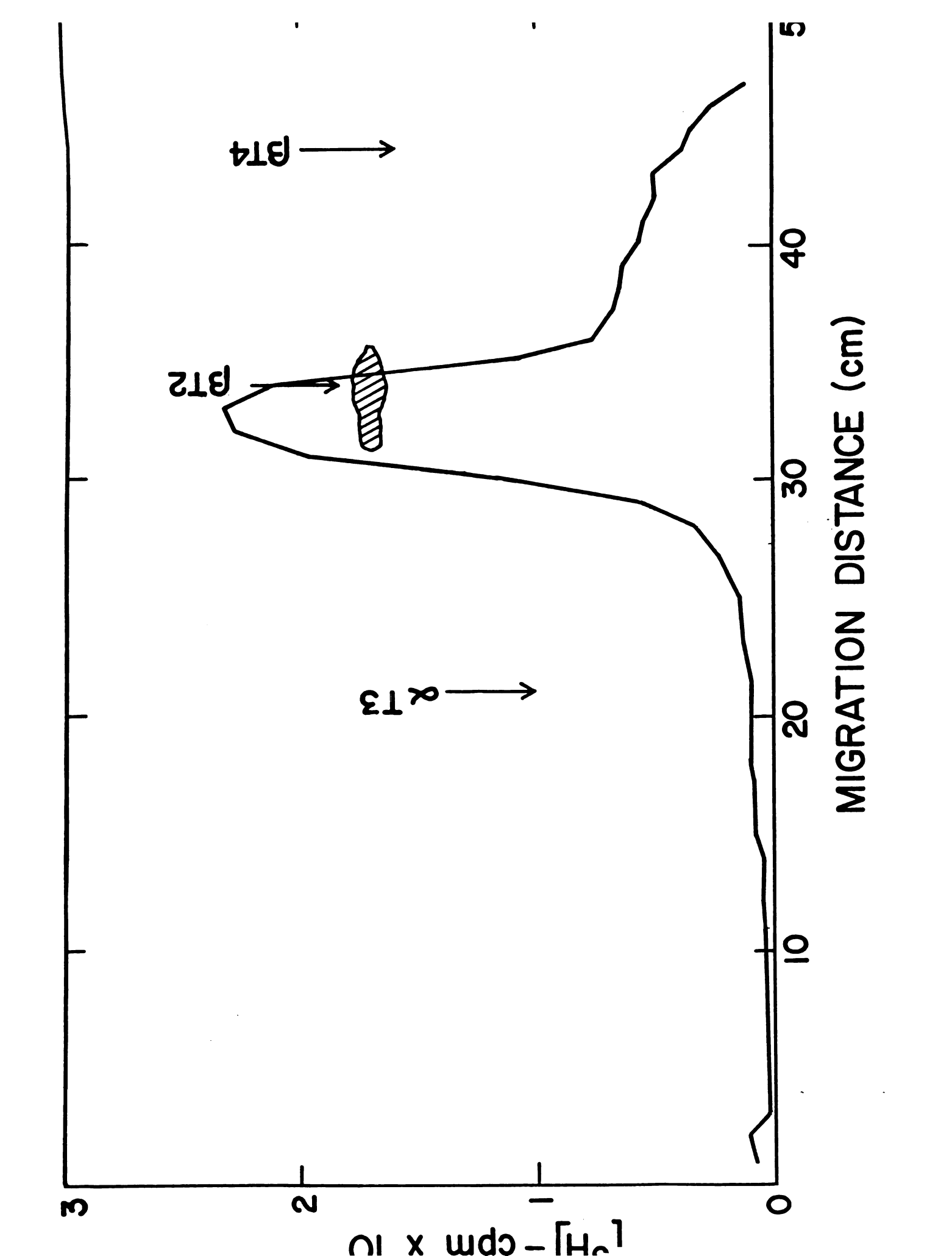
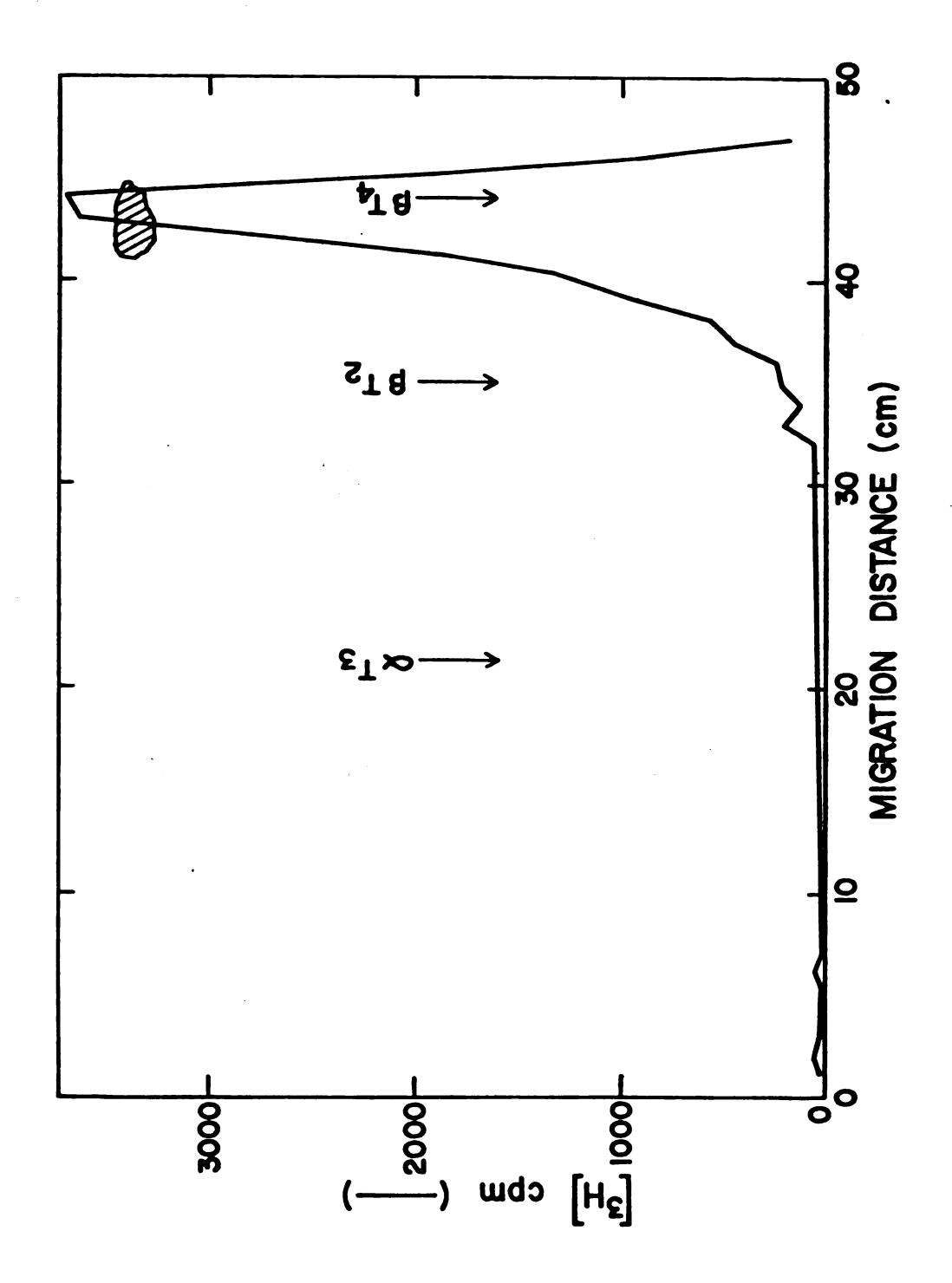


Figure 20 Paper chromatographic analysis of tryptic peptide no. 3 obtained by high pressure liquid residue located at position 837. Crosshatched area represents region of ultraviolet chromatography. This peptide was identified as BT4 corresponding to the tryptophan absorption by tryptophan.



.

H

r

t

p

ac 87

We

s; cor

001

Ter the

of

910

of elution of the tryptophan labeled tryptic peptides from the Pellionex SCX system and the Bio-yel systems is  $\alpha T3$ ,  $\beta T2$  and  $\beta T4$ .

## Determination of the $\alpha$ and $\beta$ Globin Nascent Peptide Size Distribution by HPLC of Tryptophan-Labeled Tryptic Peptides

The HPLC system was used for the analysis of the  $\alpha$  to  $\beta$  ratio in the nascent chain size distributions. Figure 21a and b shows two representative analyses of two different regions of the Bio-gel A 0.5 m size distribution corresponding to Kd 0.26 and Kd 0.59. It can be seen that the identification of  $\beta$ T4 as the latest eluting tryptic peptide is confirmed as this peptide becomes uniformly labeled later than the  $\alpha$ T3 and  $\beta$ T2 peptides, which are labeled together due to the nearly identical positions of these tryptophan residues along the polypeptide at residues  $\alpha$ 14 and  $\beta$ 15, respectively. Figure 22 shows the abrupt rise in specific activity of  $\beta$ T4 tryptic peptide represented as the increase in the ratio  $\beta$ T2/ $\beta$ T4 as a function of the distribution coefficient. Such analyses were run on highly labeled ([ $^3$ H]-tryptophan) nascent peptides whose size distribution is shown in Figure 23. Figure 24 shows the  $\alpha$  and  $\beta$  component size distributions as calculated from the value of  $\alpha$ T3/ $\beta$ T2 obtained by HPLC analysis of tryptic digestion mixtures.

The validity of this method is apparent from the substantial agreement between the  $\alpha$  size distribution obtained from tryptic analysis with the size distribution obtained directly by specific isoleucine labeling of the  $\alpha$  peptidyl tRNA fraction in the reticulocyte lysate (Figure 11).

Comparison of the  $\alpha$  and  $\beta$  profiles indicates that, the  $\alpha$  and the  $\beta$  globin profiles are significantly different, as predicted from studies

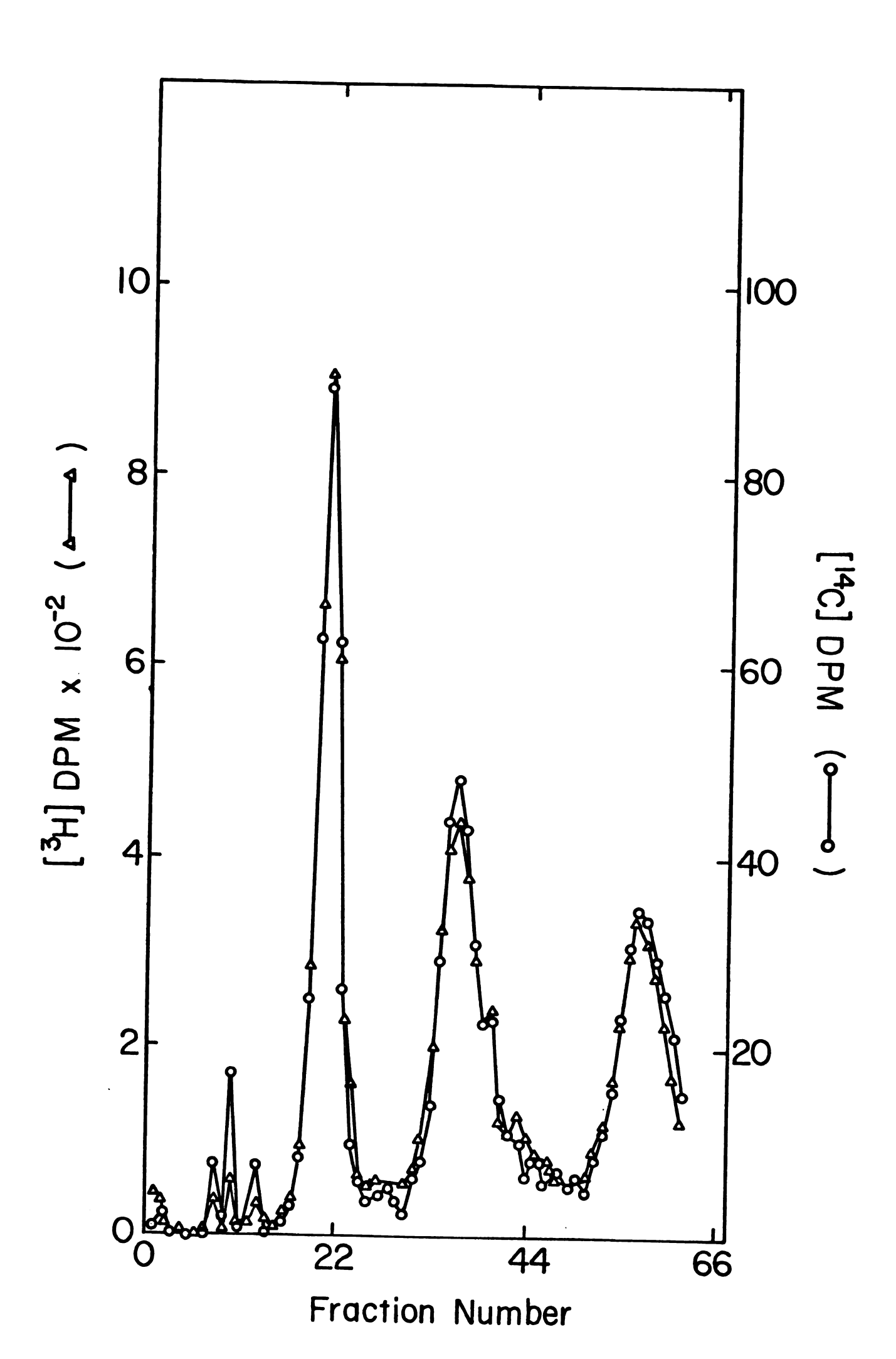
Figure 21a,b High pressure liquid chromatographic analysis of the products of tryptic digestion of L-[3H]-tryptophan-labeled nascent polypeptides corresponding to two regions of the nascent peptide size distribution.

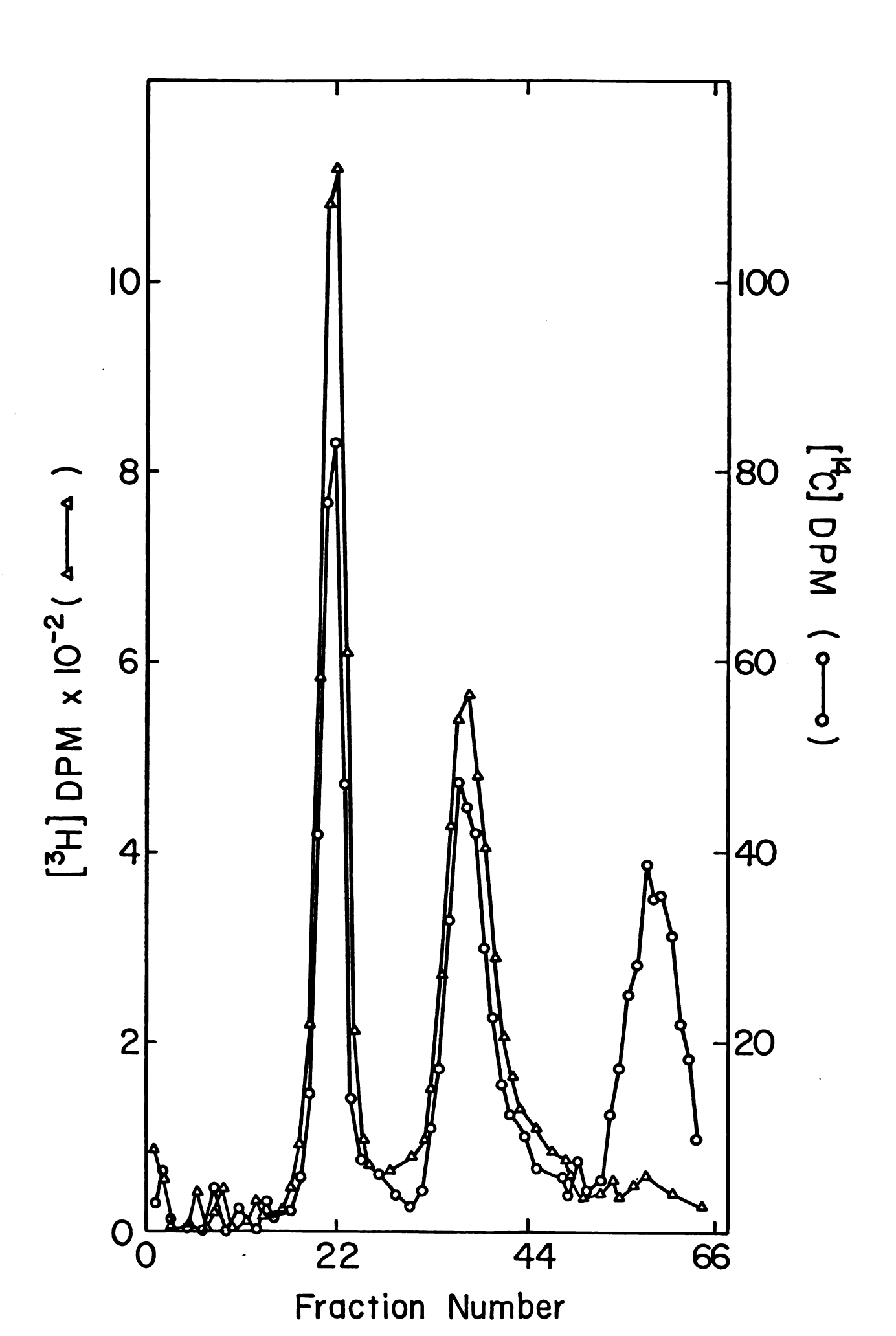
21a, Kd = 0.26

21b, Kd = 0.59 (Fig. 23)

(0-0),  $\lceil ^{14}\text{C} \rceil$  internal standard, tryptic peptides derived from uniformly labeled  $\alpha$ and B globins.

corresponding to values of the distribution coefficient greater than 0.60. (Fig. 21b). ( $\Delta-\Delta$ ), [ $^3H$ ] labeled tryptic peptides derived from nascent material. The tryptic peptide BT4 is not significantly labeled at positions in the size distribution





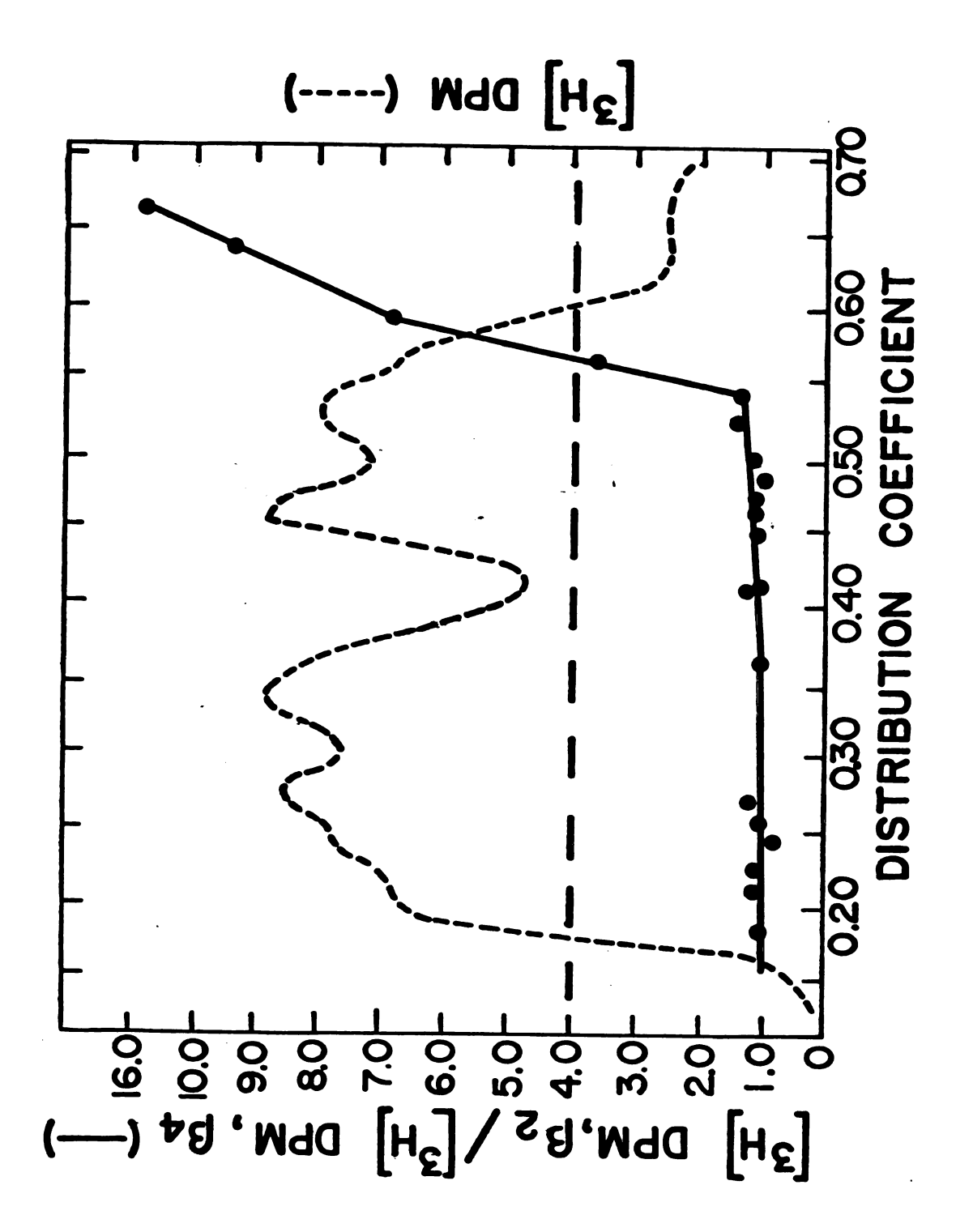
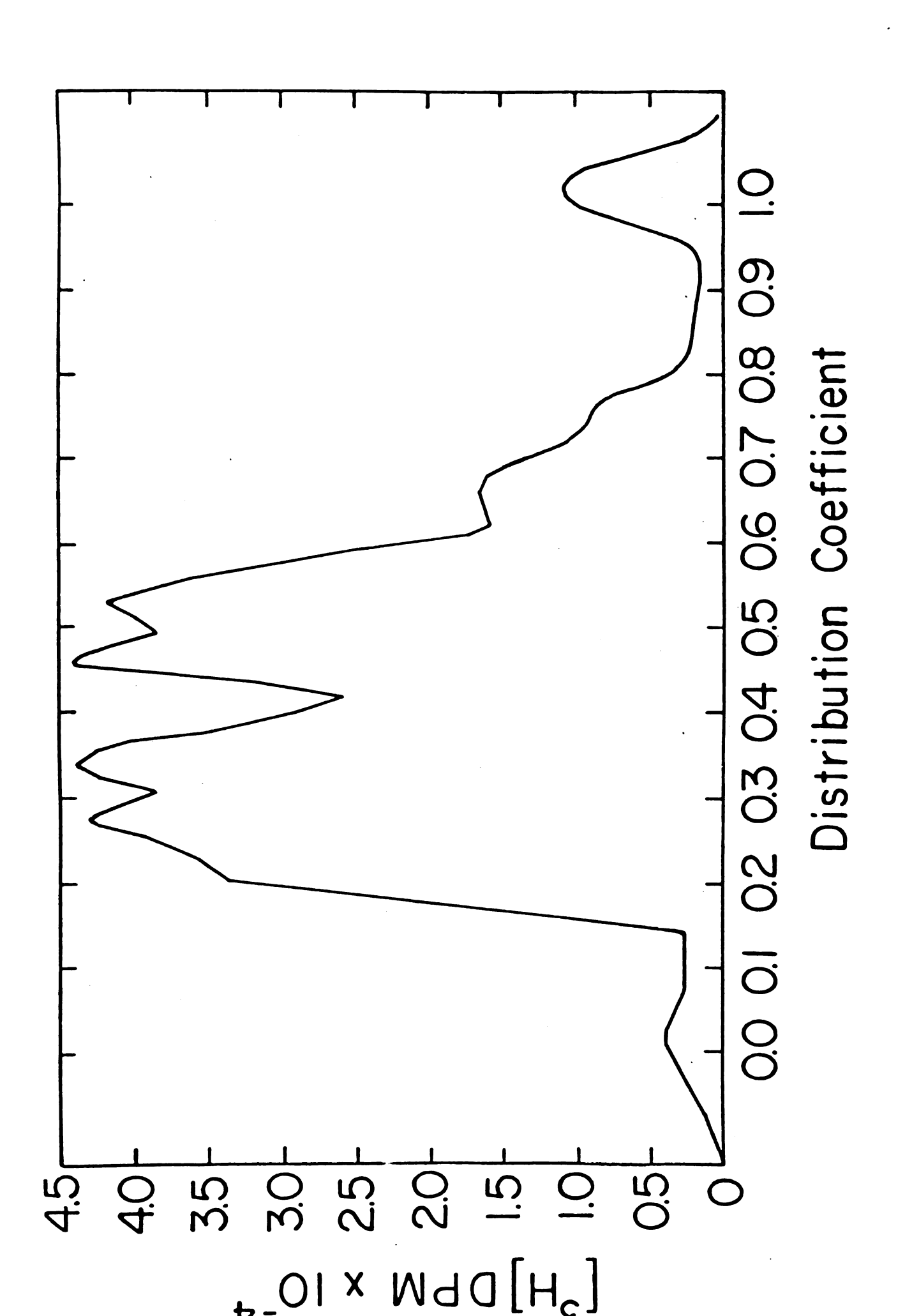
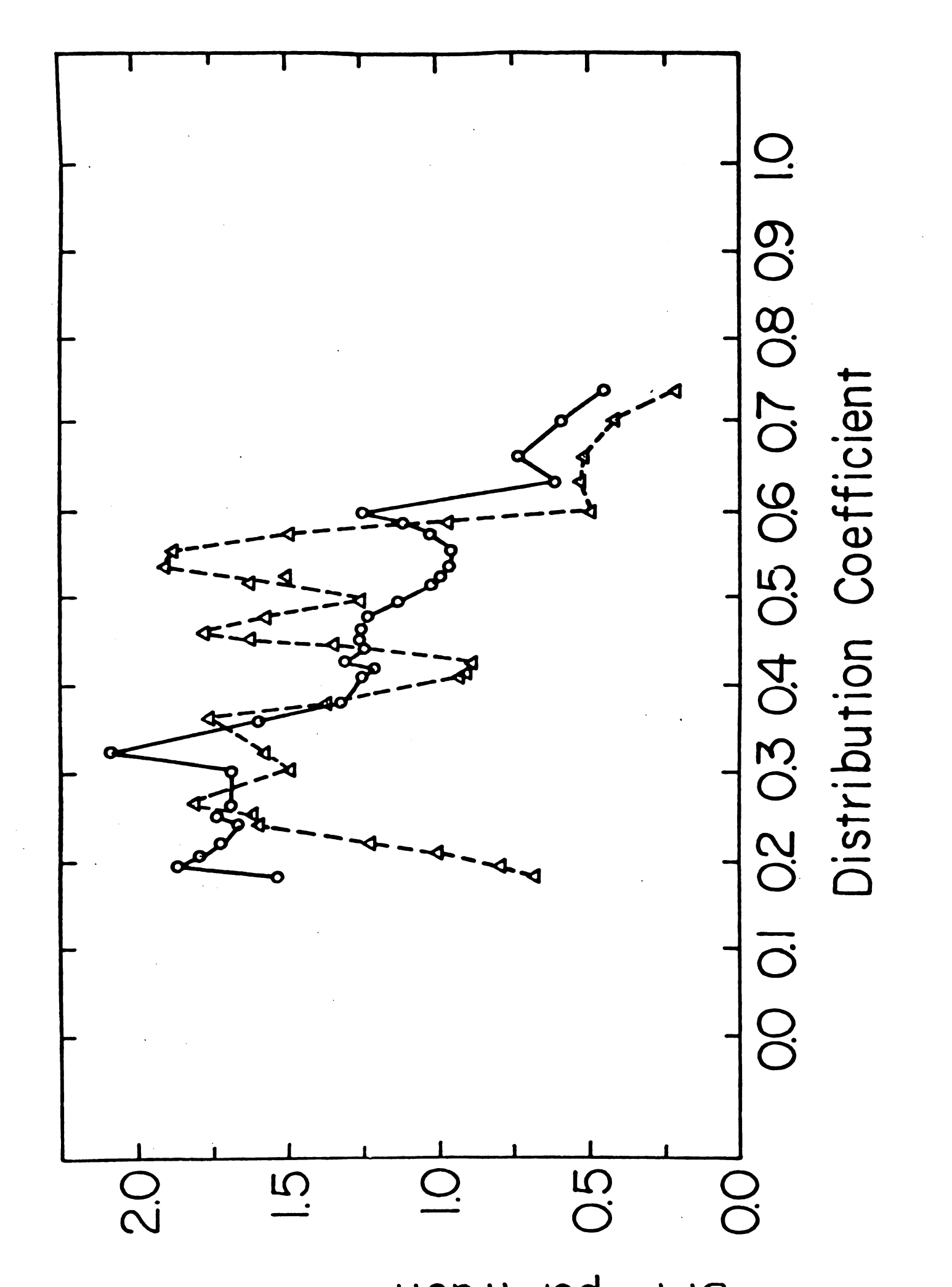


Figure 23 Bio-gel A 0.5 m size distribution profile of globin nascent peptides which were heavily labeled with L-[ $^3$ H]-tryptophan. Fractions corresponding to different values of the distribution coefficient were subjected to tryptic digestion. Quantitation of the resultant peptides BT2 and aT3 was accomplished by HPLC.



nascent peptides as determined by quantitation of tryptic peptides  $\alpha T3$  and  $\beta T2$  by high Figure 24 The mascent peptide size distribution of the  $\alpha$  globin mascent peptides and  $\beta$  globin pressure liquid chromatography.

2.0 F



of isoleucine labeled  $\alpha$  and mixed tryptophan labeled  $\alpha$  and  $\beta$  nascent peptides. The most striking difference is noted in the region from Kd .55 to .45. At this Kd the  $\beta$  nascent polypeptides show a major accumulation while very little of the  $\alpha$  nascent components are present.

Also apparent is the relatively large  $\alpha$  component in the region of completed globin chains (Kd 0.18-0.26) relative to  $\beta$ . This is consistent with the observation of Protzel and Morris of an accumulation of  $\alpha$ -globyl tRNA relative to  $\beta$  globyl tRNA and extends their observation to smaller nascent intermediates up to a Kd 0.26. This effect cannot be due to a displacement in terms of the elution volume of  $\alpha$  relative to  $\beta$ , reflecting the fact that completed  $\alpha$  globin is some 500 g/mol lighter than  $\beta$  globin since such an effect would cause  $\beta$  components to be more highly populated at lower Kd's than  $\alpha$  components, an effect which would cause an underestimate of the  $\alpha$  excess. Table 3 lists the distribution coefficient for the major  $\beta$  nascent polypeptide accumulations obtained from tryptic analysis of the tryptophan labeled size distribution for comparison. Other regions of the  $\alpha$  and  $\beta$  nascent polypeptide size distributions reflect more similarity than differences between the  $\alpha$  and  $\beta$  profiles.

## Labeling of Reticulocyte Polysomes with N-Formyl Methionyl tRNA<sub>f</sub>Met and L-[3H]-Methionine

The above analyses used selected amino acid residues as sites for radiochemical labeling in order to provide as much information as possible about the nascent polypeptide size distribution for the  $\alpha$  and  $\beta$  globin nascent polypeptides. The criterion by which a particular amino

TABLE 3

The Positions of the ß Globin Nascent Peptide Accumulations as Determined by Tryptic Analysis

β Peak	Kd	MW	Codon No.
I	0.28	12187.8	110-111
II	0.34	9579.9	87-88
III	0.46	6064.4	55-56
IV	0.53	4512.5	40-41
V	0.67	2343.6	21-22

acid was chosen was determined by the frequency and location of that residue in the sequence of the protein being studied. Since each new entry of a labeled amino acid residue into the growing nascent peptide increases the specific activity of that polypeptide, distortion of the size distribution profile can result. Since no information is obtained concerning accumulations of nascent peptides prior to insertion of the first labeled amino acid residue, it is also necessary to choose an amino acid which is as close to the N-terminus of the growing polypeptide chain as possible. To circumvent problems due to specific activity changes and, more specifically, to obtain information about the size distribution of globin nascent peptides in the region of Kd 0.75-0.95, a general method for the measurement of nascent peptide size distributions, which is independent of amino acid sequence, was adopted. Radioactive label was introduced into the N-terminal position of the nascent chains by taking advantage of the observation that yeast initiator tRNA<sub>f</sub>Met charged with methionine and formylated with a bacterial aminoacylating/formylating enzymatic extract places a permanent N-formyl methionyl residue at the N-terminus of the growing nascent polypeptides in eukaryotic derived cell-free synthesizing systems (67). Fig. 25 shows that the time course of incorporation of L-[ $^{35}$ S] formyl methionine into TCA precipitable material is linear throughout the first twenty minutes of incubation. Figure 26 shows the result of an experiment in which  $\alpha$  and  $\beta$  globin nascent chains were labeled with L-[3H]-tryptophan and L-[35S] formyl methionine (f Met). These results reveal at least one nascent peptide accumulation eluting at Kd 0.8 which is not apparent in the tryptophan profile. Another component appears as a slight

Figure 25 Measurement of the the rate of incorporation of L-[ $^{35}$ S]formylmethionine from

L-[ $^{35}$ S]fMet tRNA $^{\text{fmet}}$  into globin by the reticulocyte cell-free protein

synthesizing system.

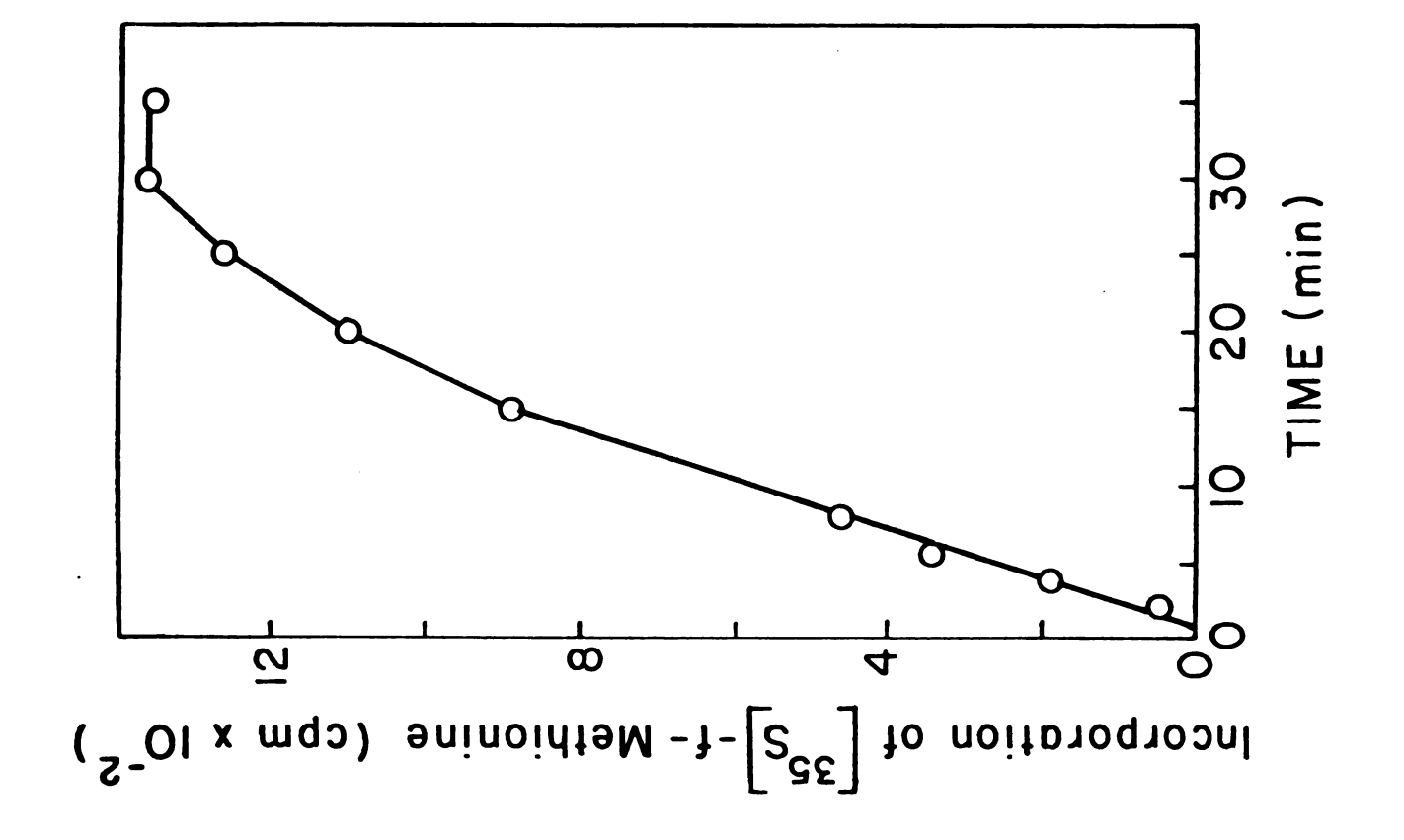
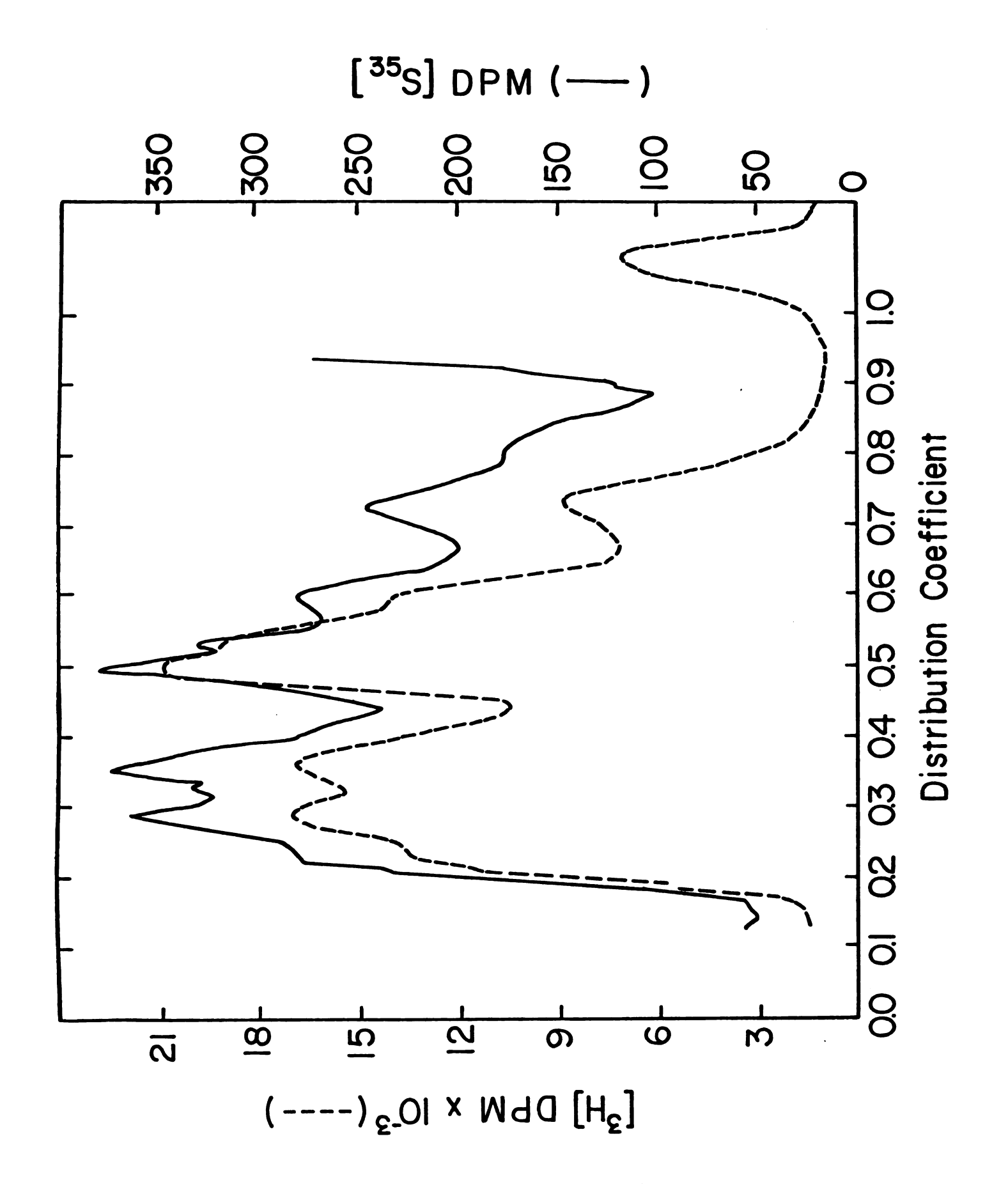
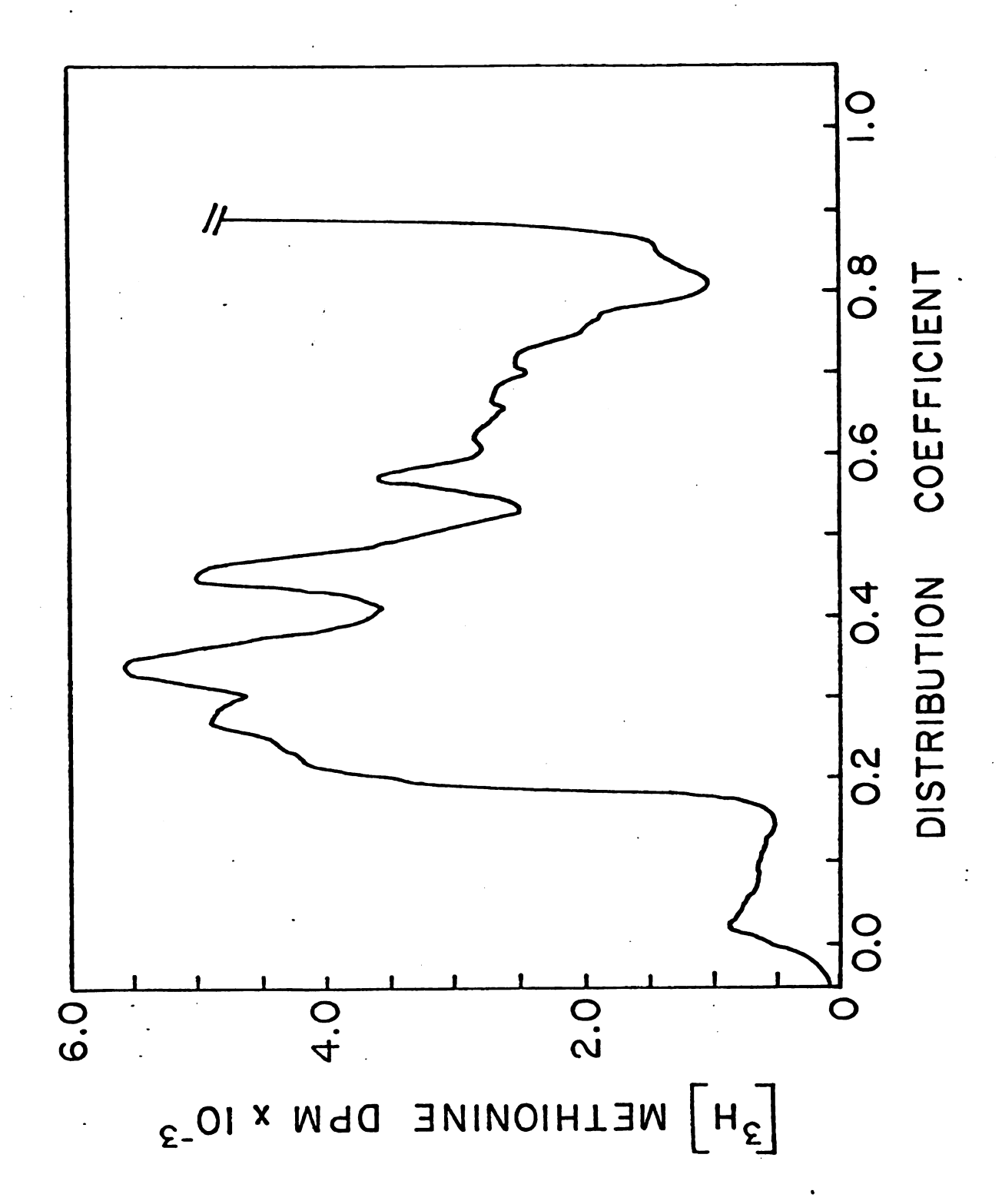


Figure 26 Bio-gel A 0.5 m analysis of the size distribution of globin nascent peptides which were



shoulder ahead of the free amino acid peak at Kd 0.92. Due to the presence of large amounts of free N-formyl methionine obscuring the small molecular weight component appearing at Kd 0.92, independent verification of this component was obtained by labeling polysomes with L-[3H]-meth-The L-[3H]-methionine labeled size distribution is complex due to the placement and subsequent removal of methionine from the N-terminus as well as labeling of the internal methionine residues at Kd 0.48 and Kd 0.61. However, it has been shown that the N-terminal methionine is not removed from the nascent globin chains until the nascent chains are at least 20 amino acid residues in length corresponding to a Kd value of 0.65 (68). The results of such an experiment are shown in Figure 27. A small molecular weight component is clearly demonstrated to elute ahead of the free L-[3H] methionine peak, confirming the previous observation obtained with  $[^{35}S]$ -f Met. The composition of the two early nascent chain accumulations in terms of the relative amounts of  $\alpha$  and  $\beta$  globin nascent peptides contributing to each was not determined. It is interesting to note the apparent loss of the prominent  $\beta$  globin mascent peptides in the region of Kd 0.45 to Kd 0.55 except for a very narrow component at Kd 0.45. This is due to the removal of the N-terminal methionine residues and the appearance of only the largest components of the accumulation previously noted at Kd 0.45 to 0.55. The narrow component at Kd 0.45 is due to labeling of B methionine residue 55 indicating that the ß accumulated ß nascent chains in the region of the size profile extending from Kd 0.45 to Kd 0.55 occur prior to and just past the B globin methionine codon 55.

labeling with L-[3H]-methionine.



## <u>Perturbation of the Nascent Polypeptide Size Distribution with</u> <u>L-O-Methylthreonine</u>

Several experiments are described which were designed to provide information on the sensitivity of the steady state nascent peptide size class accumulations to agents which might effect redistribution of ribosomal density along the mRNA molecule. L-O-methyl-threonine (L-OMT) is an isoleucine isostere and is competitive with respect to isoleucine for the isoleucyl tRNA charging reaction catalyzed by isoleucyl-tRNA synthetase. Incubation of  $\beta_{112}$  Val/Val reticulocytes or reticulocyte lysate with L-OMT is known to induce a condition of isoleucyl tRNA starvation and inhibition of ribosomal translocation of isoleucyl codons (69) of the α globin. Figure 28 shows the results of incubation of a  $\beta_{112}$  Val/Val reticulocyte lysate with L-OMT, L-[14C]-isoleucine and L-[3H]-Tryptophan. The  $\beta_{112}$  Val/Val phenotype ensures that inhibition occurs only on  $\alpha$  polysomes as has been demonstrated previously. Two peaks of shifted ribosomal density, which are observed by the altered size distribution of the nascent  $\alpha$  chains correspond to the artifically induced reduction of ribosomal translocation rate at ile codons 17 and 55. No peak is expected at isoleucine codon 10 since the first isoleucine is placed at this point and hence no label appears in the nascent peptides accumulated at this codon. A control size distribution pattern was determined using L-[ $^{3}H$ ]-Trp and L-[ $^{14}C$ ]- isoleucine similar to that shown in Figure 12 in the absence of L-OMT. It is important to note that the isoleucine label reflects the nascent peptide accumulations caused on the  $\alpha$  mRNA programmed polysomes whereas the equally distorted L-[ $^{3}$ H]-Trp profile reflects mixing of the perturbed  $\alpha$ profile with the presumably unperturbed β profile. This contribution of

Figure 28 The elution profile of  $\alpha$  (L-[  $^{14}\text{C}\xspace]-isoleucine, -----) and total$ 

(L-[<sup>3</sup>H]-tryptophan,----) globin nascent peptides which had been labeled in the presence

of 25 mM L-0-methylthreonine. The prominent accumulations at Kd's 0.48 and 0.72 represent

L-OMT induced accumulations behind ile codons 17 and 55.

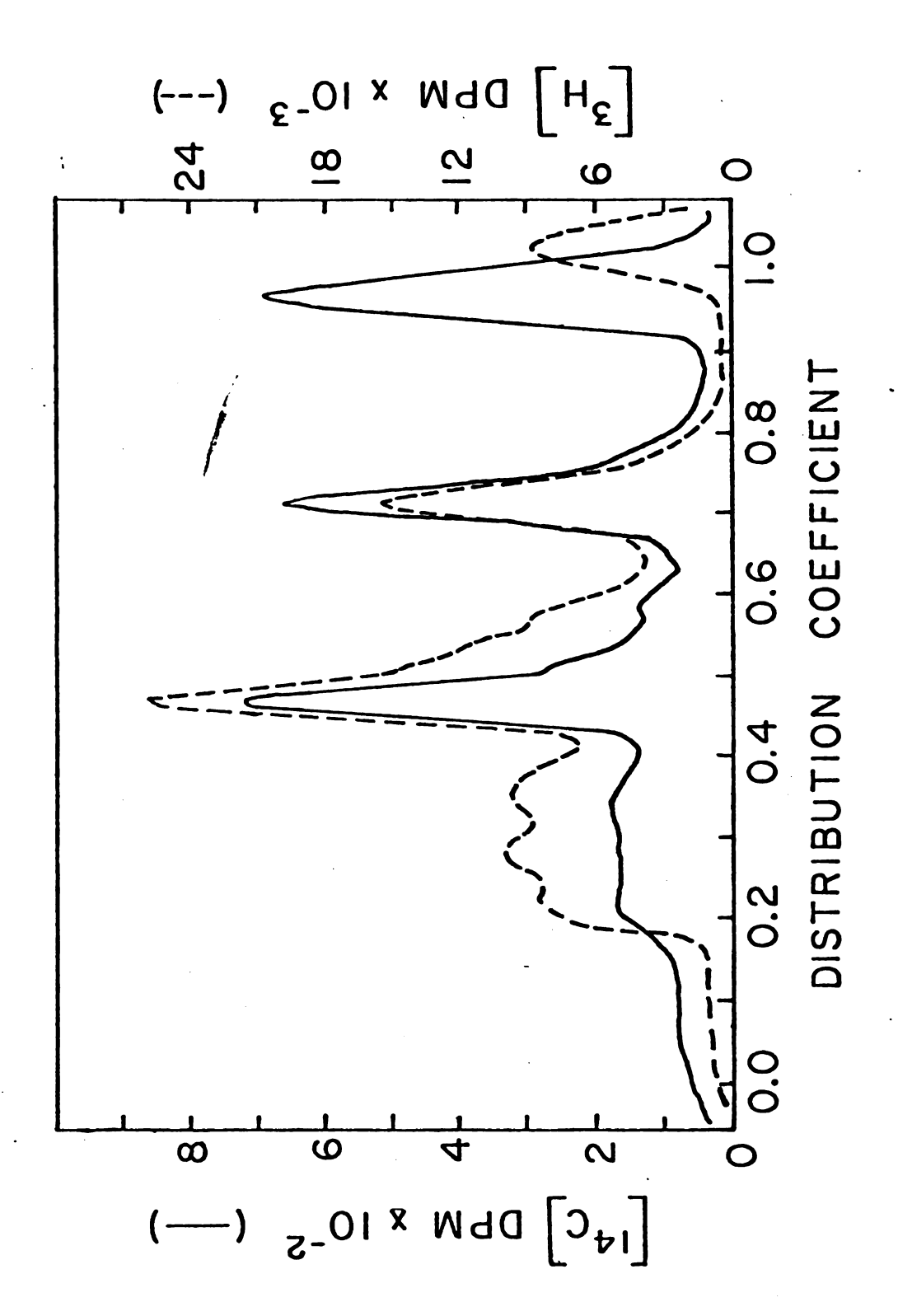
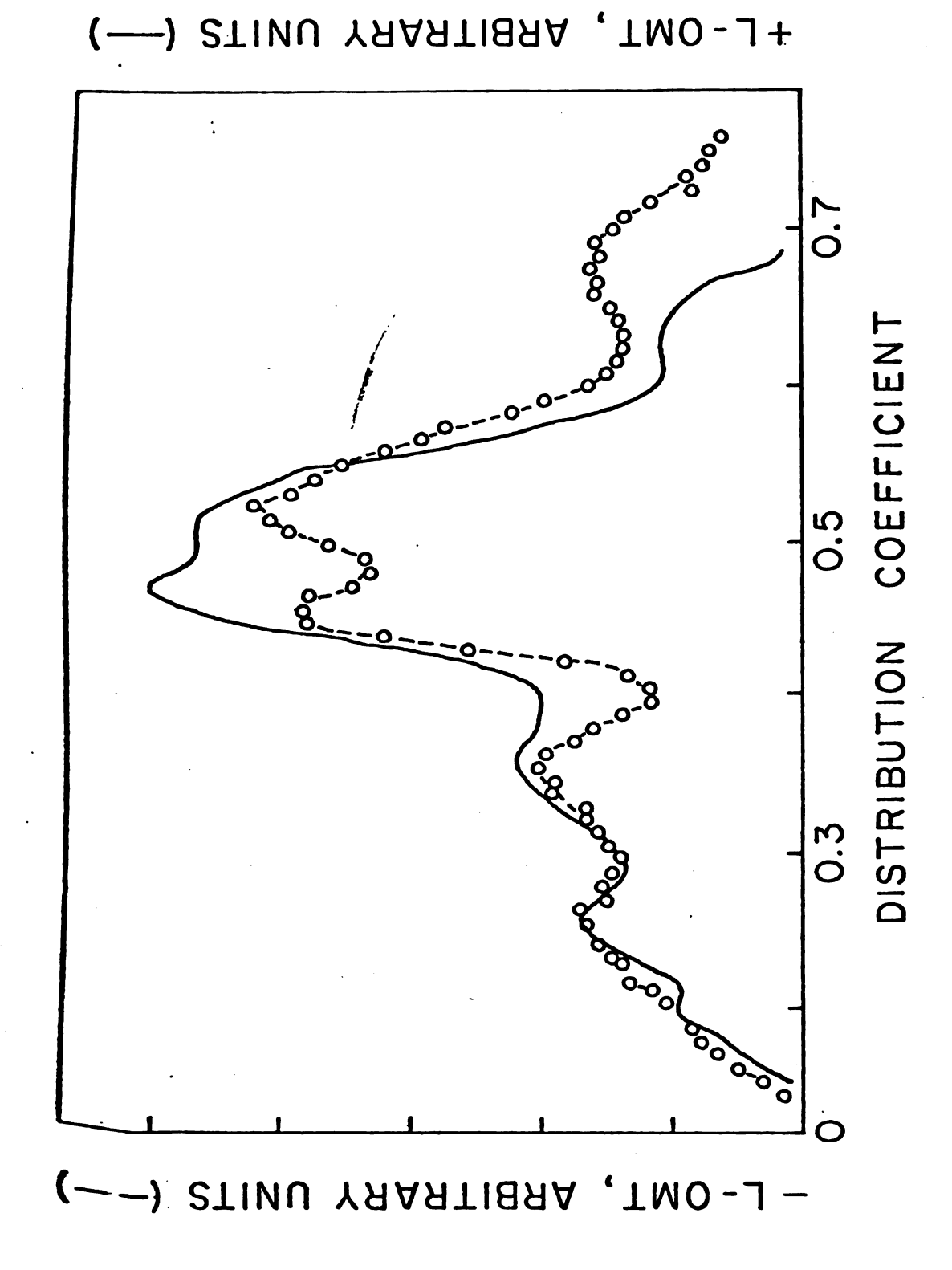


Figure 29 The residual profile obtained by subtraction of  $\alpha$  and total globin size distributions

obtained by simultaneous incorporation of L-[ $^{14}$ C]-isoleucine and L-[ $^{3}$ H]-tryptophan into nascent polypeptides in the presence (----) and absence (----) of L-O-methylthreonine.



the tryptophan labeled peptides is confirmed by the fact that subtraction of isoleucine labeled size distribution profile from the total tryptophan profile in both the control and L-OMT incubation results in residual profiles which are essentially identical (Figure 29).

## Perturbation of the Nascent Polypeptide Size Distribution with a Complimentary Deoxyribooligonucleotide

An assessment of the ability of a selected mRNA complimentary deoxyribooligonucleotide to compete with and modify mRNA secondary structure and thereby cause a perturbation of the nascent peptide size distribution was conducted. The reticulocyte lysate of a  $\beta_{112}$  Val/Val rabbit was incubated with tetradeoxycytidylic acid at a concentration of 500  $\mu$ M at 26°C and nascent polypeptides were labeled with L-[³H]-tryptophan. A parallel control incubation was conducted in the absence of the tetranucleotide and labeled with L[¹⁴C]tryptophan. After termination of the reaction with medium B plus cycloheximide and sparsomycin, the [³H] and [¹⁴C] labeled incubation mixtures were mixed and nascent peptides Purified and analyzed as a single sample to evaluate the effect of the tetranucleotide on the total  $\alpha$  and  $\beta$  nascent chain size distribution.

A second experiment was performed in exactly the same manner except that L-[ $^3$ H]Ile and L-[ $^1$ 4C]Ile were used to label the lysates incubated in the presence and absence of tetradeoxycytidylate (tetra C), respectively, to evaluate the effect, if any, of the oligonucleotide on the  $\alpha$  nascent peptide size distribution. The rationale behind this experiment is treated in detail in the discussion section.

Figure 30 shows the results of L-tryptophan labeling of the reticulocyte polysomes in the presence and absence of tetra C. This profile reflects several shifts in the composite L-[3H]-tryptophan labeled nascent peptide size distribution as compared to the control. There is a diminution of nascent peptides corresponding to Kd 0.28 and an increase in components migrating on the gel column at Kd 0.40. A second shift occurs in the region of lower molecular weight peptides. Nascent peptide components migrating at Kd 0.70 and 0.73 are seen to be shifted to higher molecular weight as reflected by a similarly shaped distribution of compounds appearing at Kd 0.64 and 0.69. A parallel experiment involving labeling of  $\alpha$  polysomes with L-[3H] or L-[14C] isoleucine with and without tetra C is shown in Figure 31. As can be seen from this figure there is no apparent difference in the control and tetra C treated isoleucine labeled lysates indicating that no effect of incubation of  $\alpha$ -globin polysomes with tetra C is observable under conditions where the L-[3H]-tryptophan labeled size distribution is effected. The B mascent peptide size distribution was the only one significantly perturbed by the presence of tetradeoxycytidylic acid.

## Analysis of the Nascent Polypeptide Size Distribution as a Function of Polysomal Size

Another approach used to define the effects of physiological levels of mRNA ribosomal loading on the nascent peptide size accumulations employed analysis of the nascent peptide size distributions present on polysomes of various size classes. A 15-50% sucrose gradient containing the elongation inhibitors cycloheximide and sparsomycin to prevent

Figure 30 The elution profile of globin nascent polypeptides which had been labeled in the presence

(0---0) or absence (0---0) of tetradeoxycytidylate.

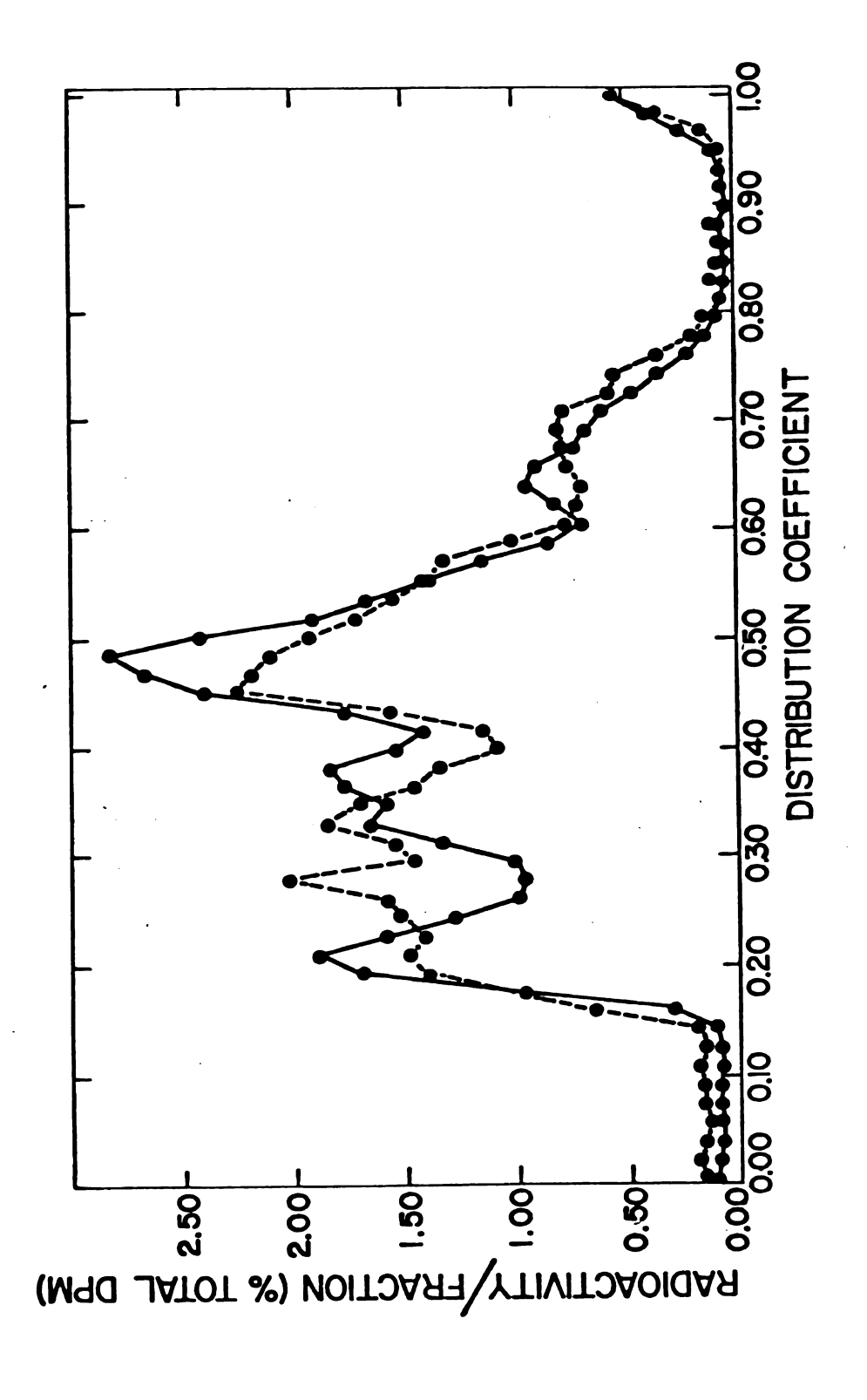
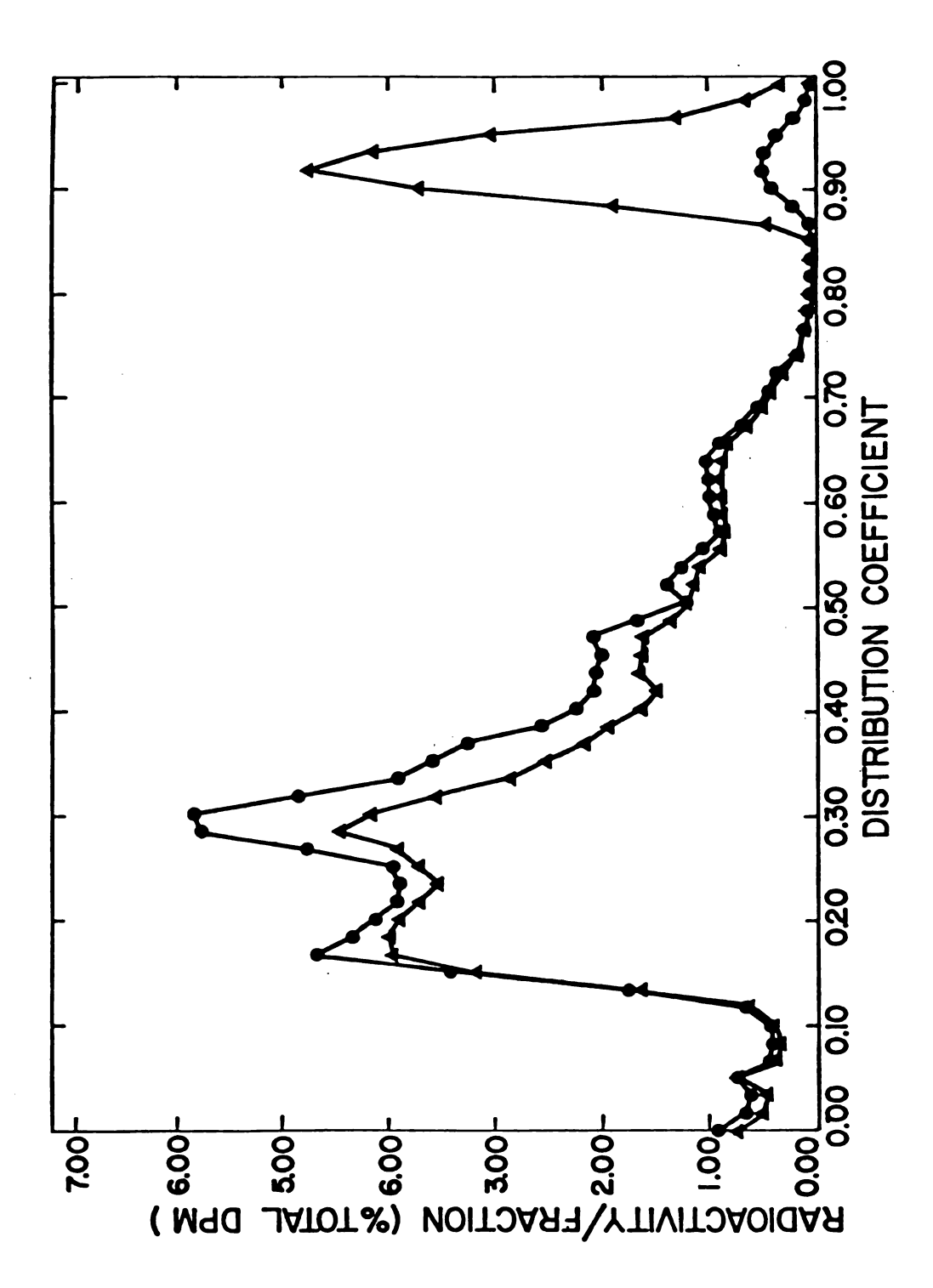
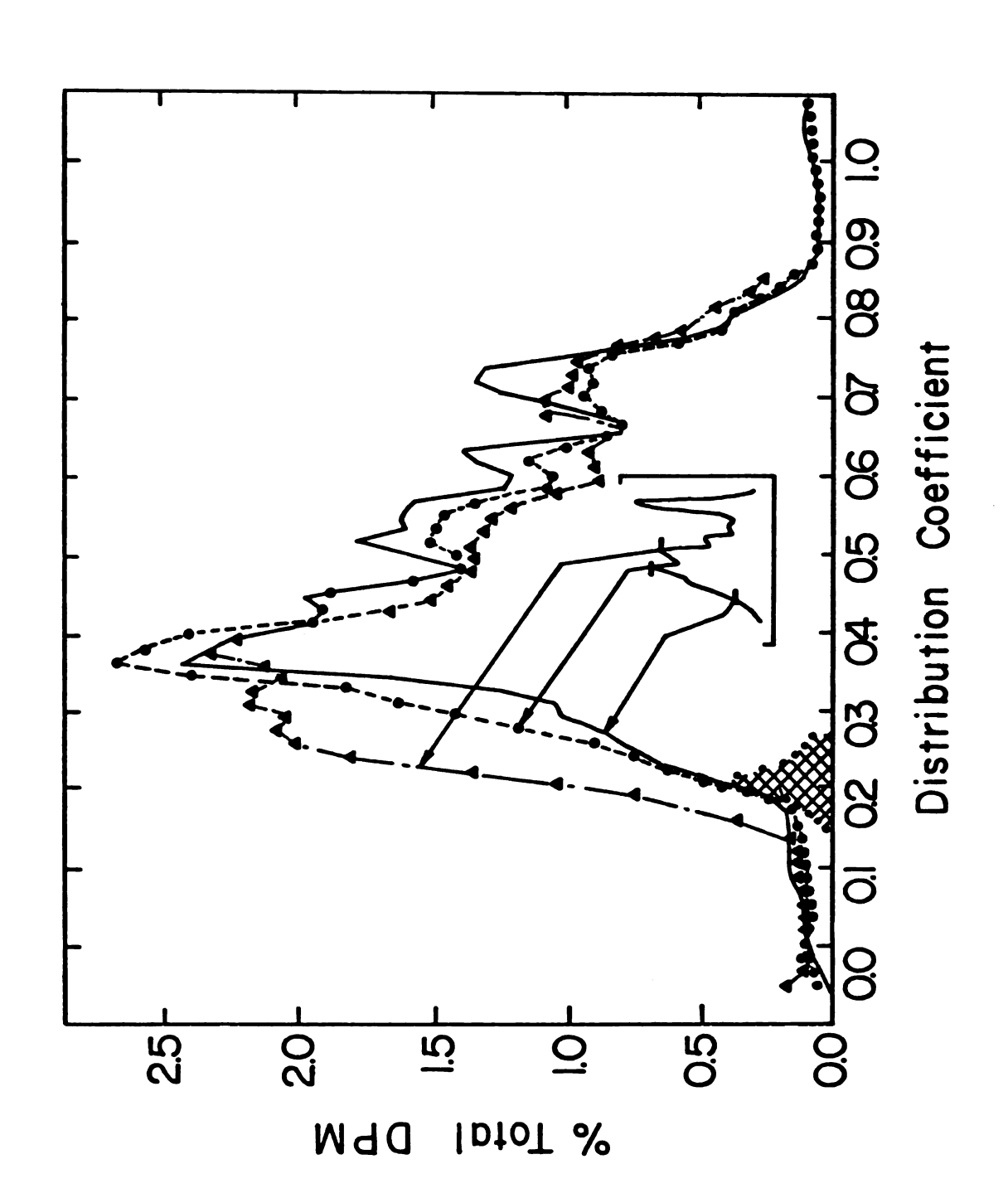


Figure 31 The elution profile of  $\alpha$  globin nascent polypeptides which had been labeled in the presence (o---o) or absence ( $\Delta$ --- $\Delta$ ) of tetradeoxycytidylate.



ribosomal run off during elongation and 0.1 mg/ml denatured globin polypeptides included as carrier material to insure against degradation of nascent peptides was used. Figure 32 typifies the results of a number of different experiments. While size distribution of the smaller nascent peptides looks essentially unaltered in the 3 size classes of polysomes examined (dimers and trimers, tetramers and pentamers and greater) there is a reproducible "filling in" of the mascent chain size distribution profile in the region of the larger nascent peptide of Kd 0.4 to 0.5. just to the 3' side of the large accumulation at Kd 0.35. A unexpected result is the reproducible demonstration of a decreasing amount of nascent chains of the size class corresponding to completed globin chains as one examines polysomes of increasing size. This observation is consistent with facilitated release or translocation of completed (or nearly completed) globin chains on larger a polysomes, possibly due to a ribosome encountering reduced secondary structural interactions on the mRNA of a polysome possessing a larger total ribosomal density. The degree of reduction of completed chains on larger polysomes may be slightly underestimated since lighter polysomes (e.g., monomers, dimers) would normally be expected to have a larger proportion of their numbers in a state of relatively higher ribosomal density at the 5' end (smaller nascent peptides) of the coding region. This effect is due to the increased probability that an inhibition which is translating at a decreased rate will be located closer to the 5' terminus of the mRNA during the interval of time necessary for a new initiation event to occur relative to uninhibited ribosomes moving at a normal translocation rate. This effect is most noticeable in dimers rather than in higher polyribosomes.

tetramer, (----); and pentamer and heavier (----) regions of the sucrose density gradient Figure 32 The elution profiles of  $\alpha$  globin nascent peptides isolated from dimer (----); trimer and polysome profile. Cross-hatched area indicates position of elution of globin standard.



It is possible that the reduction of the largest nascent peptide size classes up to and including completed globin is attributable to increased ribosomal "run off" as a function of increasing sucrose concentration, or viscosity effects or distance traversed during sedimentation in the gradient material. These seem unlikely since all size polysomes spend an approximately equal amount of time out of the milieu of the lysate.

In order to further examine the effect of polysomal size and ribosomal density on the nascent peptide size distribution and to circumvent the possibility of artifactual loss of nascent peptides during sucrose gradient centrifugation, an alternative approach was used. The  $\beta_{112}$ Val/Val reticulocyte lysate was incubated with 100  $\mu$ Ci of L-[3H] isoleucine and a concentration of aurine tricarboxylic acid sufficient to give 80% inhibition of protein synthesis (0.5 x  $10^{-6}$  M) (Figure 33). An incubation with 10.0  $\mu$ Ci of L-[14C]-isoleucine in the absence of the inhibitor was conducted in parallel with the inhibited sample. Following termination of the incubations with Medium B and cycloheximide plus sparsomycin the samples were mixed and treated as a single preparation. The results of this experiment are presented in Figure 34. Incubation of the lysate with aurine tricarboxylic acid is seen to cause a relative increase in the amount of nascent peptides towards the high molecular weight species including completed globin chains and especially in regions of the prominent mascent peptide accumulations (at Kds 0.34, 0.50, and 0.57 relative to the accumulation observed at Kd 0.71. The increase in the ratio of high molecular weight peptides relative to smaller peptides on smaller polysomes is consistent with the results obtained with inhibitors of elongation and the polysomal fractionation

Figure 33 The effect of 0.5 x  $10^{-6}$  M aurine tricarboxylic acid (ATA) on the rate of

incorporation of L-[ $^3\text{H}$ ]-isoleucine into TCA precipitable material. Control (o---o); 0.5 μM ATA (Δ---Δ).

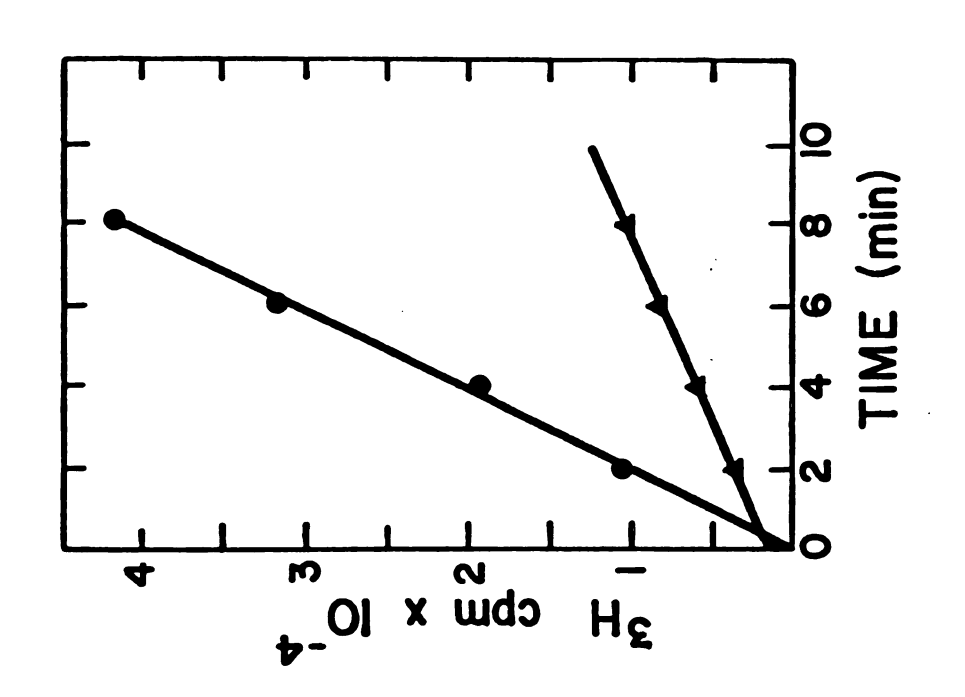
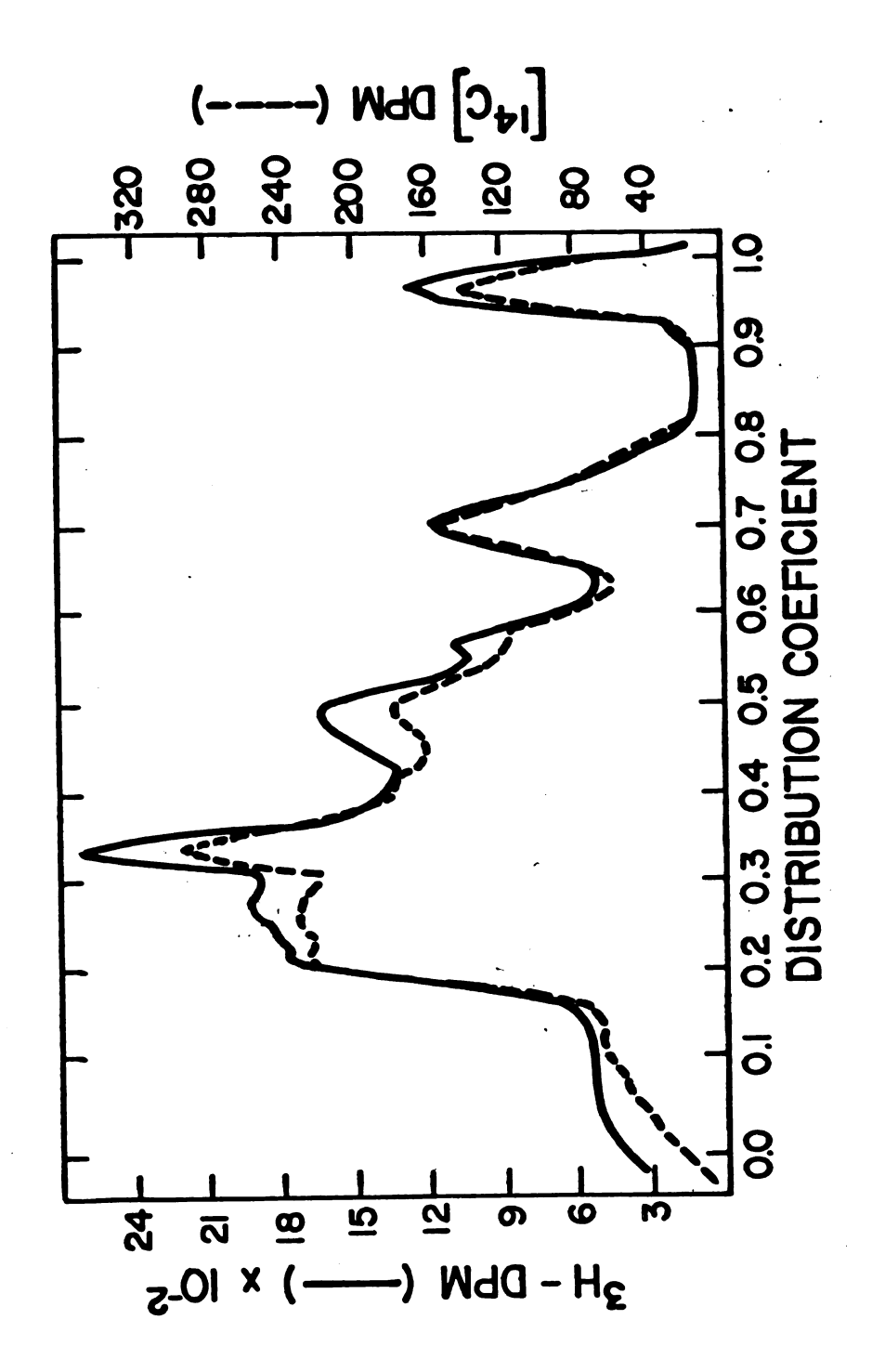


Figure 34 The elution profile of nascent peptides from aurine tricarboxylic acid inhibited (small molecular weight) polysomes as compared to the nascent peptide size distribution of inhibited polysomes. [ $^{14}$ C] control (---), [ $^{3}$ H] ATA treated (----).



(below) but approach the phenomenon differently and extend the data to very small polysomes, without exposure of the polysomes to any manipulations not encountered during a standard peptidyl tRNA preparation.

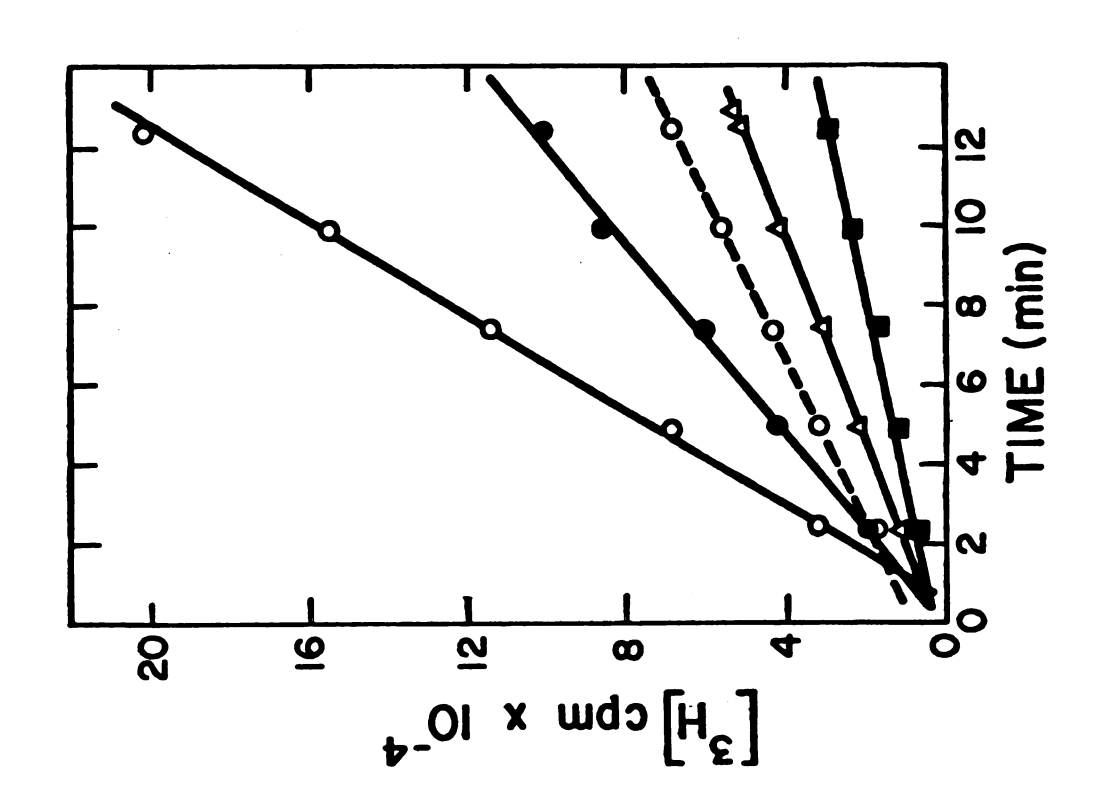
## Inhibition of Globin Translocation by Sparsomycin and Gougerotin

Inhibition of translocation to 28-30% of control by the elongation inhibitors gougerotin, sparsomycin and cycloheximide was used to increase ribosomal density on the mRNA in order to determine whether the degree of ribosomal loading of the mRNA would reflect a reduction in the nonuniformity of the nascent peptide size distribution due to an effect of Queuing of ribosomes along the mRNAs.

Preliminary studies of the dependence of elongation inhibition with inhibitor dosage in the  $\beta_{112}$  Val/Val lysate system was conducted with cycloheximide, sparsomycin and gougerotin. Levels of inhibitor necessary to give approximately 70% inhibition of protein synthesis were determined for all three and the dose dependence established for sparsomycin and cycloheximide (Figures 35 and 36). For the case of cycloheximide use of L-[14]-isoleucine as well as L-[3H]-isoleucine established that  $\alpha$  globin synthesis was inhibited with the same dose dependence as total ( $\alpha$  plus  $\beta$ ) globin synthesis (Figures 37-39). These data were reexamined by incubation of the lysate with the amounts of cycloheximide, gougerotin or sparsomycin expected to give 70-75% inhibition as is depicted in Figure 40. All these data indicate that this lysate responds, as expected, to the levels of the inhibitors administered (70).

In subsequent experiments, isoleucine was used as the label so that the  $\alpha$  globin nascent peptides were being considered with either

μM sparsomycin (●──●); 0.20 μM sparsomycin (△──△); 0.30 μM sparsomycin (■──●); and 0.35 incorporation of L-[ $^3$ H]-leucine into TCA precipitable material. Control (o---o); 0.10 Figure 35 The effect of low levels of sparsomycin and  $0.35~\mu\text{M}$  gougerotin on the rate of  $\mu M$  gougerotin (o---o).



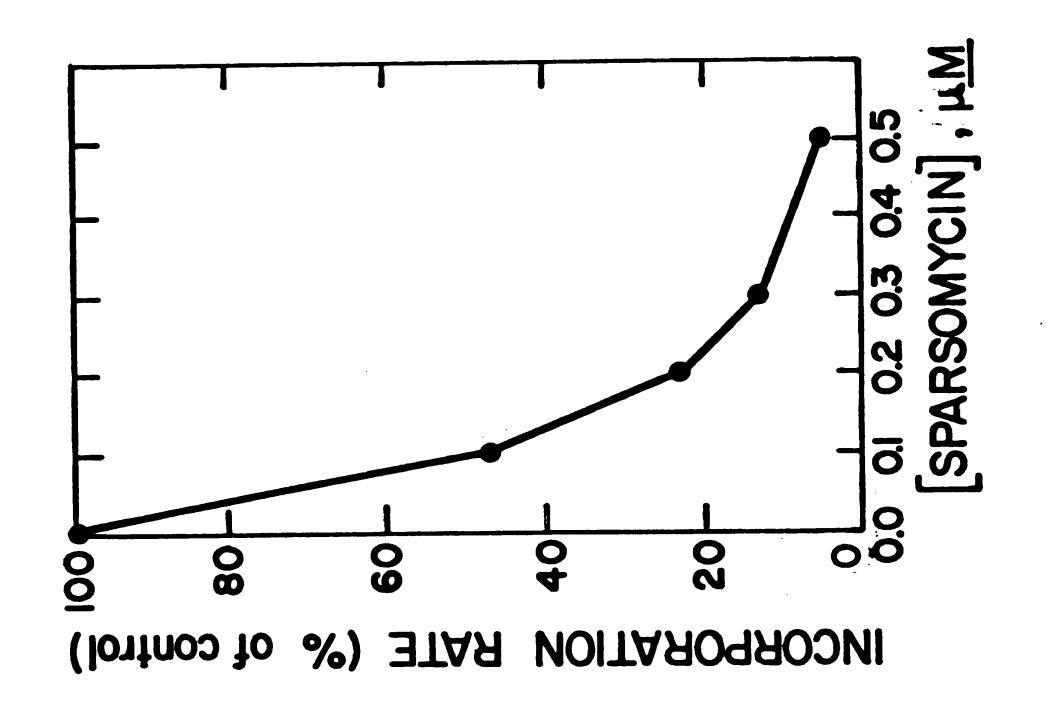


Figure 37 The effect of cycloheximide concentration on the rate of incorporation of L-[ $^3$ H]-leucine into globin. Control (0--0), 0.20 μΜ, (0--0); 0.35 μΜ (Δ--Δ); 0.50 μΜ (σ--σ).

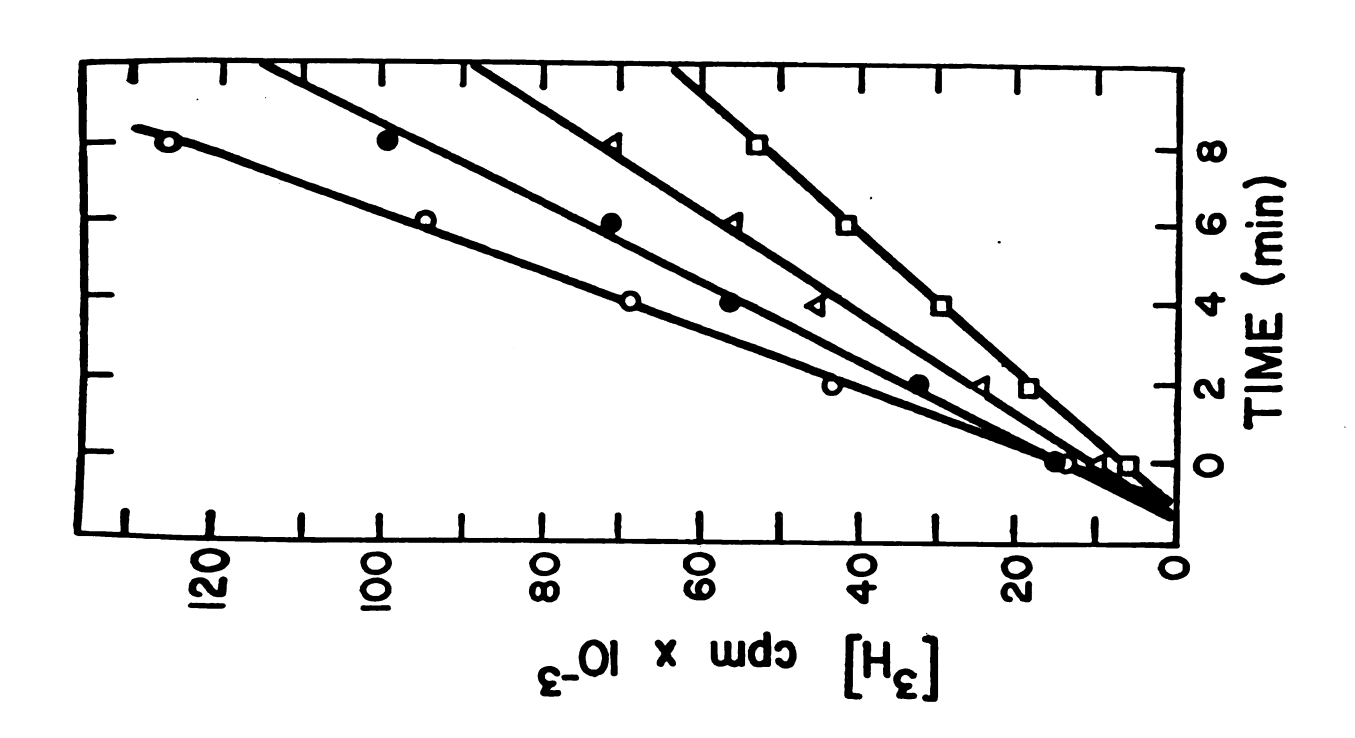
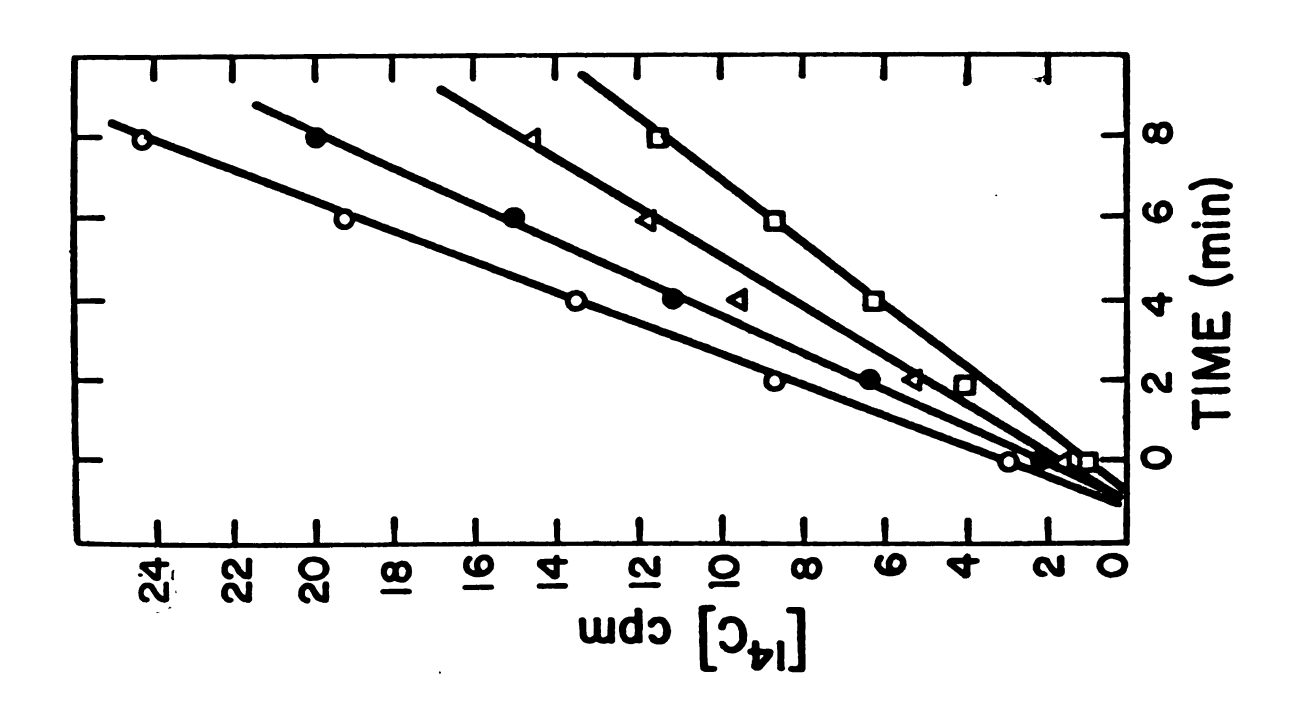


Figure 38 The effect of cycloheximide concentration on the rate of incorporation of

[14c]-isoleucine into  $\alpha$  globin. Control (o---o), 0.20  $\mu$ M, (o---o); 0.35  $\mu$ M ( $\Delta$ --- $\Delta$ ); 0.50 µM (p-0).



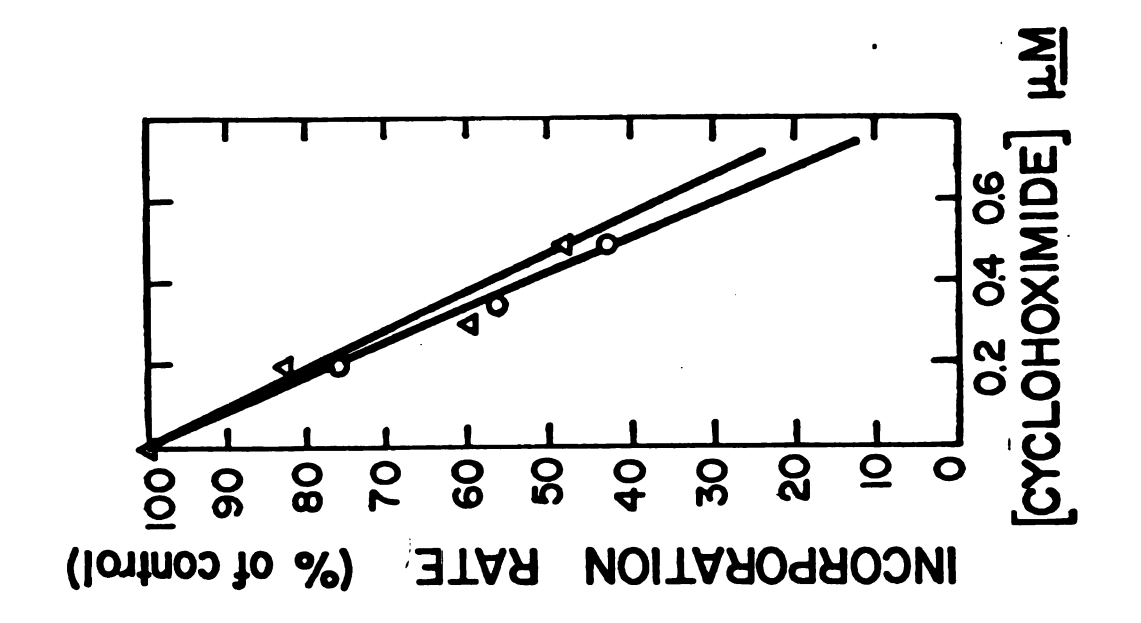
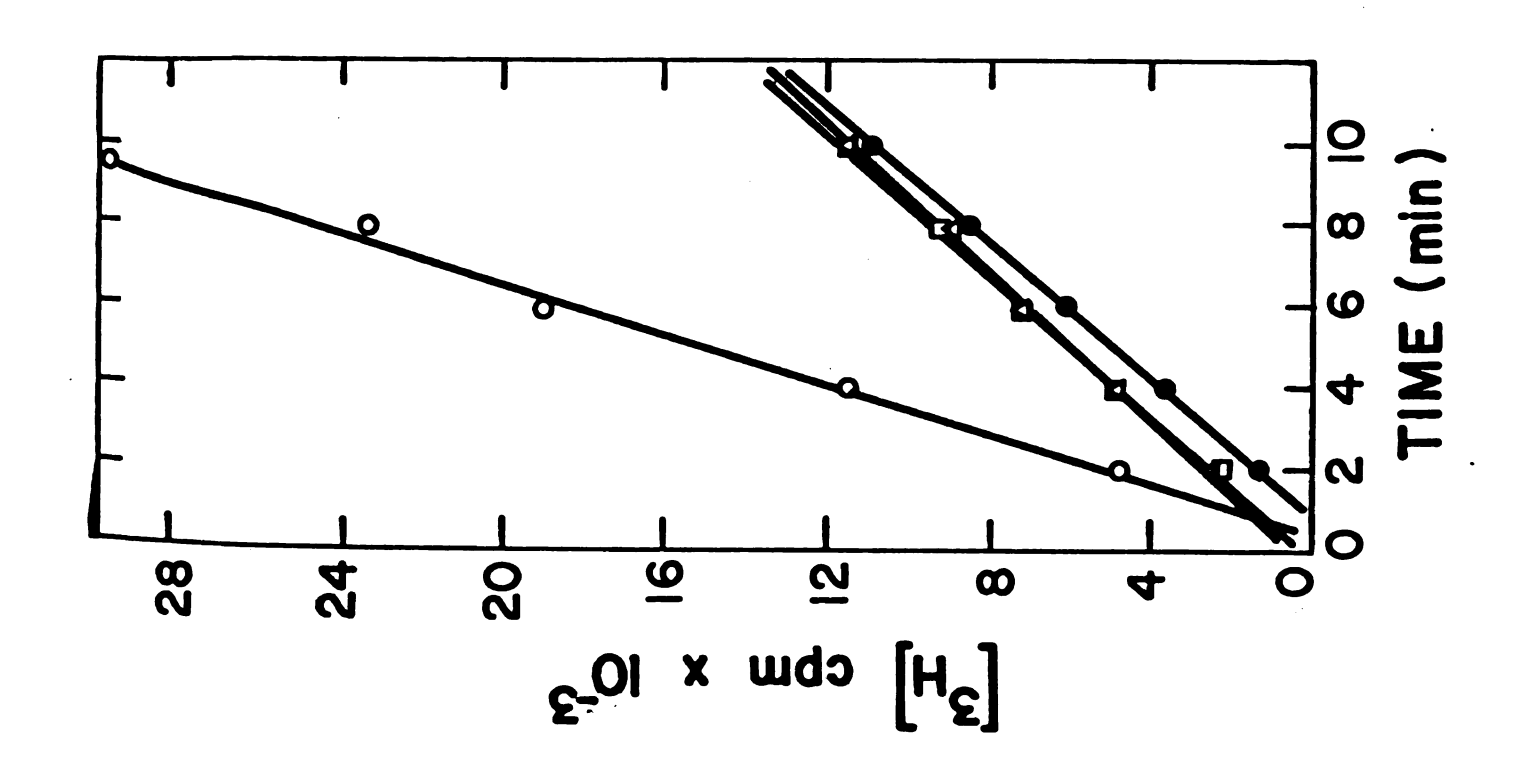


Figure 40 Demonstration of the levels of cycloheximide, sparsomycin and gougerotin which result in

approximately 70% inhibition of globin synthesis. Control (o---o), 0.18 µM sparsomycin  $(\Delta - \Delta)$ ; 0.35  $\mu$ M gougerotin ( $\bullet - \bullet$ ); 0.61  $\mu$ M cycloheximide ( $\sigma - \sigma$ ).

144



L-[<sup>]</sup>

spars

prote

addit

were catio

resul

comno.

tides. toward

peak 1

peption an obs

Which

mal ti globir

on ter

pletec

peption

termin

the do

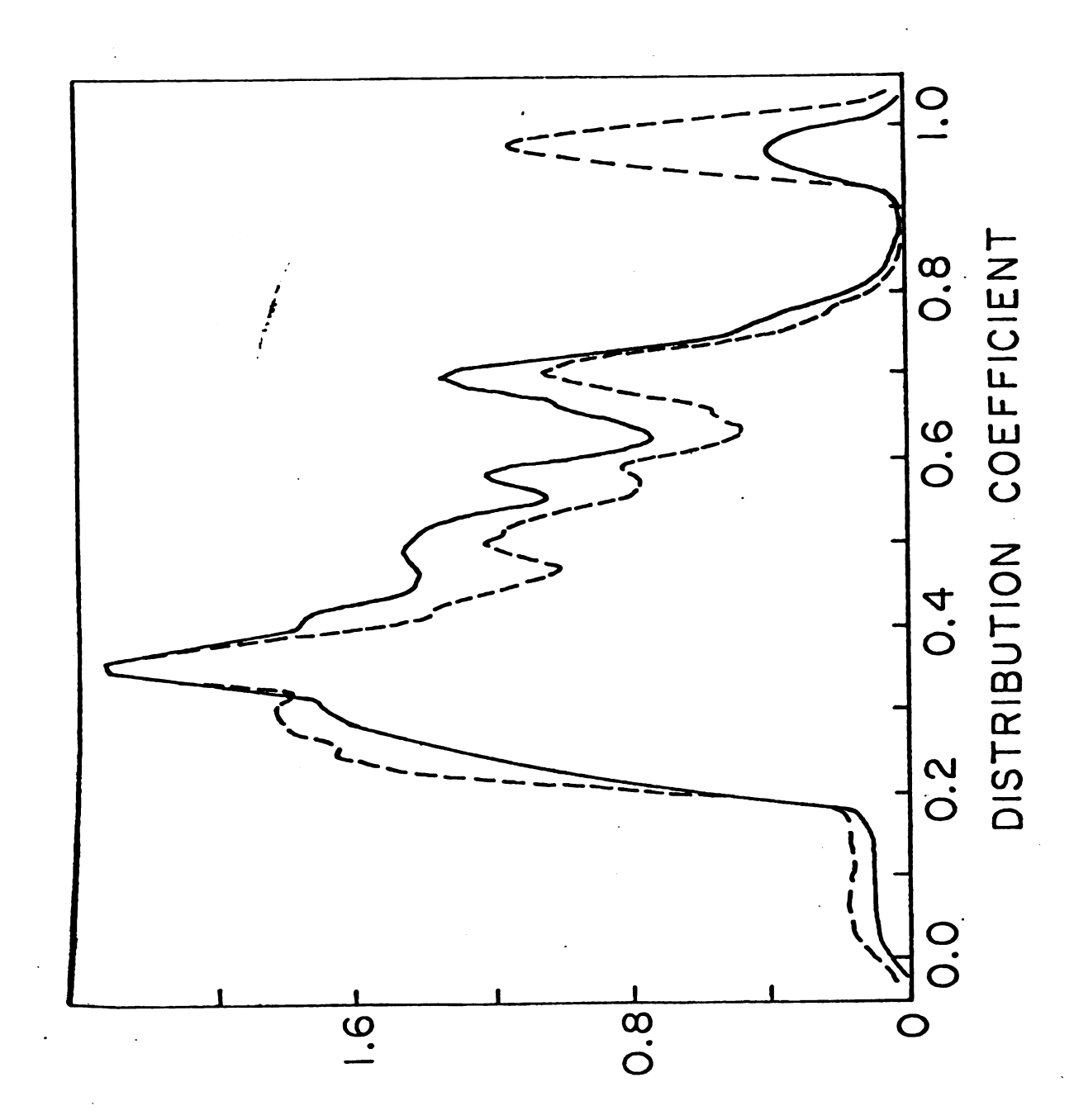
(71). Peptid

<sup>sol</sup>ely

L-[14C]-isoleucine labeled mascent peptides as the control or L-[3H]-isoleucine for inhibited treatments. Sufficient gougerotin or sparsomycin was used to give 70% inhibition of the overall rate of protein synthesis. These reactions were terminated at 10 minutes by addition of Medium B plus cycloheximide and sparsomycin. The reactions were then mixed and treated as one sample throughout the steps of purification and analysis of the peptidyl tRNA. Figure 41 and 42 show the results of the sparsomycin and gougerotin incubations compared to a common internal standard of [14C]-labeled control nascent polypeptides. These figures illustrate that ribosomal density was increased towards the smaller peptides but very little effect was observed on the peak to valley ratios except for a reproducible filling in nascent peptides at Kd 0.37 to 0.5 behind the prominent accumulation at Kd 0.34, an observation which seems to be a common characteristic of any treatment which increases ribosome density on the mRNA or conversely slows ribosomal translocation (below). A change is noted in the region of completed globins which may be due to slightly reduced effects of these inhibitors on termination relative to elongation resulting in a depletion of completed nascent peptides relative to slightly smaller sized nascent polypeptides. It should be noted however, that other studies have indicated that, where examined, the peptidyl transferase activity and the peptide termination activity of ribosomes exhibit similar properties including the dose dependence of their inhibition with sparsomycin concentration (71). This suggests that the decrease in high molecular weight nascent peptides on larger polysomes relative to smaller polysomes may be caused solely by increased polysomal size, a result that is consistent

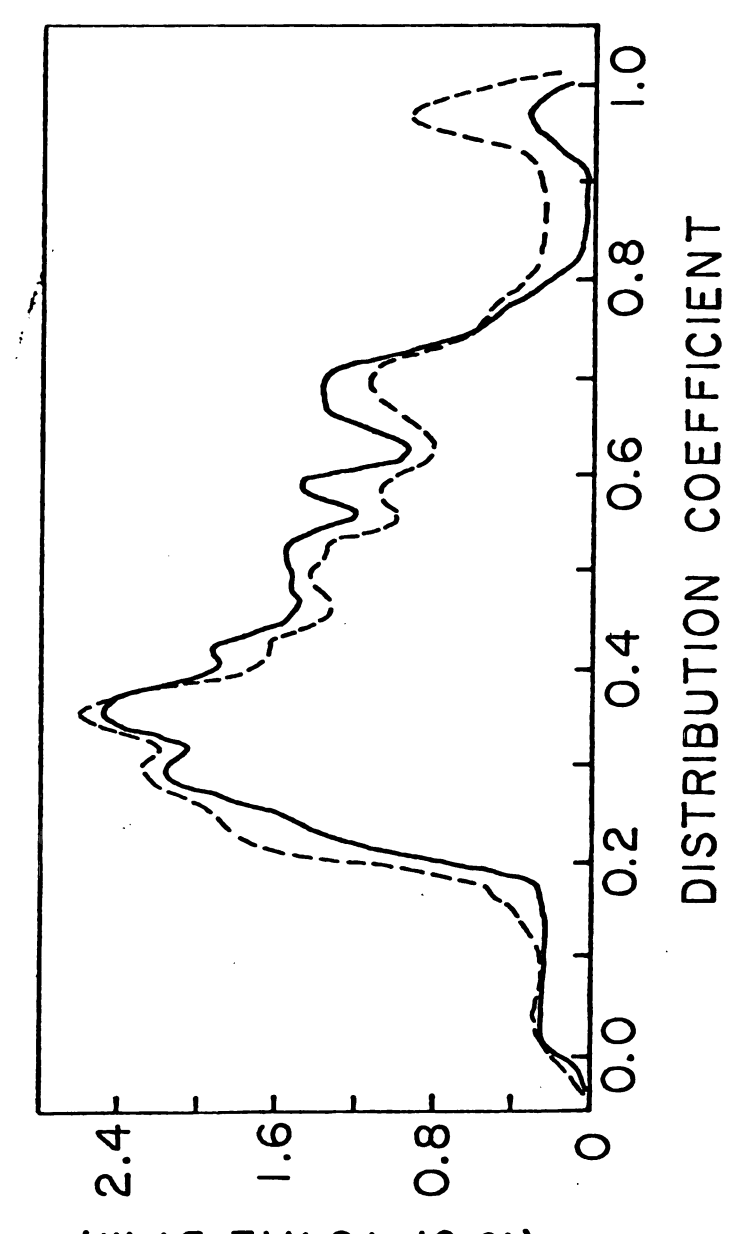
concentration of sparsomycin which results in 70% inhibition of the globin ribosomal Figure 41 The elution profile of  $\alpha$  globin mascent polypeptides which have been treated with a elongation rate. Control, (---); 70% inhibited (---).

RADIOACTIVITY/FRACTION, (% TOTAL DPM)



concentration of gougerotin which results in approximately 70% inhibition of ribosomal Figure 42 The elution profile of  $\alpha$  globin mascent polypeptides which have been treated with a elongation. Control (---); 70% inhibited, (---).

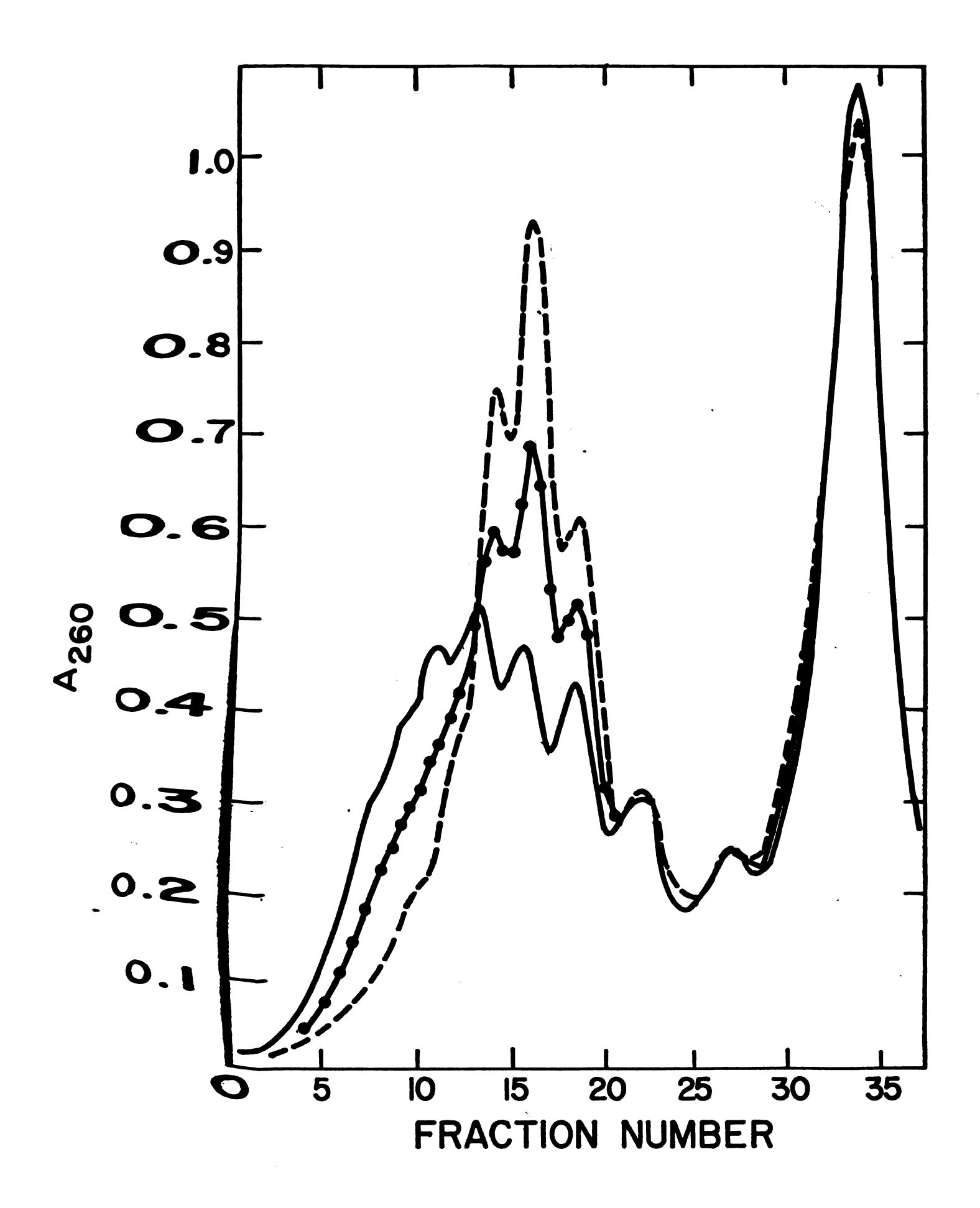
RADIOACTIVITY/FRACTION, (M90 JATOT 10 %)



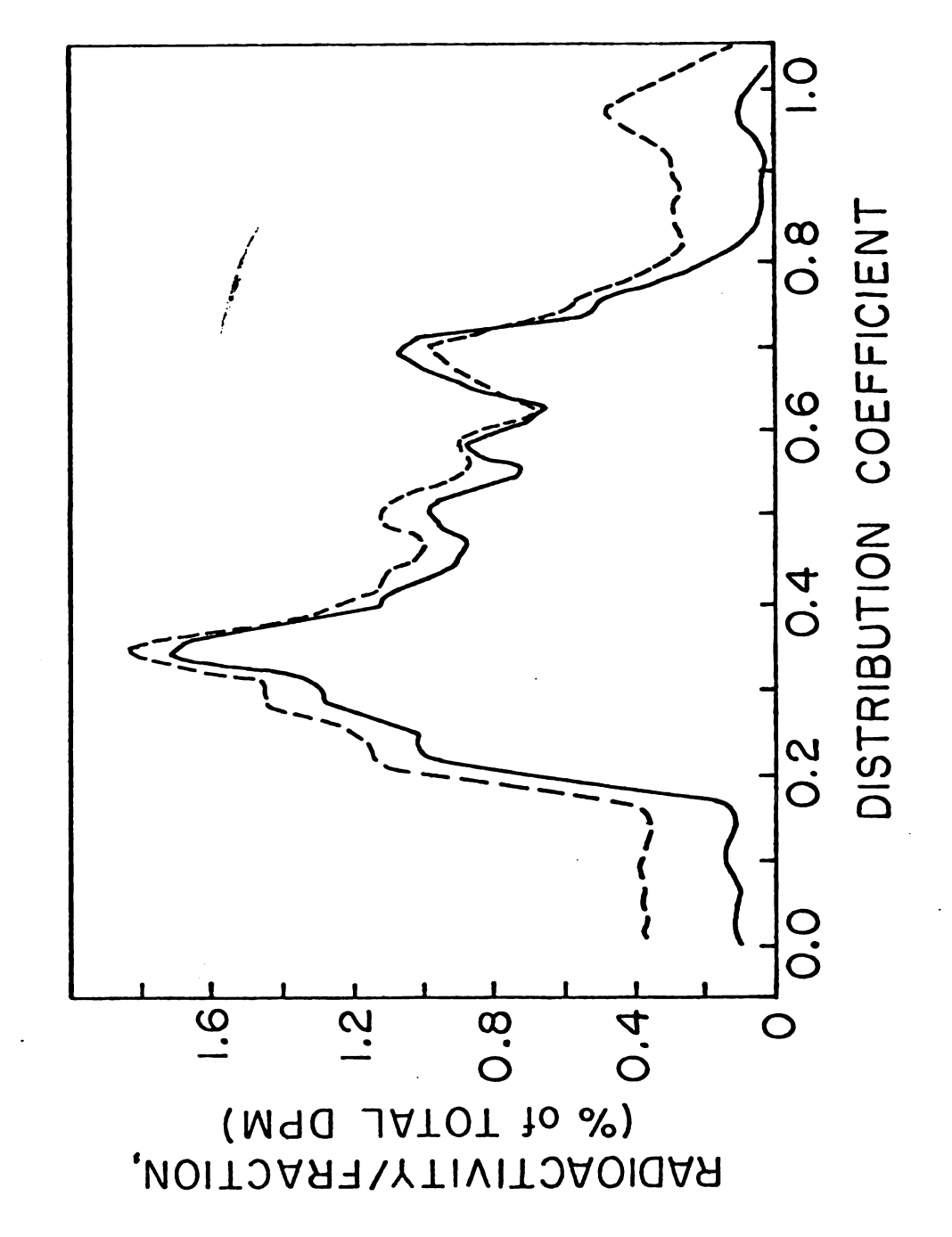
with the previous experiments.

An experiment was designed to investigate and compare the effects of the inhibition of ribosomal translocation on different nascent chain size distribution of different size class polysomes. Separate aliquots of 1 ysate were incubated in the presence or absence of sufficient sparsomycin to slow translocation to 30% of control values. Incubations were halted as usual, mixed and polysomes resolved, as before, by centrifugation on a 15-50% sucrose gradient. Parallel incubations of equal volume were also sedimented separately providing uninhibited and inhibited polysome profiles as shown in Figure 43. As can be seen, the polysomal profile of the sparsomycin inhibited reaction plus the uninhibited control profile when added together result in the observed mixed polysomal Profile. Polysomes of equal sedimentation value were obtained from the **control** and sparsomycin inhibited reactions and nascent polypeptides Prepared from the pooled fractions as indicated. Figures 44, 45, and 46 show the polysome profiles for low (dimers), medium (3-4 mers) and high (5-6 mers) polysomes. The control curves reflect the previously observed dependence of decreasing of high molecular weight nascent polypeptides with increasing polysome size as expected. Added to this trend is an increased filling in of the region from Kd 0.4-0.5 by the sparsomycin inh ibited ribosomes relative to uninhibited ribosomes on polysomes of the same sedimentation value. This latter effect seems to be due to additional "filling in" by retarded ribosomes behind the Kd 0.35 peak augmenting the effect of polysome density density alone on uninhibited Polysomes as observed above (Figure 41). An additional depletion in the region of completed globins is observed with inhibited ribosomes

separate experiment. The intermediate curve is the profile of a mixture of polysomes from The sedimentation profiles of control reticulocyte polysomes ( ----) and polysomes which equal volume of inhibited and control polysomes (•—•) used in the subsequent experihad been inhibited to 30% of the control elongation rate with sparsomycin (+--) in a ments. Figure 43

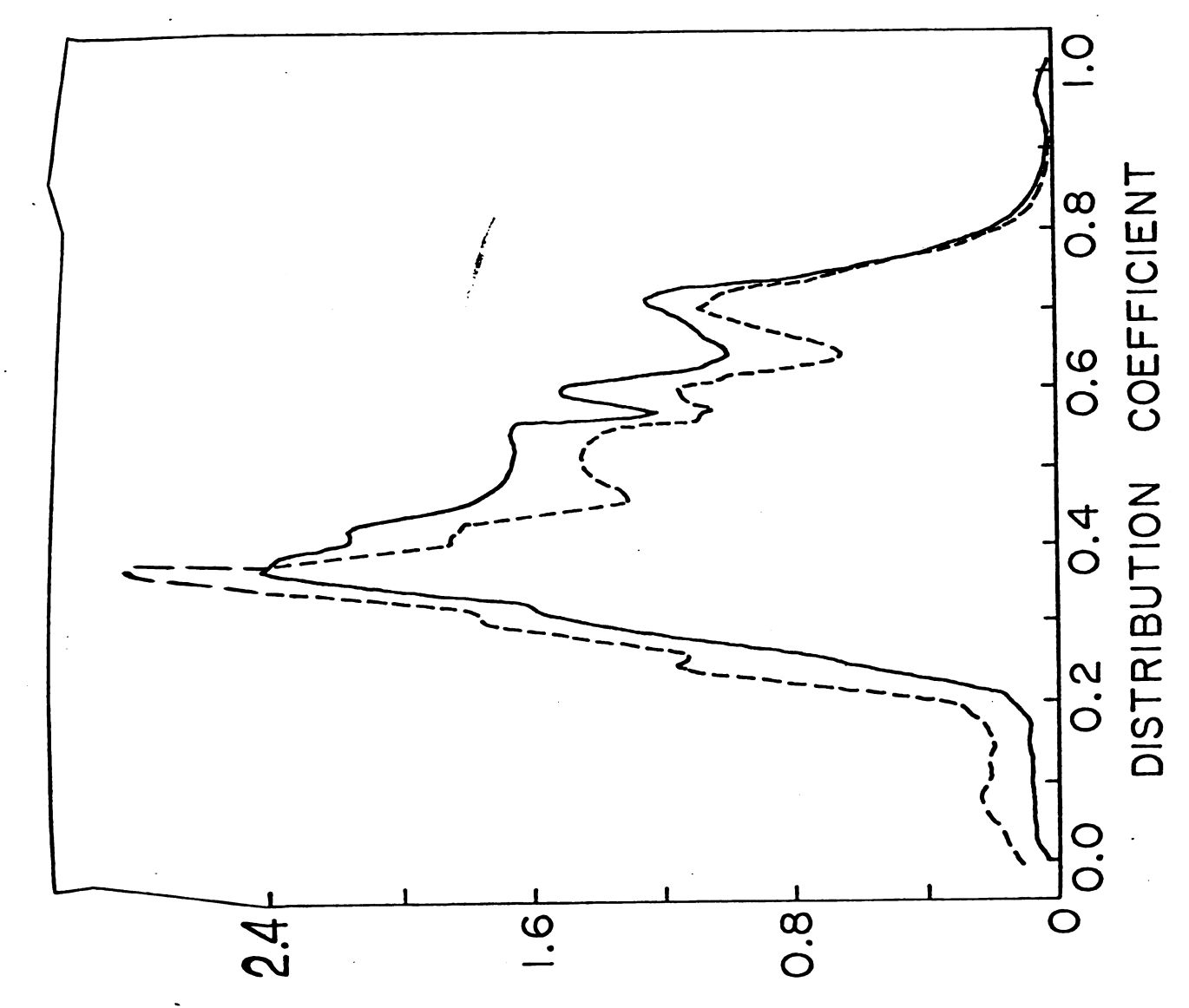


profile. The solid line reflects the size distribution resulting from sparsomycin treated dimers and the broken line reflects the size distribution from uninhibited polysomes of peptides isolated from the dimer region of the sucrose density gradient sedimentation Figure 44 The effect of low levels of sparsomycin on the size distribution of  $\alpha$  globin mascent the same sedimentation value.  $[^{14}\mathrm{C}]$  control (---);  $[^{3}\mathrm{H}]$  sparsomycin treated



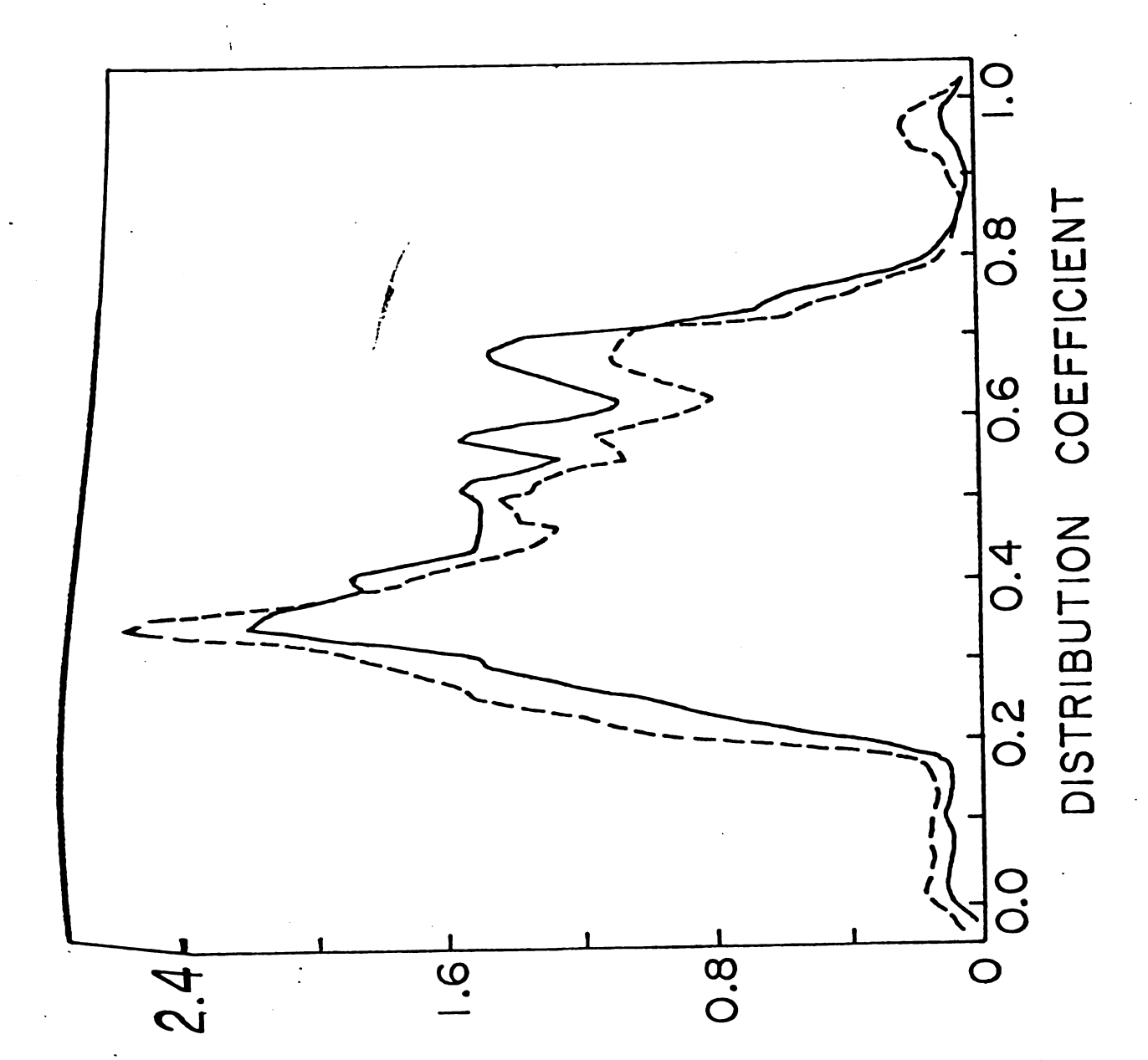
peptides from the trimer and tetramer region of the sucrose density gradient polysome Figure 45 The effect of low levels of sparsomycin on the size distribution of  $\alpha$  globin mascent profile. [14c] control (---); [3H] sparsomycin treated ( —— ).

RADIOACTIVITY/FRACTION, (% TOTA \_\_ DPM)



peptides isolated from the pentamer and hexamer region of the polysome profile.  $\lfloor 14 \zeta \rfloor$ Figure 46 The effect of low levels of sparsomycin on the size distribution of  $\alpha$  globin nascent Control ( $\longrightarrow$ ); [ $^{3}$ H] Sparsomycin treated ( $^{---}$ ).

RADIOACTIVITY/FRACTION, (% TOTAL DPM)

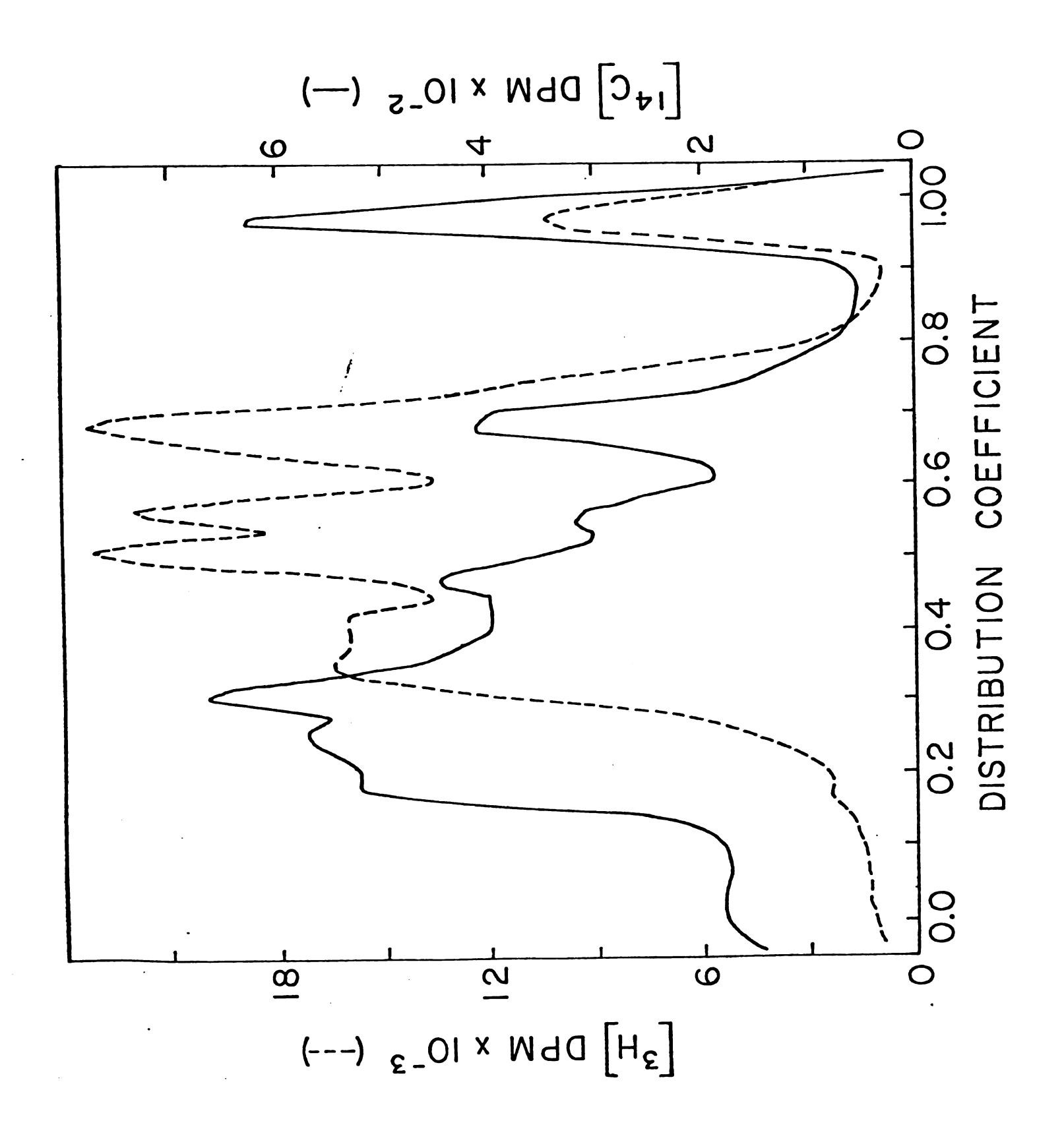


compared to uninhibited polysomes of the same sedimentation value and supports the possibility of a slight a differential effect of the inhibitor on elongation relative to termination.

## Thermal Perturbation of the Nascent Polypeptide Size Distribution

Since the studies with elongation inhibitors were designed to perturb the nascent peptide size distribution indirectly via the effect of the ribosomes on the mRNA secondary structure, a complimentary approach was sought which would allow perturbation of the nascent peptide size distribution via a direct effect on mRNA secondary structure. This was attempted by use of a temperature "shift-down" of steady state labeled translating polysomes. First, to insure that reinitiation would occur at lowered temperatures nascent peptides were labeled in an incubation conducted at 15°C for 10 minutes (Fig. 47). Steady state labeling was not attained; however, it appears that ribosomes were initiating and slowly moving into the mRNA molecule. Peaks and valleys obtained correspond approximately but not exactly to those of the internal standard incubated for the same time at 37°C. It is interesting to note that ribosomal density is very high at the 5' region relative to the 3' areas (which have not become labeled) but the mascent peptide size nonuniformity was not eliminated. Subsequent experiments were performed by thermal "shift-down" of steady state labeled polysomes from 37°C down to 22°C or 15°C. For this analysis, separate aliquots (333 microliters) of the  $B_{112}$  Val/Val lysate containing exactly 100  $\mu$ Ci of L-[ $^3$ H]isoleucine or 30  $\mu$ Ci of L-[ $^{14}$ C]-isoleucine were labeled at 37°C for 5.5  ${f minutes}$  and then the tritium containing sample was shifted down to the appropriate temperature (15°C or 22°C) and incubated for another 4.5

Figure 47 The elution behavior of  $\alpha$  globin mascent polypeptides synthesized at 15°C (---) as compared to the elution behavior of  $\alpha$  nascent peptides labeled at 37°C ( —— ).



minutes before both reactions were terminated. The [3H]-Ile labeled samples (15 and 22°C) were then mixed with equal aliquots of the L-[14C]-isoleucine labeled lysate and nascent polypeptides prepared as double label experiments. Analysis of the  $\lceil 3H/14C \rceil$  ratio and total radioactivity content in the purified peptidyl tRNA and nascent polypeptides indicated that no differential loss of [3H] nascent chains occurred during the 37°C to 22°C shift and the 37°C to 15°C shift (Table 4). Results of the analysis of the size distribution for these samples are presented in Figures 48 and 49. Thermal "shift-down" revealed a progressive diminution of nascent peptides of size class corresponding to a Kd from 0.45 to 0.55, an increase of the relative amplitude of the accumulation peak at Kd 0.35 and relative diminution of nascent polypeptides at Kd value of less than 0.35. These observations are consistent with increased hinderance to translocation at regions of the α mRNA corresponding to the Kd values of 0.60 and 0.35 with relatively little effect elsewhere in the profile. These results are also consistent with a decreased capacity of ribosomes to open hairpin structures and/or an increased stability of certain hairpin structures at reduced temperatures. As in the previous experiments, we cannot exclude other possibilities which could result in a redistribution of ribosomal density along a mRNA, such as depletion of one or more amino acyl-tRNAs or a relative change in affinities of one or more tRNAs for the "A" site of the translocating ribosome. It is known, however, that approximately 12% of the total hyperchromicity of the globin mRNAs during thermal denaturation occurs in the temperature range from 15-37°C (15) and the effect of a change in temperature on the stability of existing helical structures

TABLE 4

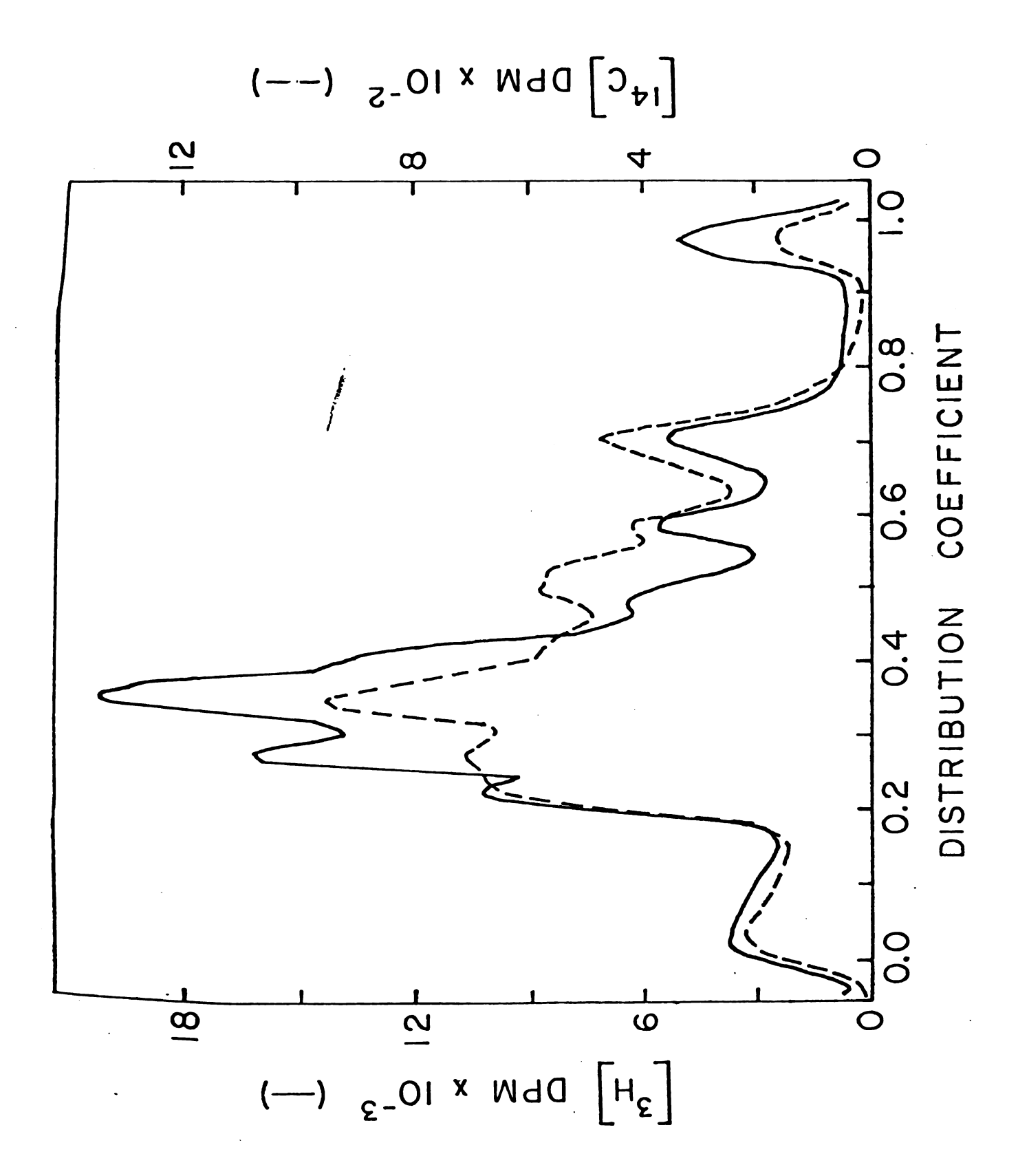
(37°C 15°C)/(37°C 22°C) The Recovery of [ $^3\mathrm{HJ}$ dpm Present in Peptidyl tRNA Relative to Control dpm ([ $^{14}\mathrm{CJ}$ ) From Polysomes Following Thermal Shift to 22°C and 15°C From 37°C Differential Loss (%) 0.74 (3H/14c)12.15 12.06 [14c]dpm in Peptidyl tRNA 27,520 32,878 [<sup>3</sup>H]dpm in Peptidyl tRNA 334,368 396,410 Description 37°C 15°C Shift 37°C 22°C Shift Sample 2

Figure 48 The elution profile of  $\alpha$  nascent peptides which had been labeled with L-[ $^3$ H]-isoleucine ([ $^3\text{H}$ ]-isoleucine,———), as compared to  $\alpha$  nascent peptides labeled continuously for 10 for 5.5 minutes at 37°C and then shifted down to 22°C for an additional 4.5 minutes

minutes at  $37^{\circ}$ C ([ $^{14}$ C]-isoleucine, ----).

DISTRIBUTION COEFFICIENT

Figure 49 The elution profile of  $\alpha$  nascent peptides which had been labeled with L-[ $^3$ H]-isoleucine ([ $^3\text{H}$ ]-isoleucine, ——), as compared to  $\alpha$  nascent peptides labeled continuously for 10 for 5.5 minutes at 37°C and then shifted down to 15°C for an additional 4.5 minutes minutes at 37°C ( $[1^4C]$ -isoleucine, ----).



is (

The

Dis

yie inp

κ<sup>+</sup>

per

Ko/

000

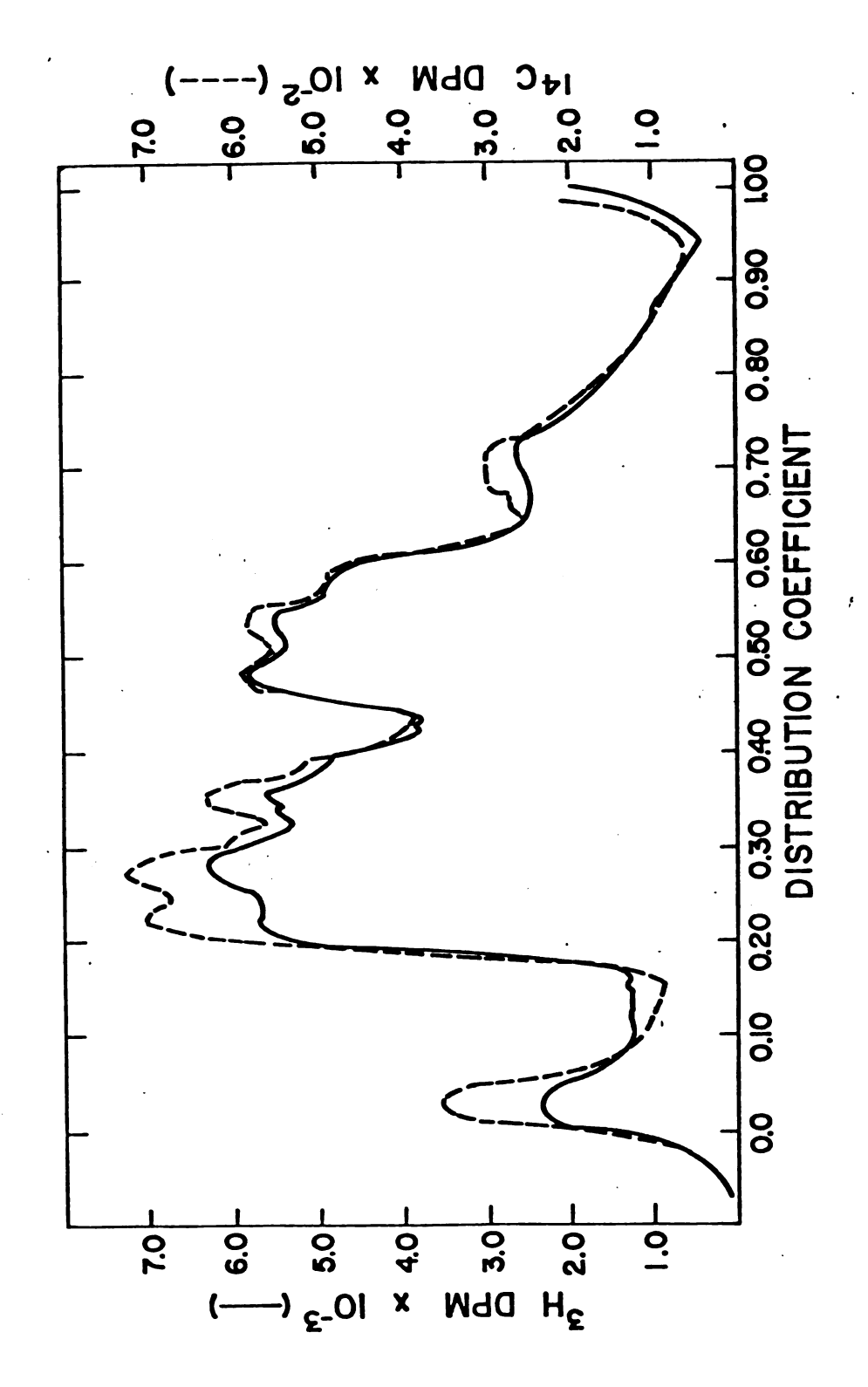
fac

is expected to be significant (18).

## The Effect of K<sup>+</sup> Concentration on the Nascent Polypeptide Size Distribution

Optomization of lysates with potassium chloride or potassium acetate yields quite different values for the translational rate optimum for input of K<sup>+</sup>. KCl optimization yields a maximal translation rate at 72 mM while KoAc raises this optima by nearly a factor of 2 to an input K<sup>+</sup> concentration of 128 mM. Preparation of nascent peptidyl tRNA was performed on two aliquots of a lysate which had been run at their KCl and KoAc optima. Figure 50 illustrates that no profound changes in the location or relative amplitudes of the nascent chain accumulation had occurred as a result of increasing the input K<sup>+</sup> concentration by a factor of 1.72 between the two salt optima for translation.

Figure 50 The effect of different levels of K<sup>+</sup> levels on the tryptophan labeled nascent peptide size distribution. 68 mM KCl (---); 132 mM KAc (---).



## Discussion

The rabbit reticulocyte contains predominantly two mRNAs coding for the  $\alpha$  and  $\beta$  polypeptide subunits of hemoglobin. Protein synthesized on polysomes directed by these mRNAs accounts for approximately 95% of the total protein synthesized in the cell, providing  $\alpha$  and  $\beta$  globins in nearly equivalent molar amounts.

Polysomes programmed for  $\alpha$  and  $\beta$  globin synthesis contain the  $\alpha$  and  $\beta$  globin mRNA molecules and (on the average) 4 to 5 ribosomes populating a coding region of approximately 435 bases (429 for  $\alpha$  globin, 442 for  $\beta$  globin) which is known to be folded into extensive regions of secondary structure in the uncomplexed mRNA molecule. Each translating ribosome contains one tRNA molecule to which is attached one nascent polypeptide intermediate in the synthesis of, in this case, an  $\alpha$  or  $\beta$  globin polypeptide.

Investigations of Protzel and Morris (48) into the properties of the population of nascent peptide intermediates involved in  $\alpha$  and  $\beta$  globin synthesis revealed that all possible nascent peptide sizes were not equally represented in the population of nascent polypeptides. Analysis of the size distribution of these intermediates revealed accumulations of certain size classes relative to others in the population. Since every ribosome contains one, and only one peptide chain, and since the size or molecular weight of the nascent polypeptide uniquely positions the associated ribosome along the coding region of the mRNA, an accumulation of a certain size class of nascent peptide may be thought of as a reduction in the translocation rate of ribosomes in the region of the mRNA corresponding to the length of the nascent peptide. The nonuniformity

of the size distribution of nascent peptides, then, indicates nonuniformity in the local rates of translation through various portions of the mRNA.

The rabbit reticulocyte lysate was chosen for the studies described in this work in light of the extensive characterization of the  $\alpha$  and  $\beta$  composite nascent peptide size distribution already achieved in this laboratory. The reticulocyte translational apparatus itself as well as the products,  $\alpha$  and  $\beta$  globin, and the  $\alpha$  and  $\beta$  globin mRNAs comprise the best characterized eucaryotic cell-free protein synthesizing system available. During the course of this work the primary sequences of the  $\alpha$  and  $\beta$  globin mRNAs have been determined by other laboratories (40,41) and several hypothetical secondary structures for these mRNAs have become available reflecting varying degrees of experimental support (38,72).

The initial problem involved resolution of the  $\alpha$  and  $\beta$  globin nascent peptide size distributions which contribute to the total globin nascent peptide size distribution thereby allowing comparison of the size distribution of two highly related, yet distinct, nascent polypeptide populations which are being synthesized simultaneously by the same biosynthetic apparatus. Analysis of such a system would not only serve as a universal control for comparison of the two mRNA molecules and their associated nascent peptides but would also serve as a starting point for studies into the possibility of  $\alpha$  and  $\beta$  mRNA structural interactions reflecting some hither to unrecognized element(s) of coordinate control of  $\alpha$  and  $\beta$  globin synthesis.

Elucidation of the  $\alpha$  globin nascent peptide size distribution in a rabbit reticulocyte lysate system which is synthesizing both  $\alpha$  and  $\beta$  globins was accomplished by taking advantage of the observation that some

rabbits exhibit a polymorphism at position 112 of the  $\beta$  globin polypeptide which results in the substitution of a valine residue for the only isoleucine residue present in the  $\beta$  globin polypeptide ( ). Reticulocytes from rabbits homozygous for this trait incorporate no radioactivity into  $\beta$  globin when incubated with radiolabel in the form of L-isoleucine.

Labeling of polysomes from such a rabbit results in a radiochemically pure population of nascent  $\alpha$  globin polypeptides. Careful analysis of this population in conjunction with internal molecular weight standards reveals at least seven prominent accumulations of nascent  $\alpha$  globin peptides.

Comparison of the  $\alpha$  chain size distribution with the tryptophan labeled nascent chain accumulations allowed tentative identification of some regions of distinct differences between the  $\alpha$  and  $\beta$  specific size distribution. The large accumulation of peptide components from Kd 0.45 to 0.55 is seen to be present in the total labeling pattern but is not a prominent feature of the  $\alpha$  pattern. The large  $\beta$  specific accumulation defines the low molecular weight boundary of the most prominent feature of the globin nascent chain size distribution, that is, the large minima observed at Kd 0.43. These data indicate landmark features of the  $\beta$  profile which contrast with the  $\alpha$  profile. The size distribution of the  $\alpha$  chain profile is nonuniform but rises in a more continuous manner with increasing molecular weight of the peptides.

It is noted that some features of size distributions are functions of the radiolabeled amino acid employed and the method of separation of the nascent peptides. An incremental increase in the size distribution profile is expected whenever a new radiolabeled residue is inserted into

the growing peptide chain, necessitating the choice of an amino acid which is located as close to the N-terminal of the growing polypeptide chain as possible while maintaining representation in the protein sequence at a minimum. Both isoleucine and tryptophan fit these criteria reasonably well. Secondly, the amplitude of the size distribution of polypeptides of constant specific activity increases towards higher molecular weight (or lower Kd value) due to the logarithmic properties of the gel filtration process employed. That is to say, more members of the possible 145 or so nascent polypeptides are eluted per unit volume at low Kd than at high Kd. Finally, a peak in the size distribution profile is to be expected at the Kd of the completed globins due to the absence of components on the lower Kd side of the elution profile.

In order to determine the  $\beta$  size distribution in the presence of  $\alpha$  synthesis and at the same time circumvent the above mentioned artifactual perturbations of the observed size distribution, two rapid, high resolution chromatographic systems were designed to permit accurate quantitation of the tryptophan label at positions 14 and 15 of the  $\alpha$  and  $\beta$  globin chain respectively, isolated as the tryptic peptides  $\alpha T3$  and  $\beta T2$ . This experimental approach allowed quantitation of the relative contributions of the  $\alpha$  and  $\beta$  nascent peptides to the tryptophan labeled nascent peptide size distribution profile.

These analyses produced an  $\alpha$  profile which was essentially identical to that observed with isoleucine labeling of  $\beta_{112}$  Val/Val lysates. The  $\beta$  pattern obtained revealed features which were quite different from the  $\alpha$  pattern. As expected, the large accumulations observed throughout the Kd range from 0.45 to 0.55 in the total size distribution are predominantly  $\beta$  specific. The  $\beta$  pattern also exhibited reduced levels of  $\beta$ 

specific nascent polypeptides compared to  $\alpha$  throughout the region of the elution profile corresponding to completed chains (Kd 0.20 to Kd 0.25). This result was not unexpected as Protzel and Morris observed an excess of  $\alpha$  globyl tRNA (completed  $\alpha$  globin still attached to tRNA) present on polysomes, as compared to  $\beta$  globyl tRNA, measured by two entirely different approaches. It should be noted that if the nonuniformity of the nascent peptide size distribution does indeed reflect nonuniform translocation rates then the size distribution profile provides a great deal of detailed information about ribosomal flux through the entire length of the mRNA coding region. However, as with most steady state measurements, information is not available regarding the kinetics of ribosomal movement through different regions of the mRNA, i.e., a particular accumulation may reflect any number of changes in elongation rate constants which result in either a net increase of flux into or decrease of flux out of the region.

It is noted that any point of isotopic placement will result in an increase in the amplitude of the profile to generate the low molecular weight side of an apparent gaussian accumulation. This is seen in the Trp and Ile size distribution profiles at a position corresponding to the placement of the first residue (at Kd 0.80). This raises the question of whether or not the accumulation at Kd 0.7-0.72 is real or simply an artifact due to the initial incorporation of label into the unlabeled growing nascent peptides. In order to investigate this possibility and to implement a general method to accomplish labeling of eukaryotic nascent peptides at as few positions as possible and as close to the N terminus of the nascent peptides as possible, L-[35s]formylmethionyl tRNA<sub>F</sub>Met was synthesized and used to label the  $\alpha$  and  $\beta$  globin

nascent peptides. The f Met residues placed at the N terminus of the globins are known to remain intact and are not removed during globin synthesis (67).

Experiments utilizing methionine and formylmethionyl tRNA revealed two nascent peptide accumulations which were undetectable by tryptophan or isoleucine labeling indicating that they correspond to peptides of length less than 10-14 amino acids. Labeling of polysomal nascent chain N termini with [35] fMet revealed at least one additional nascent chain accumulation in the population at Kd 0.82 corresponding to a region on the  $\alpha$  or  $\beta$  globin mRNA centered at codon 9. Another component was noted as a shoulder on the free amino acid peak at Kd 0.90. The latter peak was confirmed by analysis of L-[3H]-methionine labeled nascent polypeptides which exibited considerably less contamination by free amino acids in the Kd range of 0.85-0.95. The interpretation of additional accumulation in the L-[3H]-methionine profile between Kds 0.60 and 0.75 is complex and is probably due to removal of the N terminal methionine by the reticulocyte processing apparatus since these aspects of the size distribution profile are not reflected in the fMet terminally labeled nascent chain population. However, it has been reported that the N-terminal methionine residue is not removed from the growing nascent peptide until the mascent peptide has become approximately 25-30 residues long (68). Furthermore, Rich et al. (73) have observed that ribosomal structure completely protects the growing nascent peptides of less than 25-30 residues in length suggesting that the N terminal methionine is not available for processing until the ribosome has moved past the twentieth codon. Collectively, these data suggest that there are two additional accumulations in the mascent peptide size distribution of the  $\alpha$  and/or  $\beta$ globin mRNAs in the vicinity of the ribosomal binding region. Kozak has

proposed that the 40S preinitiation complex which forms with reovirus mRNA initially binds upstream from the AUG initiator codon and proceeds to "scan" the 5' noncoding mRNA sequence until it encounters the first AUG codon at which point the 60S subunit binds to form the initiation complex. Under conditions where secondary structure was weakened or eliminated the 40S preinitation complex was able to bind to the mRNA with comparable efficiency but was found to "scan" into the mRNA coding sequence, indicating a failure to bind the 60S subunit at the AUG codon (74). This led Kozak to propose that elements of secondary structure are necessary for 40S preinitiation complex recognition of the AUG initiation codon and for prevention of 40S subunit "read through". Since, for globin mRNA, the 40S complex is known to cover a much longer stretch of nucleotides (80 nucleotides), as compared to the 80S complex (27-30 nucleotides) (75,76), an element of secondary structure which would interact with the 40S subunit when it is located over the AUG initiation codon would be expected to involve sequences near the 12-13th codon or 35-40 nucleotides to the 3 side of the AUG codon. Since the 80S ribosome covers a smaller length of nucleotides, this putative secondary structural element would be expected to cause an accumulation of nascent chains of a length anywhere from 7 to 10 amino acids long if the scanning mechanism and the mRNA structures supporting that mechanism are a general feature of eukaryotic mRNAs, as has been suggested (77). Examination of the N terminal formyl methionine nascent peptide size distribution revealed two nascent peptide accumulations corresponding to peptides of length 5-7 amino acids and 9-13 amino acids both of which retard the 80S ribosome and presumably would also retard a "scanning" 40S preinitiation complex, preventing 40S movement out of the ribosomal binding site and thus providing the necessary situation for 60S binding to the 40S complex while it is located.

The presence of peptide accumulations corresponding to slow local translation rates past the first 9-10 mRNA codons is thus consistent with evidence obtained by Kozak in support of a scanning model for 80S initiation complex formation. The presence of secondary structure within the 40S ribosome binding site and its potential effect on the efficiency with which 80S initiation complexes are formed emphasizes the possibility that in cases where initiation is the rate determining step in protein synthesis the actual limiting event in the initiation or preinitiation sequence may provide a mechanism for differential control of mRNA expression at the level of initiation.

Studies were conducted to evaluate the effect of ribosomal queuing or the disruption of the normal distribution of ribosomes along the mRNA on the mascent peptide size distribution. Incubation of the  $\beta_{112}$ Val/Val lysate in the presence of L-O-methylthreonine caused L-OMT redistribution of ribosomes on the  $\alpha$  globin mRNA due to L-OMT induced pauses at the isoleucine codons as a result starvation of the biosynthetic apparatus for isoleucyl tRNA. This procedure grossly disrupts the normal polysomal structure as can be seen from the Ile labeled elution profile, but should have no effect on the ß nascent chain profile. This prediction was confirmed by formal subtraction of the L-[14C]-isoleucine from the L-[3H]-tryptophan labeled profiles in a double label experiment with L-OMT and comparison of the residual with that obtained from subtraction of control (isoleucine and tryptophan labeled) profiles obtained in the absence of L-OMT. The results of difference analysis of these profiles were found to be essentially identical, providing strong evidence that the ß nascent peptide profiles size distribution is independent of the synthesis or the size distribution of the  $\alpha$  globin

nascent chain components.

Further studies centered on the effects of ribosomal loading of the a globin mRNA caused by moderate inhibition of the rate of elongation caused by the presence of sparsomycin and gougerotin. Under conditions where a globin synthesis was inhibited to 30% of control synthesis polysomes containing a mascent peptides, as determined by Ile incorporation in a  $\beta_{\mbox{\scriptsize 112}}$  Val/Val lysate, were shifted from a maximal size of 4-mers and 5-mers to 7-mers and 8-mers. Comparison of the size distribution of the  $\alpha$  globin mascent peptides of inhibited lysates ([3H]-Ile) to that of an uninhibited lysates (preferred as an internal standard) showed an increase in ribosomal density increasing towards smaller molecular weight nascent polypeptides (the 5' end of the mRNA). However, this increase in ribosome density produced by the antibiotics caused no significant change in the shape of the size distribution. It was originally thought that an increase in ribosome density might reduce the effect of secondary structure by keeping the mRNA in an extended conformation. However, since no decrease of the nonuniformity of the nascent chain size distribution was created by decreasing ribosomal velocity, these data seem to indicate that inhibited ribosomes are retarded to the same extent as uninhibited ribosomes. Thus with the addition of elongation inhibitors, ribosome density is increased on the mRNA molecule, while the amplitude of the nascent chain accumulations increased in proportion to the ribosomal density between the putative slow translation points (profile minima).

To investigate the effect of ribosomal density on the  $\alpha$  nascent peptide size distribution, the contribution of different size polysomes to the total polysome profile was assessed. Polysomes labeled with L-isoleucine and separated on a sucrose gradient were used to prepare  $\alpha$  globin nascent polypeptides for size distribution analysis. In these analyses nascent peptides from very small polysomes (dimers) gave

essentially the same size distribution profiles as the larger polysomes. in terms of the distribution coefficients of the characteristic accumulations. There was, however, a very reproducible and continuous decrease of nascent peptides of size corresponding to completed globin polypeptides with increasing polysome size. Since these polysomes were separated on gradients which contained carrier denatured globin peptides and large amounts of sparsomycin and cycloheximide it seems unlikely that the higher molecular weight polysomes were preferentially losing complete or near complete  $\alpha$  polypeptides due to "run off" or degradation as compared to smaller polysomes which had been in the gradient for the same amount of time. It is possible that increasing sucrose concentration or some other artifact encountered during fractionation of the polysomes may have perturbed the system but it is not clear why some nascent peptide sizes would be effected differentially as compared to others. An interpretation which is consistent with the decrease in high molecular weight nascent peptides on polysomes of increasing size is that facilitated release of ribosomes on the secondary structure of the region near the terminator codon. The observation that  $\alpha$  globyl tRNA was found in excess on polysomes while  $\beta$  globyl tRNA was not may be due to the fact that  $\alpha$ globin is known to be synthesized on significantly smaller polysomes than B polysomes. This suggests a possible cause and effect relationship between the two phenomena. This result also suggests a possible relationship between the rate of initiation and the rate of release of completed polypeptides at constant elongation rates, perhaps by interaction of the 5' and 3' ends of the mRNA.

In order to study this phenomenon further, polysome size was reduced by incubation of the reticulocyte lysate with the initiation inhibitor aurine tricarboxylic acid. This experiment demonstrated that there was a increase in the larger nascent  $\alpha$  polypeptides relative to those of smaller molecular weight on the ATA induced smaller polysomes. In addition, the relative amounts of accumulated  $\alpha$  peptides increased on the smaller polysomes. Both these observations, as well as the apparent decrease of nearly completed  $\alpha$  nascent peptides on larger polysomes, is consistent with a ribosome induced unfolding of local areas of secondary structure which thus facilitates translation of regions of the  $\alpha$  mRNA which have been freed from secondary structure, possibly by regions of the mRNA far removed in sequence from one another, drawing support for the possibility of long range effects of ribosomal loading on mRNA secondary structure.

Studies were conducted to assess the sensitivity of the a nascent polypeptide size distribution to changes in ionic strength. Reticulocyte lysates have been shown to have different apparent K+ requirements depending on whether acetate or chloride is present as the counterion. This has been attributed to an inhibitory effect of chloride ion in the system ( ). A lysate optimized with KCl and with KAc was found to incorporate maximally at input concentrations of 72 and 132 mM, respectively. Total tryptophan nascent peptide prepared from incubations at either level of input K+ showed no significant differences in the nascent peptide size distribution consistent with an absence of significant effect of K+ concentration over this concentration range on mRNA secondary structure or the distribution of ribosome density across the mRNA. Changes in K+ concentration are known to produce changes in the thermal stability of a number of mRNAs including the globin messenger

RNA as well as other natural and synthetic polynucleotides. The absence of an effect here may be due to our inability to observe the dependence of the nascent chain size profile with ionic strength values over a wide enough range.

Analyses of the  $\alpha$  globin size distribution as a function of temperature were conducted under several different experimental conditions. Incubation of the lysate at 15°C demonstrated that initiation proceeds at this reduced temperature. Analysis of the mascent chain size distribution indicated that steady state labeling of the mascent chains is not achieved at this temperature in 10 minutes. Nascent polypeptides towards the 5' end of the mRNA were found to be heavily labeled but synthesis had failed to proceed into the coding region of beyond that associated with a Kd of 0.5 or less. Although ribosomes were densely populating the 5' mRNA region, the size distribution was still nonuniform. This finding could indicate that a tighter mRNA configuration is present at 15°C and impedes ribosomes more efficiently due to lower rates of thermal "breathing" of secondary structure and also indicates the presence of more or different structures at 15°C than are present at 37°C. It is known from hyperchromism and circular dicroism measurements on globin mRNA conducted as a function of temperature that 10-12% more secondary structure is present at 15°C compared to 37°C. A shift in this distribution does not seem to be due solely to slower ribosomal transit since inhibition of elongation produced with gougerotin or sparsomycin had no such effect on the nascent peptide elution profile.

Since steady state labeling had not been achieved under the above conditions, further experiments relied on the transfer of polysomes which had achieved steady state labeling of  $\alpha$  globin with [3H] isoleucine at

37°C to an incubation temperature of 22°C or 15°C. Following termination of the incubation as described in Methods the reaction mixture was combined with [14C]-Ile labeled nascent peptides synthesized at 37°C as a control and internal standard. These experiments showed almost no effect of the temperature shift to 22°C in the low molecular weight regions of Kd values > 0.5. However, a redistribution of approximately 12% of the labeled mascent peptides occurred as an apparent loss of labeled material from regions corresponding to Kd 0.35 to 0.4 with an apparent increase in the prominent accumulation at Kd 0.27 suggesting that ribosomes may be accumulating at a point of hinderance giving rise to this accumulation as well as decreased flux past the point of accumulation characterized at Kd 0.52. This interpretation is consistent with an apparent "runoff" of nascent peptide components corresponding to molecular weights higher than the accumulation of Kd 0.27. The shift to lower temperatures (15°C) from 37°C resulted in a pronounced effect on ribosomal flux producing fine structure in the elution profile corresponding to nearly gaussian accumulations at the Kd's corresponding to accumulations seen at normal incubation temperatures but producing as well as an increase of the effects noted at the first shift down temperature at Kd values less than 0.35. Again, these data contrast with those obtained for lowered ribosomal transit rates at 37°C produced by gougerotin and sparsomycin in that a shift in the distribution coefficient of at least 1 component was observed in the 37°C/15°C thermal shift experiment demonstrating that ribosomal flux in specific regions of the mRNA are affected by the lowered temperature which is not simply due to retarded ribosomal translocation and is consistent with an effect of the known increase in secondary structure for the globin mRNAs in vitro throughout

this (15°-37°) temperature range. We cannot, of course, exclude any of a number of potential mRNA sequence specific effects which may be postulated to have occurred. These effects include possible changes in the association constant of an amino acyl tRNA for the ribosomal "A" site or amino acyl tRNA starvation due to a reduced aminoacylation activity or a change in the growing peptide conformation any of which could modify a local translocation rate constant. Thermal stabilization of helices is the most plausible explanation for which considerable independent physical data exists.

An alternative approach to the effect of mRNA secondary structure on ribosomal translocation rate was designed to assess the effect of sequence specific oligonucleotide binding in order to perturb the dynamic structure of a translating mRNA molecule. Of the limited possibilities for a structurally complimentary oligonucleotide available to us, tetradeoxy C was chosen. This choice was dictated by the fact that the tetra C:tetra G duplex would have sufficient stability to exist at a reasonable concentration at 26°C and under the conditions of ionic strength approximated in the lysate by a minimal K<sup>+</sup> concentration of 132 mM. The sequence -GGGG- occurs only twice in the coding region of the ß mRNA and does not occur at all in the  $\alpha$  sequence, nor are there any G runs longer than 4 in either mRNA molecule. This choice was also dictated by concern over the known ability of complimentary oligonucleotides to bind to the anticodon regions of certain tRNA molecules. The most probable instance where this type of interaction could occur is the case of the proline isoacceptor tRNA whose anticodon contains a tri G sequence. Of the tri C proline codons present in the  $\alpha$  and  $\beta$  mRNAs, all 5 occur in the  $\alpha$  globin mRNA. Thus if the nascent peptide elution profile were to change due to

tetra C interference with some aspect of prolyl tRNA function, this effect would be expected to be apparent in the  $\alpha$  globin size distribution at those places corresponding to tri C proline insertion points. The presence of tetra C was found to have no significant effect on the  $\alpha$  size distribution compared to an internal control under conditions where several significant effects were noted in the tryptophan labeled ( $\alpha$  and  $\beta$ ) nascent chain size distribution. One of these effects is a shift in the tryptophan nascent peptide accumulation at Kd 0.72 to an accumulation of nascent peptides of larger molecular weight. This shift was totally absent in the  $\alpha$  specific labeling pattern and furthermore occurred in a region where neither mRNA codes for any proline residues. The observed shift of nascent peptides occurred at a point corresponding to the position of the first tetra G sequence in the  $\beta$  mRNA, the only oligo G sequence of greater than two residues in this region of either mRNA.

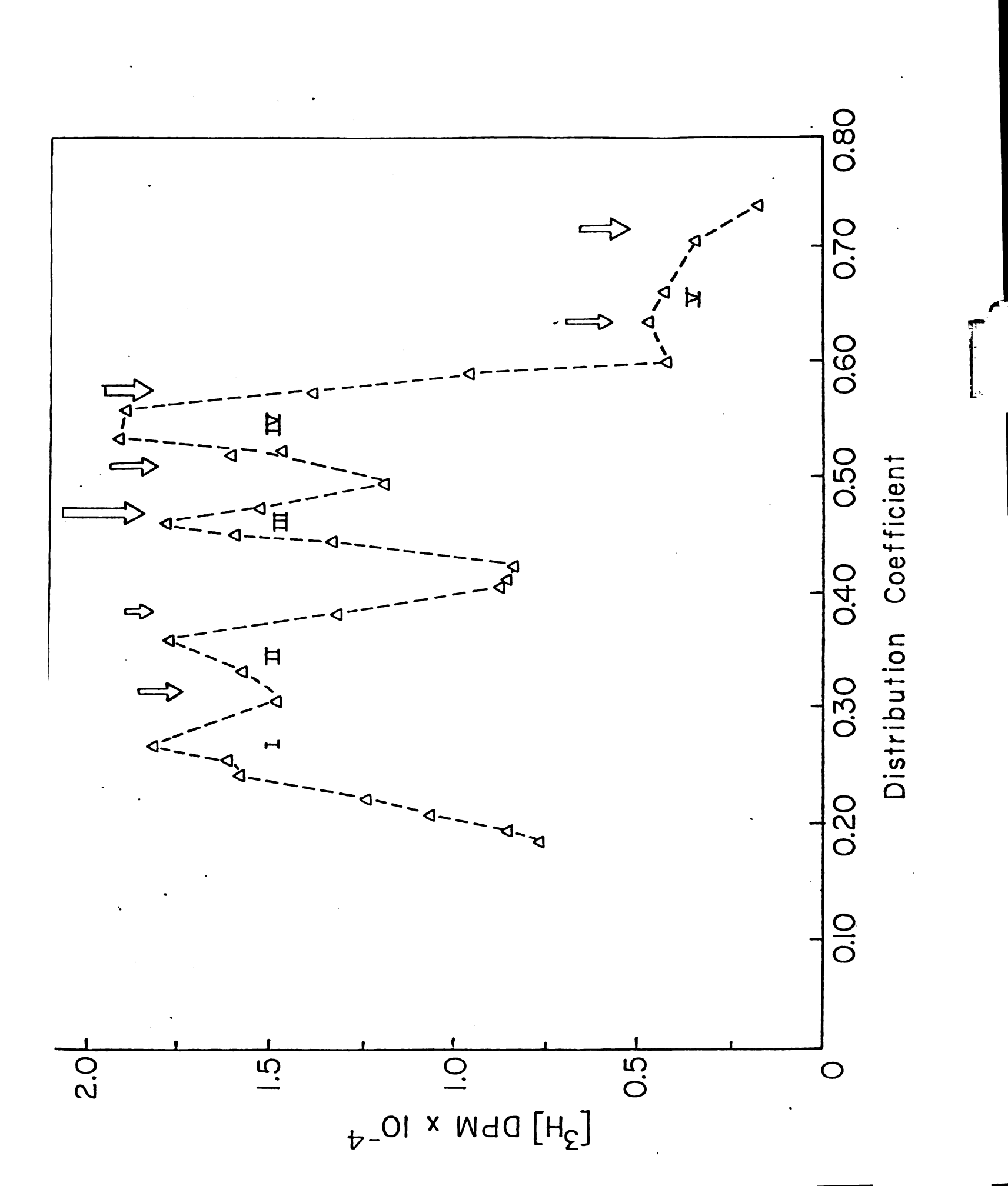
The simpliest interpretation of this result is that the high concentration of the oligonucleotide served to perturb the equilibrium of a hairpin structure which had given rise to the Kd 0.72 accumulations shifting these accumulations to a new hairpin structure farther downstream. The experiments discussed thus far were designed in an attempt to gain insights into the origin of the nonuniformity of the nascent peptide accumulations.

All studies using perturbative techniques are subject to many criticisms due to the complexity of this system and hence do not rigorously prove a relationship exists between the translocation rate of an RNA bound ribosomal complex and the secondary structure of the RNA template. The results presented herein represent a contribution to a growing body of observations consistent with the hypothesis that mRNA

secondary structure causes changes in the local rates of ribosomal translocation. Clearly, independent confirmation must be sought for the effect of RNA secondary structure on ribosomal translocation as well as all other aspects of ribosome and ribosomal subunit-RNA interactions.

In this respect the work of Wurst et al. (32) and Pavlakis et al. (38) on the secondary structural analysis of the  $\alpha$  and  $\beta$  globin mRNA molecules using enzymatic probes of RNA structure provides one such approach. The methodology developed by these workers relies on the use of S<sub>1</sub> nuclease as well as other nucleases to preferentially cleave single stranded regions of mRNA molecules which have been labeled with  $[^{32}P]$  on the 5' end of the RNA molecule. This technique is performed in parallel with sequencing reactions and thus allows the determination of those nucleotide sequences which are single stranded regions. A histogram representing the number and intensity of nuclease cleavage sites of the RNA plotted as a function of Kd of the mascent peptide size distribution analysis allows comparison of nuclease susceptible single stranded regions with the nascent polypeptide size distributions. Figure 51 shows the \$ mRNA nuclease susceptible sites, as determined by Pavlakis et al. (79) correlated with the ß mascent peptide size distribution. Alignment of the nuclease accessible regions of the ß nucleotide sequence with the ß nascent chain size distribution was accomplished by the use of marker [14C] globin CnBr peptides used as internal standards and [14C]-ile labeled, L-OMT induced, nascent chain accumulations (see Figures 8, 9 and 26).

It can be seen from Figure 51 that a significant number of the nuclease cleavage points fall in regions of  $\beta$  profile minima providing support for the hypothesis that ribosomes have an increased probability



of being found immediately 5' to double-stranded regions in the mRNA and that a relatively low probability exists (as reflected in a high translocation rate) of ribosomes being found at the 5' end of single stranded regions. The most significant correlation present in these data is that between the highly nuclease susceptible region of the ß globin mRNA as shown by the numerous nuclease cleavages throughout 8 codons 50-56 and the heavy accumulation of ß globin mascent peptide components located from Kd 0.45 to Kd 0.55. These data indicate that, in this case, accumulated  $\beta$  nascent peptides correspond to ribosomal density immediately adiacent to sequences which are inaccessible to single strand specific nucleases and hence are at the 5' terminus of stable 8 globin mRNA structure, and at the 3' end of a stretch of single stranded structure. The location of the  $\beta$  nascent chain accumulations is compared with the nuclease susceptibility data provided by Pavlakis et al. in Figure 52. Recently published secondary structure maps of the rabbit α and β 5'-terminal regions, which extend into the coding regions of these mRNAs reveal the additional correlation between nascent chain accumulations and mRNA secondary structure alluded to in the discussions of tetra C induced perturbation of the ß mascent peptide size distribution and fMet detected "early" nascent peptide accumulation mapping in this region. The location of these accumulations are presented in Figures 53a and 53b. It can be seen in Figure 53b that tetra C interaction and destabilization of the large ß hairpin centered at codon 14-15 would be expected to shift the accumulation to the next hairpin region at codon 24-25 as was observed. Also mRNA structures predict the low molecular weight accumulations. revealed by fMet and Met labeling of nascent chains, at points within and slightly past the 40S ribosomal subunit and 80S ribosome protected

Figure 52 Correlation between the location of points of S<sub>I</sub> nuclease susceptibility of the ß globin  $\ensuremath{\mathsf{mRNA}}$  as a function of the distribution coefficient and the location of the  $\beta$  globin nascent peptide accumulations. Arrows indicate nuclease susceptibility. Sphéres

indicate ribosomal density.

192

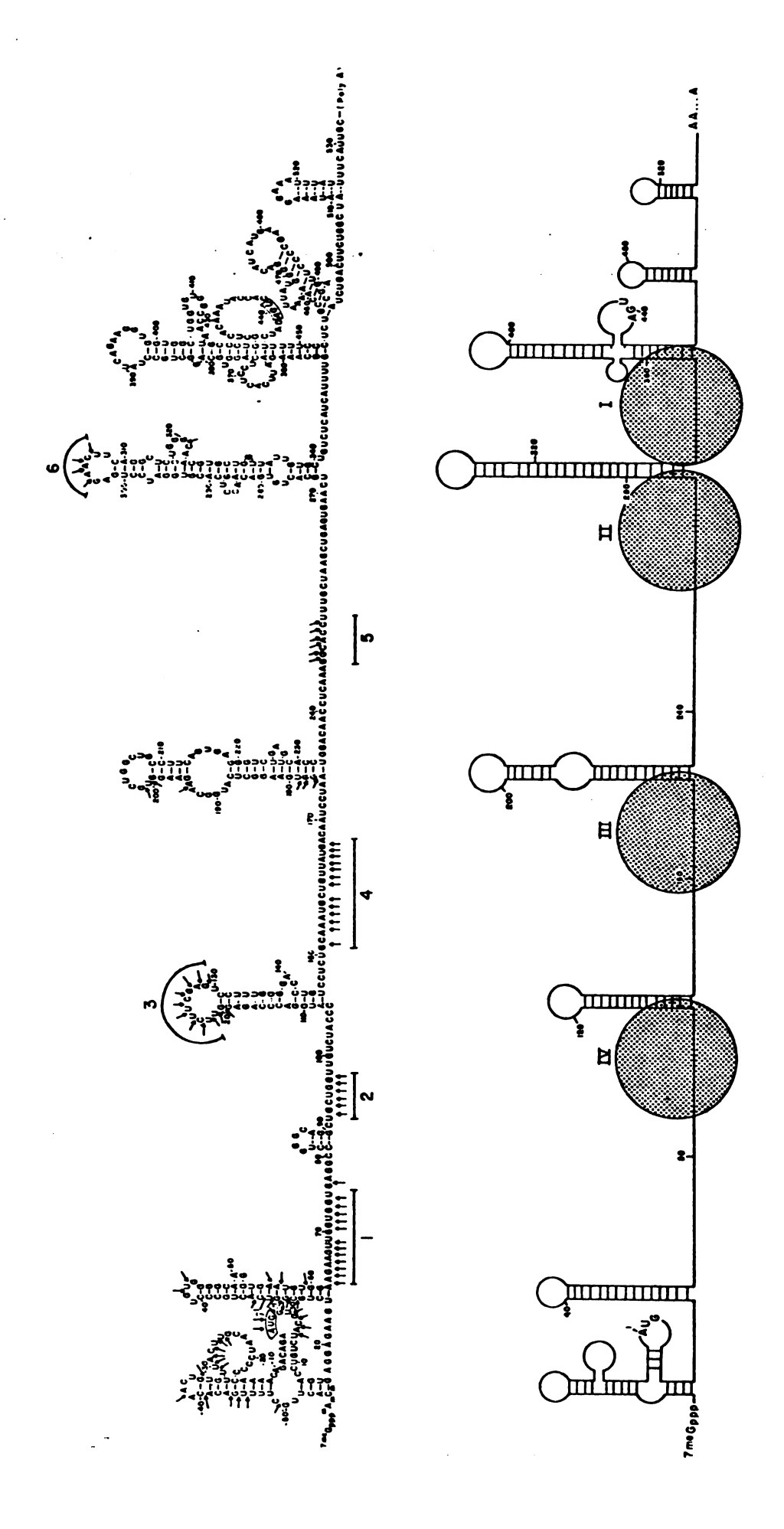
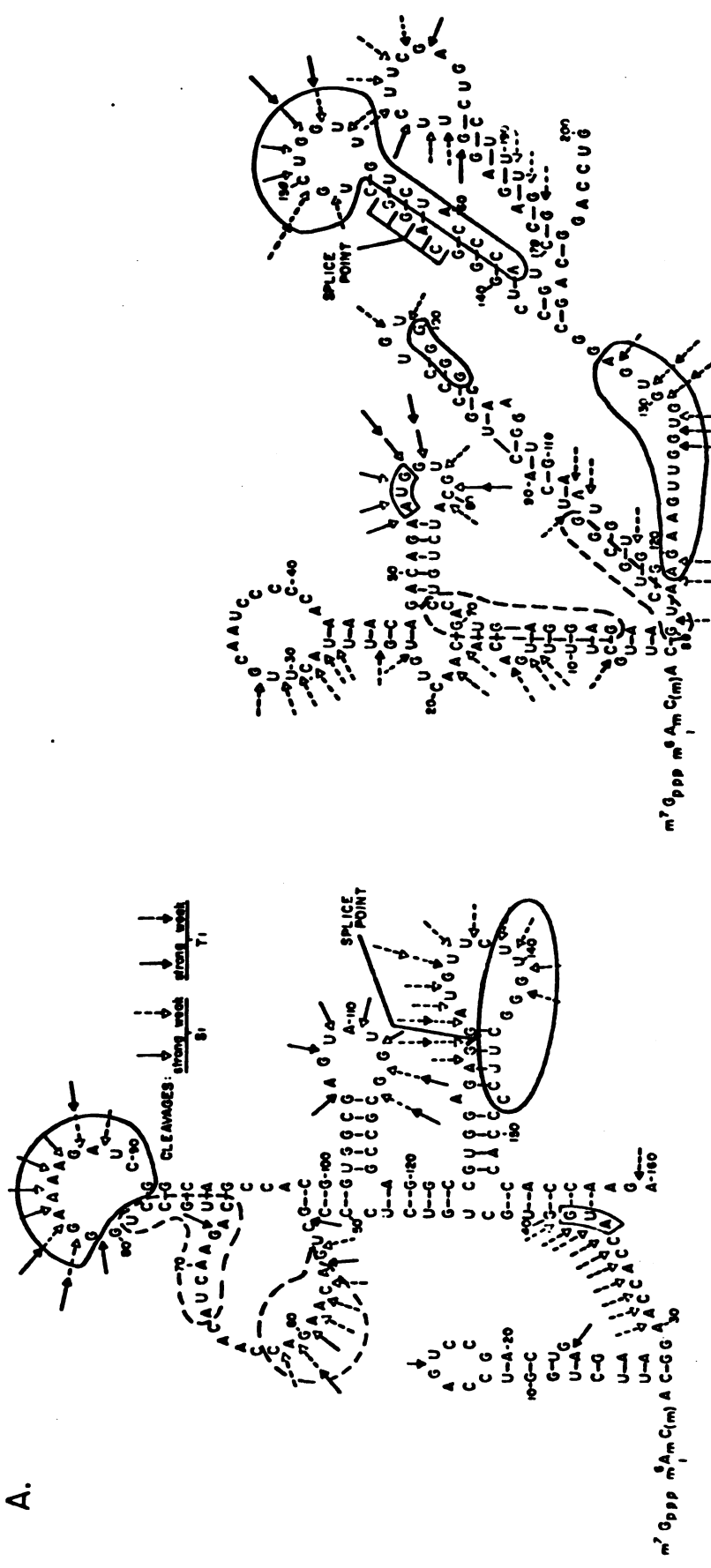


Figure 53 A comparison of the location of the small molecular weight nascent peptide accumulations with the proposed structures for the 5' regions of the rabbit  $\alpha$  and  $\beta$  globin mRNAs.



d-GLOBIN MRNA

A-GLOBIN MRNA

regions in both α and β globin mRNAs as discussed above.

The nascent peptide accumulations are consistent with secondary structural elements ahead of the 7-8th amino acid position or 21-24th codon nucleotide and the 10-16th amino acid corresponding to codon nucleotides 30-45 and in essential agreement with the structures proposed by Pavlakis et al. for these regions. It must be emphasized that while the nascent peptide accumulation at Kd 0.7 is known to be due to both  $\alpha$  and  $\beta$  components, the identity of the lower molecular weight accumulations have not been determined and may be  $\alpha$  and/or  $\beta$  in composition.

The studies presented here and previously support the view that mRNA molecules have characteristic, nonrandom structures in terms of the locations and stabilities of helical or tertiary structural interactions. We extend this hypothesis by proposing that portions of these structures are present in the coding region of mRNA molecules effectively modulate the rate of ribosomal movement through various regions of the mRNA. Data presented here and by others support the hypothesis that the resultant effect of secondary structure on stabilization of polysomal size and the distribution of ribosomal density on the mRNA may effect a number of aspects of mRNA function including initiation, termination and elongation rates, and mRNA structural and functional half life. It should be noted that several lines of evidence suggest that the nonuniformity of the nascent peptide size distribution is not due to partial proteolysis of nascent polypeptides. The size distribution profiles were unchanged when labeling was conducted in the presence of phenylmethylsulfonylfluoride (80) or when excess denatured globins were added as carrier. Most significant, however, is the appearance of at least two and possibly

three accumulations of nascent peptides of less than 30 amino acids (Kd 0.65) in the size distribution. Several workers have shown that peptides of this size are completely protected from proteolysis by the 80S ribosomal structure as cited above.

## References

- 1. Lodish, H.F. (1974) Nature 251, 385.
- 2. Shumacher, G., Ehring, R., (1975) Molec. Gen. Genet. 136, 41.
- Sonenberg, N., Rupprecht, K.M., Hecht, S.M., Shatkin, A.J. (1979)
   Proc. Nat. Acad. Sci. 76, 4345.
- 4. Bolton, P.H., Kearns, D.R. (1977) Biochem. 16, 5729.
- 5. Steitz, J.A., Sprague, K.U., Steege, D.A., Yuan, K.C., Laughrea, M., Moore, P.B. (1977) Nucleic Acid-Protein Recognition, Academic Press, Inc., New York, New York.

•

- 6. Proudfoot, N.J. (1977) Nature 265, 499.
- 7. Seeman, N.C., Rosenberg, J.M., Suddath, F.L., Kim, J.J.P., Rich, A. (1976) J. Mol. Biol. 104, 109.
- Rosenberg, J.M., Seeman, N.C., Dav, R.O., Rich, A. (1976) J. Mol. Biol. 104, 145.
- 9. Yathindra, N., Sundaralingam, M. (1976) Nucl. Acids Res. 3, 729.
- 10. Quigley, G.J., Rich, A. (1976) Science 194, 796.
- 11. Sundaralingam, M. (1973) In 'Conformation of Biological Molecules and Polymers," The Jerusalem Symposium on Quant. Chem. Biochem., Eds. E. D. Bergman, and B. Pullman 5, 417-456, Academic Press, New York.
- 12. Wang, A.H.J., Quigley, G.J., Kolpak, F.J., Crawford, J.L., Van Boom, J.H., Van der Marel, G., Rich, A. (1979) Nature 282, 680.
- 13. Holder, J.W., Lingrel, J.B. (1975) Biochem. <u>14</u>, 4209.
- Van, N.J., Holder, J.W., Woo, S.L.C., Means, A.R., O'Malley, B.W. (1976) Biochem. <u>15</u>, 2054.
- 15. Bretani, M., Salles, J.M., Zinner, K., Faljoni, A., Bretani, R. (1978) Biochem. Biophys. Res. Commun. 83, 124.
- 16. Gralla, J., Belisi, C. (1974) Nature <u>248</u>, 330.
- 17. Delisi, C., Crothers, D.M. (1971) Biopolymers 10, 1809.
- Martin, F.H., Uhlenbeck, O.C., Doty, P. (1971) J. Mol. Biol. <u>57</u>, 201.
- 19. Gralla, J., Crothers, D.M. (1973) J. Mol. Biol. 78, 301.
- 20. Tinoco, I., Uhlenbeck, O.C., Levine, M.D. (1971) Nature 230, 362.

- 21. Tinoco, I., Borer, P.N., Dengler, B., Levine, M., Uhlenbeck, O.C., Crothers, D.M., Gralla, J. (1973) Nature 245, 40.
- 22. Pipas, J.M., McMahon, J.E. (1975) Proc. Nat. Acad. Sci. USA <u>72</u>, 2017.
- 23. Studnicka, G.M., Rahn, G.M., Cummings, I.W., Salser, W.A. (1978) Nucl. Acids Res. 9, 3365.
- 24. Freier, S.M., Tinoco, I. (1975) Biochem. 14, 3310.
- 25. Wrede, P., Pongs, O., Erdmann, V.A. (1978) J. Mol. Biol. 120, 83.
- 26. Adams, J.M., Cory, Spahr, P.F. (1972) Eur. J. Biochem. 29, 469.
- 27. Adams, J.M., Jeppeson, P.G.N., Sanger, F., Barelle, B.G. (1972) Nature 223, 1009.
- 28. Min Jou, W., Haegeman, G., Ysebaert, M., Fiers, W. (1972) Nature 237, 82.
- 29. Flashner, M.S., Vournakis, J.N. (1977) Nucl. Acids Res. 4, 2307.
- 30. Pavlakis, G., Vournakis, J.N., in press.
- 31. Vass, J.K., Maden, E.H. (1978) Eur. J. Biochem. <u>85</u>, 241.
- 32. Wurst, R.M., Vournakis, J.N., Maxam, A.M. (1978) Biochem. 17, 4493.
- 33. Maxam, W.A., Gilbert, W. (1977) Proc. Nat. Acad. Sci. 74, 560.
- 34. Ross, A., Brimacombe, R. (1979) Nature 281, 271.
- 35. Lodish, H.F. (1970) J. Mol. Biol. 50, 689.
- 36. Lodish, H.F., Robertson, H.D. (1969) CSHSQB 34, 655.
- 37. Tooze, J., Weber, K.J. (1967) J. Biol. Chem. 28, 311.
- 38. Pavlakis, G.N., Lockard, R.E., Vamvakopoulos, N., Rieser, L., RajBhandary, V.L., Vournakis, J.N. (1980) Cell 19, 91.
- 39. Legon, S., Robertson, H.D., Prensky, W. (1976) J. Mol. Biol. <u>106</u>, 23.
- 40. Efstratiadis, A., Kafatos, F.C., Maniatis, T. (1977) Cell 10, 571.
- 41. Heindell, H.C., Liv, A., Paddock, G.V., Studnika, G.M., Salser, W.A. (1978) Cell <u>15</u>, 43.
- 42. Ball, L.A. (1973) J. Theo. Biol. 41, 243.
- 43. MacDonald, T., Gibbs, J.H., Pipkin, A. (1968) Biopolymers  $\underline{6}$ , 1.

- 44. MacDonald, C.T., Gibbs, J.H. (1969) Biopolymers 7, 707.
- 45. Lodish, H.F., Bergmann, J.E. (1979) J. Biol. Chem. 254, 11927.
- 46. Lodish, H.F., Jacobsen, M. (1972) J. Biol. Chem. 247, 3622.
- 47. Cohen, P.S., Lynch, Walsh, M.L., Hill, J.M., Ennis, H.L. (1977) J. Mol. Biol. 114, 569.
- 48. Protzel, A., Morris, A.J. (1973) J. Biol. Chem. 248, 7438.
- 49. Chaney, W.G., Morris, A.J. (1978) Arch. Biochem. Biophys. 191, 734.
- 50. Chaney, W.G., Morris, A.J (1979) Arch. Biochem. Biophys. <u>194</u>, 283.
- 51. Schimke, R.T., Farhang, P. (1979) J. Biol. Chem. 254, 7636.
- 52. Allen, E.H., Schweet, R.S. (1962) J. Biol. Chem. 237, 760.
- 53. Lingrel, J.B., Borsook, H. (1963) Biochem. 2, 309.
- 54. Darnbrough, C., Legon, S., Hunt, T., Jackson, R.J. (1973) J. Mol. Biol. 76, 729.
- 55. Dintzis, H. (1961) Proc. Nat. Acad. Sci. USA 47, 247.
- 56. Winterhaltzer, K.H., Huehns, E.R. (1964) J. Biol. Chem. <u>239</u>, 3699.
- 57. Slabough, R.C., Morris, A.J. (1970) J. Biol. Chem. <u>245</u>, 6182.
- 58. Nozaki, Y., Tanford, C., in S.P. Colowick and N.O. Kaplan (Eds.), Methods in Enzymology, Vol. II, Academic Press, New York, 1967, p. 715.
- 59. Fish, W.W., Mann, K.G., Tanford, C. (1969) J. Biol. Chem. <u>244</u>, 4989.
- 60. Ringer, S. (1886) J. Physiol. <u>7</u>, 291.
- 61. Wood, G.T., Schaeffer, J.R. (1975) Anal. Biochem. 63, 135.
- 62. Blakesely, R.B., Boezi, J.A. (1977) Anal. Biochem. 82, 580.
- 63. Schroeder, W.A., Jones, R.T., Cormick, J., McCalla, K. (1962) Anal. Biochem. 34, 1570.
- 64. Hunt, T., Hunter, Munro, A. (1968) J. Mol. Biol. <u>36</u>, 31.
- 65. Shamsuddin, M., Mason, R.G., Cohen, C., Tissot, R., Honig, G.R. (1973) Arch. Biochem. Biophys. <u>158</u>, 922.
- 65b. S-330 and LS-230 Liquid Scintillation Systems, Operating Manual Beckman Instruments, Inc., Fullerton, CA, 92634, pp. 20-22.
- 66. Lodish, H.F., Housman, D., Jacobsen, M. (1971) Biochem. 10, 2348.

- 67. Housman, D., Jacobs-Lorena, M., RajBhandary, U.L., Lodish, H.F. (1970) Nature 227, 913.
- 68. Jackson, R., Hunter, T. (1970) Nature 227, 672.
- 69. Hori, M., Rabinowitz, M. (1968) Proc. Nat. Acad. Sci. 39, 1349.
- 70. Lodish, H.F. (1971) J. Biol. Chem. 246, 7131.
- 71. Vogel, Z., Zamir, A., Elson, D. (1969) Biochem. 8, 5161.
- 72. Salser, W. (1977) CSHSQB 42, 985.
- 73. Malkin, L.I., Rich, A. (1967) J. Mol. Biol. 26, 329.
- 74. Kozak, M. (1980) Cell <u>19</u>, 79.
- 75. Legon, S. (1976) J. Mol. Biol. 106, 37.
- 76. Legon, S., Model, P., Robertson, H.D. (1977) Proc. Nat. Acad. USA 74, 2692.
- 77. Kozak, M. (1978) Cell 15, 1109.
- 78. Cahn, F., Lubin, M. (1978) J. Biol. Chem. 253, 7798.
- 79. Pavlakis, G.N., Vournakis, J.N., personal communication.
- 80. Morris, A.J., Chaney, W.G., unpublished data.

<b>u</b> '		